

**CONTROL OF FEAR LEARNING BY NEUROMODULATION OF
PERISOMATIC INHIBITORY INTERNEURONS OF THE BASOLATERAL
AMYGDALA**

AN ABSTRACT

SUBMITTED ON THE TWELFTH DAY OF APRIL 2021

TO THE NEUROSCIENCE PROGRAM

IN PARTIAL FULFILLMENT OF THE REQUIREMENTS

OF THE SCHOOL OF SCIENCE AND ENGINEERING

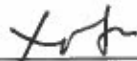
OF TULANE UNIVERSITY

FOR THE DEGREE

OF

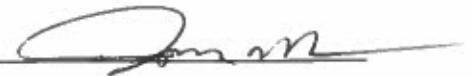
DOCTOR OF PHILOSOPHY

BY

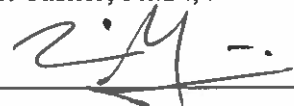


Xin Fu

Approved:



Jeffrey G. Tasker, Ph.D., Advisor



Nicholas W. Gilpin, Ph.D.



Laura A. Schrader, Ph.D.



Hai Huang, Ph.D.

Abstract:

The basolateral amygdala is a medial temporal lobe structure critically involved in the associative fear learning by imparting negative valence to the incoming sensory cues, a process that is profoundly regulated by the ascending neuromodulatory signals (e.g., norepinephrine) carrying information of the emotional states of the animals. The inhibitory parvalbumin (PV)- and cholecystokinin (CCK)- expressing basket cells in the BLA selectively innervate the perisomatic region of the principal neurons to effectively control the ensemble activities and neural oscillations, which play important roles in the populational coding of fear memory formation. Mounting evidence shows that inhibitory interneurons are major targets for neuromodulation and are activated by multiple neuromodulators via their cognate GPCRs coupled to Gq signaling pathways. However, the roles of Gq-triggered neuromodulatory activation of perisomatic targeting interneurons in the regulation of BLA population neural activity and fear acquisition remain unknown. Here, with combined chemogenetics, patch clamp electrophysiology, and genetic manipulation, I identified two different patterns of inhibitory postsynaptic currents (IPSCs) in the BLA principal neurons generated by chemogenetic and $\alpha 1A$ noradrenergic Gq activation of presynaptic PV and CCK interneurons that exert opposite effects on the acquisition of conditioned fear. Activation of Gq signaling induced repetitive bursts of action potentials showing fast acceleration of frequency in the PV interneurons that deliver synchronized phasic IPSC outputs to the principal cells. This Gq-mediated phasic activity transformed tonic action potentials into a burst firing pattern in the PV cells, which drove phasic firing in the principal neurons, and it suppressed BLA gamma oscillations in vivo. In contrast, Gq activation of CCK interneurons through $\alpha 1A$

adrenoreceptors and hM3D designer receptors generated singular trains of synchronized rhythmic IPSCs showing a stable frequency at around 4 Hz in the principal neurons. Both NE-induced CCK- and PV-type IPSCs in the BLA principal neurons were lost in a global $\alpha 1A$ knockout mouse line. Selective re-expression of $\alpha 1A$ adrenoreceptors in the PV interneurons restored the repetitive bursts of IPSCs in the principal neurons of the $\alpha 1A$ knockouts and facilitated the acquisition of fear memory, and activation of restored $\alpha 1A$ noradrenergic signaling in the BLA CCK interneurons of the $\alpha 1A$ knockouts predominantly induced rhythmic IPSCs and inhibited fear learning. These data showed dissociable roles of two types of perisomatic-targeting interneurons in controlling fear learning via the generation of distinct patterns of inhibitory synaptic outputs in response to a stress signal. This provides a possible cellular mechanism of how stress can fine tune associative fear learning by balancing the contribution of patterned perisomatic inhibition.

**CONTROL OF FEAR LEARNING BY NEUROMODULATION OF
PERISOMATIC INHIBITORY INTERNEURONS OF THE BASOLATERAL
AMYGDALA**

A DISSERTATION

SUBMITTED ON THE TWELFTH DAY OF APRIL 2021

TO THE NEUROSCIENCE PROGRAM

IN PARTIAL FULFILLMENT OF THE REQUIREMENTS

OF THE SCHOOL OF SCIENCE AND ENGINEERING

OF TULANE UNIVERSITY

FOR THE DEGREE

OF

DOCTOR OF PHILOSOPHY

BY



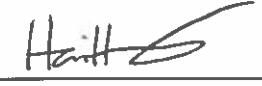
Xin Fu

Approved: _____


Jeffrey G. Tasker, Ph.D., Advisor


Nicholas W. Gilpin, Ph.D.


Laura A. Schrader, Ph.D.


Hai Huang, Ph.D.

© Copyrights by Xin Fu, 2021

All Rights Reserved

Acknowledgement

I am so fortunate to have Dr. Jeffrey Tasker as the mentor for my PhD training in neuroscience. This adventure would have been a miserable one for me without your consistent guidance and support. Thank you for having your door open whenever I need your help for my research project and life. Your encouragement, patience and brilliant ideas are deeply appreciated.

I would also like to thank my committee members, Dr. Laura Schrader, Dr. Nicholas Gilpin, and Dr. Hai Huang. Your advice and feedbacks are invaluable for the development of my project.

Thank you to the people in Tasker Lab, Dr. Shi Di, Dr. Laura Harrison, Dr. Zhiying Jiang, Dr. Chun Chen, Dr. Grant Weiss, Dr. Jenifer Rainville, Marco Fisher, and Hunter Bernstein. Thank you for teaching me the lab techniques, helping me with my project, and giving me the suggestions when I had problems with my experiments. Your passion and generous hands make the Tasker lab a very friendly and joyful working environment.

Last but not least, I would like to thank my wife Dainan Li and my parents for their constant support. Thank you for always believing in me and giving me the strength to pursue my ambitions.

Table of content

Acknowledgement	ii
Table of content	iii
List of figures	vi
1. Introduction:	1
1.1 Associative fear memories and Pavlovian fear conditioning	1
1.1.1 Associative fear learning	1
1.1.2 Pavlovian Fear conditioning.....	2
1.2 Amygdala neural circuitry and fear memory formation	3
1.2.1 Amygdala complex is critical for learned fear	3
1.2.2 Intrinsic connectivity and information flow in the amygdala.....	4
1.2.3 Synaptic plasticity in the fear circuits.....	6
1.3 The basolateral amygdala	8
1.3.1 Cellular composition of BLA	9
1.3.2 CCK and PV basket cells in the BLA.....	11
1.3.3 Fear and extinction neurons in the BLA.....	13
1.3.4 PFC-BLA neural oscillation and fear expression	14
1.3.5 Neuromodulation in the BLA.....	16
1.3.6 Glucocorticoids.....	17
1.3.7 Norepinephrine	18
1.4 Rationale of this study:	21
2. Chapter 2: Methods	23

2.1 Animals.....	23
2.2 Intracerebral virus injection	23
2.3 Fear conditioning and retrieval	24
2.4 Histology.....	25
2.5 Brain slice electrophysiology	27
2.6 Local field potential recordings in the BLA and frontal cortex.....	29
2.6.1 Field potential recording <i>in vivo</i>	29
2.6.2 Extracellular field data analysis.....	29
2.6.3 Cannula fabrication and intra-BLA infusions	30
2.7 Statistical analysis	31
3. Chapter 3: Oscillatory switch in emotional brain state by neuromodulation- induced burst firing in parvalbumin interneurons of the basolateral amygdala.....	32
3.1 Abstract	32
3.2 Introduction	33
3.3 Experimental design.....	35
3.4 Results	36
3.4.1 Gq activation in BLA PV interneurons stimulates repetitive bursts of IPSCs .	36
3.4.2 Norepinephrine stimulates PV neuron-mediated repetitive IPSC bursts.....	46
3.4.3 Gq activation of PV cells alters the firing pattern of PV interneurons and principal neurons	58
3.4.4 Gq activation in BLA PV neurons promotes state switches in amygdalo-frontal networks <i>in vivo</i>	61

3.4.5 α 1A noradrenergic Gq activation of PV interneurons enhances fear memory formation	66
3.5 Discussion.....	70
4. Chapter 4: Neuromodulatory activation of CCK interneurons in the BLA stimulates patterned perisomatic inhibition to restrain fear learning.....	77
4.1 Abstract	77
4.2 Introduction	78
4.3 Experimental design.....	81
4.4 Results	82
4.4.1 NE stimulates synchronized rhythmic perisomatic inhibitory synaptic inputs to BLA principal neurons by activating CCK basket cells.....	82
4.4.2 Expression of α 1A adrenoreceptors on the BLA CCK interneurons	88
4.4.3 Gq activation of CCK interneurons drives the rhythmic trains of IPSCs in the BLA	90
4.4.4 Activation of α 1A adrenergic signaling in CCK interneurons suppresses conditioned fear learning	95
4.5 Discussion.....	99
5. Unified discussion.....	107
6. References	112
7. Biography.....	141

List of figures

Figure 1. Intrinsic connectivity of the amygdala	6
Figure 2. Different synaptic connectivity and molecular expression in the CCK and PV basket cells.....	13
Figure 3. Gq activation of PV interneurons generates repetitive IPSC bursts.....	38
Figure 4. IPSC bursts mediated by Gq activation of PV cells are sensitive to P/Q-type calcium channel blockade.....	39
Figure 5. Gq-dependent IPSC burst generation in PV interneurons.....	41
Figure 6. Rhythmic burst firing activity induced by Gq activation of PV interneurons...	43
Figure 7. Synchronized PV-Gq-activated IPSC bursts in paired recordings of BLA principal neurons	45
Figure 8. NE activates repetitive IPSC bursts in principal neurons that originate from PV interneurons	48
Figure 9. NE induces rhythmic burst firing activity in PV interneurons	50
Figure 10. α 1A adrenoceptor-dependent NE stimulation of IPSC bursts.....	53
Figure 11. Expression of α 1A adrenoceptors in BLA PV interneurons	55
Figure 12. Serotonin 5-HT _{2A} receptor activation of IPSC bursts.....	57
Figure 13. Gq activation switches the firing pattern of PV interneurons from tonic to phasic.....	59
Figure 14. Gq activation of PV interneurons transforms the activity of BLA principal neurons	60
Figure 15. Gq signaling in BLA PV interneurons desynchronizes gamma oscillations in amygalo-frontal circuits in vivo.	62

Figure 16. Noradrenergic activation of BLA Gq signaling desynchronizes gamma oscillations in amygdalo-frontal circuits in vivo.	64
Figure 17. Rescue of Gq signaling in PV interneurons in global adra1A KO mice	67
Figure 18. Rescue of Gq signaling in PV interneurons in global adra1A KO mice facilitates the formation of fear memory	69
Figure 19. Summary diagram of facilitation of fear expression by PV-Gq modulation of BLA-PFC gamma oscillation	71
Figure 20. NE stimulates trains of rhythmic IPSCs in the BLA principal neurons	84
Figure 21. NE-induced IPSC trains undergo transient and complete DSI.....	86
Figure 22. NE-induced IPSC trains are synchronized between BLA principal neurons ..	87
Figure 23. Expression of α 1A adrenoreceptors in BLA CCK interneurons	89
Figure 24. Chemogenetic activation of BLA CCK interneurons stimulates IPSCs in the BLA principal neurons	91
Figure 25. Serotonin 5-HT _{2C} receptor activation of rhythmic IPSC trains	94
Figure 26. Rescue of α 1A adrenoreceptors in the BLA CCK interneurons restores rhythmic IPSC trains	96
Figure 27. α 1A adrenoreceptors in BLA CCK interneurons suppress fear acquisition....	98
Figure 28. Summary diagram of suppression of fear learning by Gq activation of rhythmic IPSCs from CCK interneurons.....	100
Figure 29. Summary diagram of dissociable roles of NE-stimulated CCK and PV perisomatic inhibition in fear learning	108

1. Introduction:

1.1 Associative fear memories and Pavlovian fear conditioning

1.1.1 Associative fear learning

Fear is an innate emotional state elicited by threatening stimuli that activates a battery of physiological and behavioral defense responses of an organism, such as increased sympathetic activation and glucocorticoid release, freezing, and potentiated startle (Duvarci & Pare, 2014; Hamm & Weike, 2005; LeDoux, 2014). The fear system that detects and responds to threats mobilizes energy and resources to prepare the organism for effective avoidance and escape depending on the proximity of the threatening stimulus (Fadok et al., 2017; Lang et al., 1997), which is fundamental for survival and, as a corollary, is evolutionally conserved. Moreover, the fear system is not hardwired but shows strong plasticity, allowing a previously innocuous stimulus associated with an aversive outcome to activate the fear responses by itself. The ability to form associative fear memory in an experience-dependent manner dramatically expands the range of stimuli that can activate the fear system, which enables the animals to better adapt to an ever-changing and volatile environment. However, dysregulation of normal fear learning, including excessive and overgeneralized fear learning, is maladaptive and underlies several neuropsychiatric disorders, such as posttraumatic stress disorders (PTSD), phobia, and panic disorder (Lissek et al., 2010; Zoellner et al., 2020). Currently, exposure therapy has been used in the treatment of these fear disorders, but it has a high dropout rate and never permanently removes the maladaptive fear (Schottenbauer et al.,

2008; Trouche et al., 2013). Thus, a deeper understanding of the neural mechanisms of how the fear system encodes associative fear memories may help the development of better therapeutics to treat these mental illnesses.

1.1.2 Pavlovian Fear conditioning

One of the behavioral procedures most widely used in laboratories to investigate the neural mechanisms of associative fear learning is Pavlovian fear conditioning. In this paradigm, rodents (mice or rats) learn to associate a biologically neutral conditional stimulus (CS; like a tone), with a nociceptive unconditioned stimulus (US; like a mild electrical foot shock). After several times of contingent pairings of CS and US (foot shocks co-terminate with the tones), the animals form a stable and long-lasting fear memory, and express a conditioned response (CR; often as freezing) both to the tone (cued fear memory) and the training context (context A; contextual fear memory). No associative fear memory is learned when the US is randomly applied relative to the CS (Johansen et al., 2011; Kim & Jung, 2006). Whereas the contextual fear memories are assessed by putting the animals back in the context A without CS exposure, cued fear memories are tested by presentation of the CS in a context with different texture, illuminance, and smell (context B). Typically, the amount of freezing, defined as a complete lack of motion except respiration for at least 2 seconds, is used as a proxy of the level of fear memory.

Formation of conditioned fear memory can be divided into three different phases, which are acquisition, consolidation, and reconsolidation (Johansen et al., 2011). During fear acquisition, the association of CS and US is learned, and animals quickly develop

conditioned freezing to the CS presentations during the fear conditioning training and during a short-term memory test in a different context right after the training. Fear consolidation is the process that stabilizes the newly acquired fear memory into a persistent long-term memory, which generally takes about 24 hours in the rodents. Activation of a consolidated memory during fear retrieval 24 hours after fear conditioning renders the memory labile again, a process termed reconsolidation that allows the animal to incorporate new environmental information into the previously formed memory traces. Drugs and treatments that are administered before fear conditioning are considered to target fear acquisition when they affect the freezing behavior during training and during the short-term memory test. If a drug or a treatment is administered before or right after fear conditioning does not influence the short-term fear memory but affects the fear retrieval 24 hours later, it is considered to regulate fear consolidation. Drugs and treatments are thought to regulate fear reconsolidation if they are applied after fear retrieval and exert effects on the memory tested 24 hours after drug application.

1.2 Amygdala neural circuitry and fear memory formation

1.2.1 Amygdala complex is critical for learned fear

A rich body of evidence from human and animal studies has pinpointed the amygdala complex in the medial temporal lobe as a brain structure crucial for the acquisition, consolidation, and expression of associative fear memories. Pilot studies in rhesus monkeys showed that bilateral amygdala lesions caused pronounced alterations in emotional behavior, particularly those related to fear processing (Klüver & Bucy, 1937;

Weiskrantz, 1956). This finding has been confirmed with neuropsychological and functional brain imaging studies in humans. Patient B.P. with bilateral amygdala damage exhibited impaired recognition of fear expression (Adolphs et al., 1994) as well as fear-facilitated memory formation (Cahill et al., 1995). Consistently, fMRI imaging studies showed that the amygdala is activated when the subjects are presented with fearful faces (Morris et al., 1996), and during fear conditioning (LaBar et al., 1998). In animals, lesion of amygdala attenuates fear acquisition, which eventually leads to a decrease in fear expression (Blanchard & Blanchard, 1972; Kim et al., 1993). While the lesion studies provide little temporal information of the role of the amygdala complex in the regulation of different phases of fear learning, experiments of temporary inactivation of the amygdala with infusion of muscimol, a GABA_A receptor agonist, right before fear conditioning and fear expression show amygdala activity is necessary for fear acquisition as well as fear retrieval (Helmstetter & Bellgowan, 1994; Muller et al., 1997; Wilensky et al., 1999). Moreover, extensive studies with post-training intra-amygdala drug infusion revealed an essential role of amygdala in the consolidation of stress-induced facilitation of fear memory (McGaugh, 2004; Roozendaal et al., 2009). Taken together, these studies demonstrate a critical role of amygdala complex in the processing of all the phases of fear memory.

1.2.2 Intrinsic connectivity and information flow in the amygdala

Anatomically, the amygdala complex is comprised of a group of heterogeneous nuclei that are generally divided into lateral amygdala (LA), basolateral amygdala (BLA), central lateral amygdala (CeL), central medial amygdala (CeM), and intercalated cell masses (Duvarci & Pare, 2014). To put the information flow inside the amygdala in a

very simplistic way, the multimodal sensory inputs of CS and US from thalamus and cortex funnel into the LA, which is then relayed to the BLA and CeL, and from there, to the CeM, the output nucleus of the amygdala that sends long-range projections to various downstream fear effector regions, including the hypothalamus, periaqueductal gray area, and nucleus reticularis pontis caudalis to regulate the heart rate, glucocorticoid secretion, freezing, and fear potentiated startle response (Duvarci & Pare, 2014; Parsons & Ressler, 2013) (Figure 1). The BLA connects to the CeM through both direct glutamatergic excitatory output and indirect inhibitory output via intercalated cells, and it has been proposed that the relative weight of the excitatory and inhibitory input from the BLA to the CeM is regulated during fear learning. The BLA also makes reciprocal connections with the prefrontal cortex (PFC) and hippocampus, which are critical for the generation of sustained CS-induced neural activation in the BLA and formation of contextual fear memories (Amano et al., 2011; Duvarci & Pare, 2014). In the CeL, reciprocally connected inhibitory circuits send projections to the CeM, which control the CeM activity through a mechanism of disinhibition. Traditionally, the LA is thought as the primary and sole entry site for the sensory inputs, where convergence of the CS and US induces synaptic plasticity in the LA principal cells during memory encoding. However, recent work showed that the CeL also receives the sensory inputs of the CS and US and undergoes synaptic plasticity during the acquisition of fear memory (Cicchi et al., 2010; Haubensak et al., 2010; Li et al., 2013; Penzo et al., 2014). Thus, there are multiple routes and regulation sites in the amygdala that work in parallel to control conditioned fear learning.

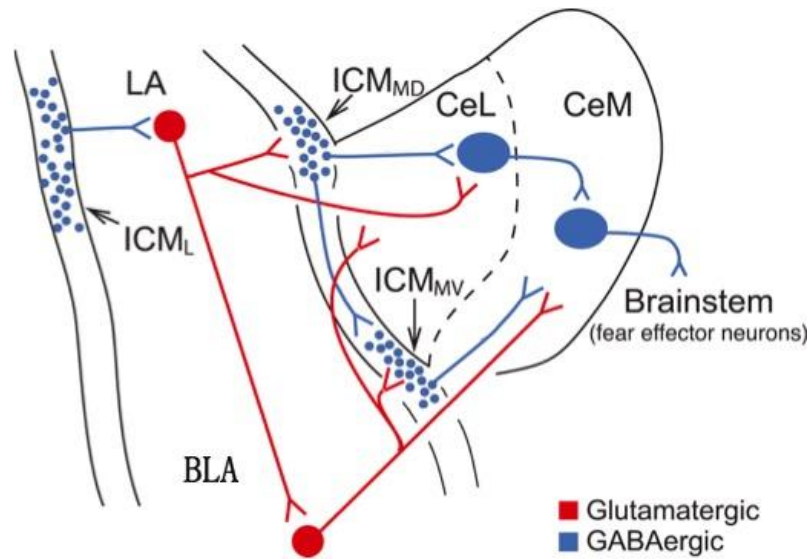


Figure 1. Intrinsic connectivity of the amygdala

The LA sends excitatory projections (labeled as red) to the BLA and CeL, which in turn activate and inhibit the CeM projection cells, respectively. The intercalated cell masses embedded in the external (ICM_L) and intermediate capsule (ICM_{MD} , ICM_{MV}) gate the information flow from BLA to CeM, from LA to CeL, and sensory input to the LA through feedforward inhibition (labeled as blue). Adapted from Duvarci & Pare, 2014.

1.2.3 Synaptic plasticity in the fear circuits

One of the cellular mechanisms underlying the formation of associative fear memory is long-term potentiation of the synapses conveying the CS information in the fear circuits. Extensive studies support the idea that CS gains its ability to activate the fear circuits and conditioned fear responses through Hebbian potentiation of its synaptic strength to the LA principal neurons. It has been shown that CS-US pairing in an auditory fear conditioning paradigm enhances both the evoked field potential in the LA by the tone or stimulation of the auditory thalamus (Rogan et al., 1997; Schafe et al., 2005) and CS-evoked single unit spiking (Goosens et al., 2003; Quirk et al., 1995). Moreover, as

predicted by the Hebbian theory that a strong depolarization of the LA neurons by the US instructs the enhancement of the concurrent weak response induced by CS, pairing the CS with optogenetically stimulated activation of the LA principal neurons mimicking the US is sufficient to produce conditioned fear (Johansen et al., 2010). At last, blockade of synaptic plasticity by blocking the AMPA receptors insertion and intracellular MAPK signaling impairs fear learning (Rumpel et al., 2005; Schafe et al., 2005). Therefore, the process of fear learning appears to occur in a scenario in which before fear conditioning, CS only elicits weak responses in the LA and is unable to trigger a fear response. During fear conditioning, the US generates strong depolarizations in the LA principal neurons, which strengthens the coincident CS-induced weak responses. As a result, CS becomes more effective in activating the LA neurons and the downstream pathways.

As mentioned earlier, the LA is not the only place that undergoes plastic synaptic change during associative fear conditioning. *In vivo* single unit recordings show that the CeL contains two populations of reciprocally connected CeM-projecting cells that develop either excitatory or inhibitory responses, termed CeL_{on} and CeL_{off} cells, to a conditioned stimulus presentation after fear conditioning (Ciocchi et al., 2010). These data suggest that fear learning disinhibits the CeM by lifting the tonic inhibition from the CeL_{off} cells through activation of the CeL_{on} cells. While the CeL_{off} cells are further shown to be positive for PKC δ (Haubensak et al., 2010), the CeL_{on} cells appear to express somatostatin (SOM) and activation of SOM population produces unconditioned fear in the naïve animals (Fadok et al., 2017; Li et al., 2013). As the PKC δ and SOM cells exist before fear conditioning, whether a cell in the CeL acquires an ON or OFF response is predetermined by their molecular profile instead of a stochastic selection from an initially

homogenous group. One possible cellular mechanism for the induction of opposing CS-induced neural activities in the CeL is biased experience-dependent plasticity at the synapses onto the ON and OFF cells. By measuring the amplitude of evoked excitatory postsynaptic currents in the CeL cells, it has been shown that under basal conditions, synaptic connection from LA to CeL SOM-positive neurons is weaker than those to SOM-negative cells. However, fear conditioning selectively enhances synaptic transmission from LA to the CeL SOM-positive cells while weakening the ones to the SOM-negative cells (Li et al., 2013). This indicates that fear conditioning resets the relative contribution of functionally distinct neuron ensembles in the CeL to controlling the CeM output, which allows the plasticity in the LA to trigger a conditioned fear response.

1.3 The basolateral amygdala

The BLA is cortical like and occupies a central position in gating the information flow from the LA to the CeM and communicating with the prefrontal cortex and hippocampus. Complementary to the synaptic plasticity in the LA and CeL, recent studies suggest that dynamic temporal and spatial control of the inhibitory synaptic inputs to the BLA principal neurons and changes in the oscillatory population activities in the interconnected PFC and BLA circuits also underlie the encoding and expression of fear memories (Herry & Johansen, 2014; Wolff et al., 2014). Furthermore, it has been well established that the BLA dependent fear memory formation is profoundly modulated by stress and the ascending neuromodulatory inputs carrying emotional arousal, like norepinephrine. This section focuses on details of the cellular composition of the BLA,

oscillatory activities between the PFC-BLA circuit during fear expression, and the role of stress hormones and neuromodulators in the regulation of conditioned fear in the BLA.

1.3.1 Cellular composition of BLA

The BLA shares a similar cellular composition with the hippocampus and cortex, that is about 80% glutamatergic excitatory principal neurons and 20% inhibitory GABAergic interneurons (Spampanato et al., 2011). While the principal cells send long-range projections out to other brain areas, like the CeM, prefrontal cortex, and hippocampus, axons of the interneurons are mostly restricted to the BLA, although a small population of somatostatin-positive interneurons close to the external capsule have been found to project to the basal forebrain (McDonald et al., 2012). Despite their relatively small number in the BLA, the local inhibitory interneurons represent a highly heterogeneous population. Recent experiments with cell type-specific opto- and chemogenetic manipulations of different types of interneurons have begun to elucidate their important roles in regulating the BLA neural output and fear learning (Krabbe et al., 2019; Wolff et al., 2014). Before getting into their function, a commonly used classification of the interneurons based on the expression of molecular markers and their postsynaptic connectivity will first be discussed.

Classification of BLA interneurons based on expression of molecular markers: similar to their hippocampal and cortical counterparts, the BLA interneurons can be characterized based on their expression of calcium binding proteins and neuropeptides. The calcium binding proteins calbindin (CB) and calretinin (CR) are differentially expressed in two nonoverlapping populations of BLA interneurons. CB expressing

interneurons can be further divided into parvalbumin (PV)-positive, somatostatin (SOM)-positive and some of the large somata cholecystokinin (CCK)-positive interneurons (McDonald, 2020; Spampanato et al., 2011). Some of the SOM-positive neurons also express neuropeptide Y (NPY) (McDonald, 1989). The CR-positive interneurons often co-express VIP and CCK, and exhibit small somata and bitufted dendrites (Mascagni & McDonald, 2003). Thus there are at least four different types of interneurons that exist in the BLA, which are PV-positive interneurons, SOM-positive interneurons, large-soma CCK interneurons, and small-soma interneurons with overlapping expression of CCK, VIP and CR. Oddly, mRNA expression of these markers obtained from single-cell PCR does not fully match the results from the immunohistochemical staining (McDonald, 2020; Spampanato et al., 2011), suggesting either the mRNAs of the molecular markers are not translated into the protein or the expression of the proteins is too low to be detected by immunostaining.

Classification based on postsynaptic connectivity: another widely used criterion to classify the interneurons is the cellular compartment of the postsynaptic principal cells on which they make synaptic connections. The dendritic inhibitory cells, for example the SOM-positive interneurons, mainly (78% of axon terminals) target the spines and shafts of distal dendrites of the principal neurons (Muller et al., 2007), which are proposed to gate synaptic integration and plasticity, generation of calcium-dependent dendritic spikes, and back-propagation of the action potentials from the soma to the dendritic compartment (Freund, 2003). In comparison, the CCK- and PV-positive basket cells and PV-positive axo-axonic Chandelier cells preferentially target the perisomatic region of hundreds of principal neurons, including the proximal dendrites, soma, and the axon initial segment

(Vereczki et al., 2016). Importantly, both CCK-positive and PV-positive basket cells are electrically coupled within their category to form a syncytium (Freund, 2003; Woodruff & Sah, 2007b). The perisomatic inhibition is thought to control the spike timing, synchronization of ensembles of BLA principal neurons, and oscillations (Ryan et al., 2012; Woodruff & Sah, 2007a). The spatially separated dendritic and perisomatic inhibitory inputs to the BLA principal neurons are further regulated temporally to control the neural network activity during fear memory encoding. In an elegant study, Wolff et al. observed that PV interneurons are activated during CS presentation, which inhibit the SOM-positive interneurons and promote fear learning by disinhibiting the dendrites of the BLA principal neurons. However, during foot shocks, both PV and SOM interneurons are inhibited, allowing an enhanced US response and the association of CS and US to take place (Wolff et al., 2014).

1.3.2 CCK and PV basket cells in the BLA

Although both target the perisomatic region of the principal neurons, the CCK and PV basket cells exhibit differences in their electrophysiological properties, synaptic input connectivity, and synaptic transmission. While the PV-positive basket cells fire high-frequency (up to more than 100 Hz), short-duration action potentials with little or no frequency accommodation (Ascoli et al., 2008; Woodruff & Sah, 2007b), and are normally referred to as fast-spiking interneurons, the CCK basket cells exhibit a regular firing at a much lower frequency (Veres et al., 2017). In the hippocampus and cortex, the PV basket cells receive extensive incoming excitatory glutamatergic input and are excited reliably to mediate feed-forward inhibition to the principal neurons (Freund & Katona, 2007; Marek et al., 2018). However, PV cells in the BLA receive only a few cortical

glutamatergic inputs, but strong inputs from the principal neurons inside the BLA, which are apt for feedback inhibition (Guthman et al., 2020; Smith et al., 2000) (Fig. 2). In comparison to the PV interneurons, not only do the CCK basket cells receive less than half the number of glutamatergic synapses, but also the excitatory synapses on the CCK basket cells contain less AMPA receptors (Andrási et al., 2017) (Fig. 2). As a result, the miniature excitatory postsynaptic currents (mEPSCs) in the CCK basket cells show a much lower frequency and smaller amplitude than those in the PV basket cells (Andrási et al., 2017). Lastly, the PV and CCK basket cells in the BLA form electrical and chemical synaptic connections with other homotypic (i.e., like) basket cells (Andrási et al., 2017; Woodruff & Sah, 2007b) (Figure 2).

The axon terminals of the CCK and PV interneurons also display several differences that endow distinct properties to their inhibitory synaptic transmission to the principal neurons. The CCK basket cells specifically utilize voltage-gated N-type calcium channels at the terminals for synaptic transmission, whereas the PV basket cells exclusively use the voltage-gated P/Q-type calcium channels at the synapse to release GABA (Chu et al., 2012; Wilson et al., 2001) (Figure 2). Consistent with a looser coupling of N-type channels to the calcium sensors than the P/Q-type channels at the active zone, the CCK synapses, but not the PV synapses, exhibit extensive asynchronous release after stimulation by a train of action potentials (Barsy et al., 2017; Hefft & Jonas, 2005). Moreover, similar to the hippocampus and cortex, the expression of cannabinoid receptor type 1 (CB1R) is restricted to the CCK basket cells in the BLA interneurons (Katona & Freund, 2008; Katona et al., 2001) (Figure 2). Accordingly, activation of CB1 receptors through exogenous CB1 agonist or endogenous cannabinoid (eCB) by

depolarization of the postsynaptic neurons selectively suppresses the transmission at the CCK terminals, with no effect on the PV-mediated synaptic release (Freund & Katona, 2007; Rovira-Esteban et al., 2017; Vogel et al., 2016; Wilson & Nicoll, 2001).

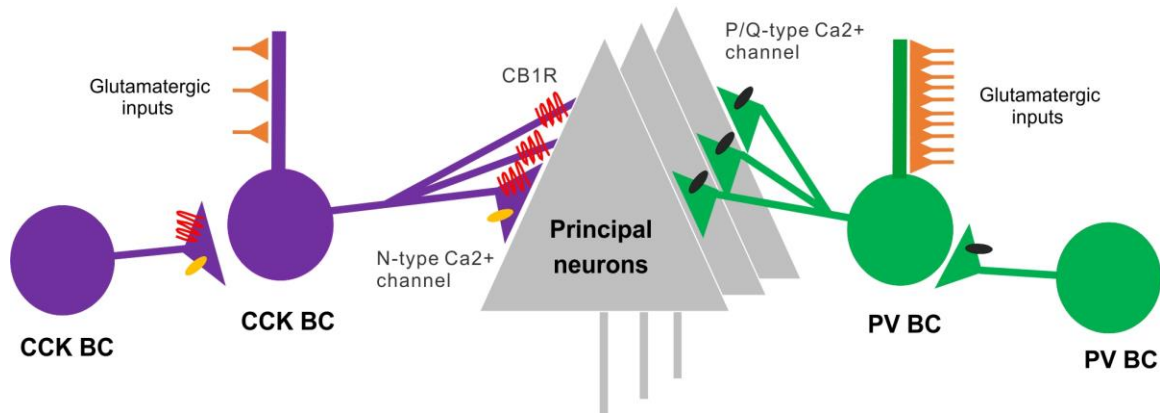


Figure 2. Different synaptic connectivity and molecular expression in the CCK and PV basket cells

The CCK and PV basket cells innervate the perisomatic region of a large number of principal neurons through their extensive axon branches, which are critical to control the spike timing and populational activity. The CCK BCs receive a small number of glutamatergic inputs and selectively express CB1 receptors and N-type calcium channels at their axon terminals. In contrast, the PV interneurons receive robust glutamatergic inputs and exclusively express P/Q-type calcium channels at the terminals. Both CCK and PV BCs form synaptic connections with other BCs within their own category. Adapted from Freund, 2003 and Andrasi et al., 2017.

1.3.3 Fear and extinction neurons in the BLA

Similar to the LA, some of the principal neurons in the BLA, termed fear neurons, develop CS-evoked responses after fear conditioning (Amano et al., 2011; Herry et al., 2008). Another group of neurons in the BLA, termed extinction neurons, do not show an

increase of firing during CS presentation initially during fear expression, instead, they develop CS-evoked responses after fear extinction (Herry et al., 2008). As the BLA makes strong reciprocal connections with the PFC, the activity of these fear and extinction neurons may propagate fear information to the PFC during fear memory expression and extinction. Supporting this hypothesis, inactivation of the BLA with muscimol blocked the CS-evoked activation of the principal neurons in the prelimbic region (PL) of the PFC (Sotres-Bayon et al., 2012). Whereas the PL has been shown to promote fear expression and inhibit fear extinction (Burgos-Robles et al., 2009), the infralimbic region (IL) of the PFC facilitates fear extinction and suppresses fear expression (Sierra-Mercado et al., 2011). Intriguingly, the BLA fear neurons have been found to project to the prelimbic region (PL) of the PFC while the extinction neurons selectively target the IL of the PFC (Senn et al., 2014). As a result, selective inhibition of the IL-projecting extinction neurons in the BLA interferes with extinction of fear memory and an opposite effect is observed with inhibition of the PL-projecting fear neurons (Senn et al., 2014).

1.3.4 PFC-BLA neural oscillation and fear expression

Emerging evidence has revealed the neural oscillations particularly in the theta and gamma band width between the interconnected BLA and PFC circuits are critically involved in the retrieval of conditioned fear memory. During fear memory recall, a coordinated 4 Hz oscillatory activity between the PFC and the BLA emerges, which synchronizes spiking activity of the principal neurons between the two structures and predicts the onset of the freezing episodes (Karalis et al., 2016). Directionality analysis further showed that the BLA-PFC 4 Hz oscillation is entrained by the oscillatory activity

in the PFC. Accordingly, optogenetic induction of an artificial 4 Hz oscillation in the PFC is sufficient to drive freezing in naïve animals (Karalis et al., 2016). One possible mechanism to generate oscillation in the PFC during fear expression is the regulation of its intrinsic inhibitory control by fear conditioning. Supporting this idea, another study elegantly showed that CS presentations during fear retrieval inhibit the activity of PV interneurons in the PFC, which disinhibit the principal neurons and reset the local theta oscillations (Courtin et al., 2014).

In addition to the case of the theta oscillation, gamma oscillation and gamma-theta coupling in the BLA-PFC circuit have also been associated with fear memory retrieval. In a discriminative fear conditioning paradigm, animals learn to associate the CS+ (paired with foot shocks) and CS- (not paired with foot shocks), with fear and safety respectively. With this procedure, Stujenske et al. observed that CS+ presentations promote the theta-gamma coupling between the PFC and the BLA and suppress the gamma power (70-120 Hz) in the BLA, which are associated with a fear state and higher freezing level. In comparison, presentation of the safety signal CS- increases the gamma power (70-120 Hz) in the BLA (Bocchio & Capogna, 2014; Stujenske et al., 2014). These findings collectively suggested the gamma oscillation in the BLA might be modulated during the switch of fear and safety emotional states of the animals. Given the important role of the perisomatic targeting basket cells in sculpting the population activity and neural oscillation, experiments with cell type-specific manipulation will be needed to address their function in switching the oscillatory state of the amygdala neural circuits during emotional processing.

1.3.5 Neuromodulation in the BLA

Activation of the fear system by threatening stimuli is accompanied by the activation of the stress response in the brain as well as in the periphery. In the brain, stress activates the ascending monoamine modulatory systems and triggers the release of neuromodulators, like norepinephrine (NE), throughout the brain, which promotes an arousal state and enhances the processing of the threatening cues (Rodrigues et al., 2009). In the periphery, activation of the sympathetic system and HPA axis stimulates the release of NE and epinephrine from the adrenal medulla and glucocorticoids (GCs) from the adrenal cortex. While the GCs readily cross the blood brain barrier (BBB), the peripheral NE and epinephrine do not cross the BBB and may indirectly affect the brain through the ascending visceral nerves (Rodrigues et al., 2009). Therefore, activation of the fear system by threat stimulates the release of stress hormones (like NE and GCs), which feed back to the circuits and mediate the brain state-dependent modulation of information processing. Particularly, the BLA has a rich expression of glucocorticoid receptors as well as dense staining for axon fibers positive for tyrosine hydroxylase (TH), dopamine beta hydroxylase (DBH), and norepinephrine transporter (NET), which are the enzymes and transporter for norepinephrine synthesis and uptake (Muller et al., 2009; Stringfield et al., 2016; Zhang et al., 2013). Consistently, studies with lesion and region-specific pharmacological manipulations show an essential role of the BLA in mediating the effect of stress and stress-related neuromodulation on the facilitation of fear memory formation (McGaugh, 2004), which are discussed below with emphasis on the glucocorticoids and norepinephrine.

1.3.6 Glucocorticoids

Once the circulating GCs get into the brain, they bind to the high-affinity mineralocorticoid receptors (MRs) or low-affinity glucocorticoid receptors (GRs) and modulate neural activity and behavior. While GCs exert a biphasic modulation on neural excitability and LTP induction by dose-dependent activation of the MRs and GRs in the hippocampus (de Kloet et al., 1999; Joëls & de Kloet, 1992; Pavlides & McEwen, 1999; Pavlides et al., 1996; Rodrigues et al., 2009), both low and high concentrations of GCs are shown to enhance neural excitability of the BLA principal neurons (Duvarci & Paré, 2007). In addition to the direct postsynaptic effect on the principal neurons, recent experiments revealed that GCs also modulate the synaptic transmission in the BLA. At inhibitory synapses, application of GCs triggered the release of eCB from the principal neurons and induced a long-lasting suppression of the frequency of mIPSCs in the BLA principal neurons from naïve animals, an effect reversed by blocking eCB synthesis and CB1 receptors (Di et al., 2016). Moreover, The GC-induced suppression of inhibition in the slice is occluded by a prior acute restraint stress, which triggers high glucocorticoids in the circulation (Di et al., 2016). At the glutamatergic synapses, glucocorticoids increase the frequency of mEPSCs in naïve animals when the circulating glucocorticoids are low (Karst et al., 2010). However, a metaplasticity is observed when the slices were harvested from animals with a prior stress. Instead of a facilitation of excitatory transmission, glucocorticoid application induced a rapid and long-lasting suppression of the frequency of mEPSCs in the BLA principal neurons (Karst et al., 2010).

A large body of evidence shows glucocorticoids enhance the formation of fear memory by modulating the BLA. Post-training systemic or intra-BLA administration of

glucocorticoids or GR agonist enhanced fear memory consolidation (Lupien & McEwen, 1997; McGaugh, 2004; Zorawski & Killcross, 2002). Moreover, lesion of the BLA blocked the memory facilitation induced by systemic GC administration (Roosendaal et al., 1996). GC-mediated facilitation of memory consolidation involves interaction with β -adrenergic signaling as concomitant injection of β -adrenoreceptor antagonist blocked the systemic or intra-BLA administration of GCs or glucocorticoid agonist (Quirarte et al., 1997). Additionally, recent experiments suggest the endocannabinoid is an important mediator of glucocorticoid-induced memory enhancement in the BLA through a membrane glucocorticoid receptor. Post-training intra-BLA infusion of CB1 receptor antagonist AM251 blocked memory enhancement by intra-BLA infusion of both glucocorticoids and CORT-BSA, a membrane-impermeable version of the GCs (Atsak et al., 2012; Campolongo et al., 2009).

1.3.7 Norepinephrine

Norepinephrine is generally considered as an arousal signal in the brain that modulates a variety of cognitive functions including vigilance, attention, and memory processing. The BLA receives extensive noradrenergic inputs from the Locus Coeruleus (LC) and the concentration of NE in the BLA is significantly elevated during stressful encounters (McIntyre et al., 2002). Once NE is released from the noradrenergic fibers, it binds to the different subtypes of adrenergic receptors that are coupled to different G protein signaling pathways. The adrenergic receptors appear to localize to different cell types and different cellular compartments to produce multiplex modulation of BLA neural activity, which further influences the formation of conditioned fear memory (Giustino & Maren, 2018; McGaugh, 2004).

There are three different classes of adrenoreceptors, which are the $\alpha 1$, β and $\alpha 2$ adrenoreceptors. Each class has three subtypes: $\alpha 1$ receptors include $\alpha 1A$, $\alpha 1B$, and $\alpha 1D$; β receptors include $\beta 1$, $\beta 2$, and $\beta 3$; and $\alpha 2$ receptors include $\alpha 2A$, $\alpha 2B$, and $\alpha 2C$. The $\alpha 1$ adrenoreceptors are generally coupled to the Gq signaling pathway, which activates phospholipase C (PLC) and mobilizes intracellular calcium, leading to neuronal excitation. The β adrenoreceptors are Gs coupled, which activates adenylyl cyclase and downstream cAMP cascades. The $\alpha 2$ adrenoreceptors are coupled to Gi signaling and inhibit the activity of adenylyl cyclase and cAMP formation, which generally reduces neuronal excitability. Several biochemicals that selectively target the G α proteins have been used to understand intracellular signaling pathways. Pertussis toxin (PTX) catalyzes the ADP-ribosylation of G α_i protein and selectively inhibits the activation of the Gi-coupled signaling pathway (Katada, 2012). In comparison, Cholera toxin (CTX) selectively catalyzes the ADP-ribosylation of G α_s protein and blocks the G α_s -mediated intracellular cascade (Haan & Hirst, 2004). Two recently reported depsipeptides, YM-254890 and FR900359, block the transition of G α_q protein from GDP-bound to GTP-bound states, which selectively inhibits the activation of the G α_q pathway (Schrage et al., 2015; Takasaki et al., 2004).

Alpha 2 adrenoreceptors are generally localized at the axon terminals at different synapses (Gilsbach & Hein, 2012). Specifically, at the terminals of noradrenergic neurons, $\alpha 2$ adrenoreceptors function as autoreceptors that suppress the exocytosis of norepinephrine in a negative feedback mechanism. Elevation of extracellular NE levels by blocking $\alpha 2$ adrenoreceptors induced significant cFOS expression in the BLA (Singewald et al., 2003), while blunting extracellular NE with $\alpha 2$ adrenoreceptor agonist

during fear conditioning attenuated cued fear learning and cFOS expression in the BLA (Frances Davies et al., 2004).

Compelling evidence from the literature demonstrates β receptor activation increases BLA neural activity and fear memory consolidation. Fear conditioning induced a long-lasting increase of firing activity in the BLA by increasing norepinephrine release from the LC (Giustino et al., 2020). This effect was blocked by systemic or intra-BLA administration of the β adrenoceptor antagonist propranolol (Giustino et al., 2020). Optogenetic activation of the LC noradrenergic fibers in the BLA also increased the firing of some of the principal neurons in the BLA and promoted anxiety-like behavior, which was also blocked by inhibiting β adrenoceptors with propranolol (McCall et al., 2015; McCall et al., 2017). In the brain slice, activation of β adrenergic signaling enhanced the excitability of the BLA principal neurons by downregulation of the calcium-activated small conductance potassium channel (SK) through recruitment of the protein kinase A pathway (Faber et al., 2008). Behaviorally, post-training infusion of NE and β receptor agonist in the BLA enhanced the consolidation of fear memory, while blocking the β receptors and the downstream cAMP signaling cascade in the BLA prevented memory enhancement by stress (McGaugh, 2004).

Interest in understanding the function of $\alpha 1$ adrenergic function rises in part as the $\alpha 1$ antagonist prazosin clinically exhibits a promise in treating some of the PTSD symptoms, including nightmares and frequent sleep disturbance (Breen et al., 2017; Hendrickson & Raskind, 2016; Singh et al., 2016). In the BLA, activation of the $\alpha 1A$ adrenoceptors stimulates a robust increase in synaptic inhibition, possibly by activating the putative presynaptic CCK interneurons (Braga et al., 2004; Kaneko et al., 2008).

Intriguingly, traumatic stress exposure desensitized the NE facilitation of inhibition in the BLA (Braga et al., 2004). The role of $\alpha 1$ activation in the BLA in fear memory formation is controversial (Ferry et al., 1999; Gazarini et al., 2013; Lazzaro et al., 2010; Lucas et al., 2019), possibly due to a lack of receptor subtype- and cell type-specific pharmacological and genetic manipulations.

1.4 Rationale of this study:

The inhibitory neural circuitry in the BLA dynamically sculpts the output of the principal neurons to regulate fear memory encoding and expression. BLA-dependent memory processing is profoundly modulated by the neuromodulators carrying stress and arousal signals. Although emerging evidence shows the interneurons are major targets for neuromodulation, the role of cell type-specific neuromodulatory activation of the BLA interneurons in the regulation of BLA neural activity and fear learning remains to be determined. Here, combining chemogenetics and brain slice electrophysiology, I observed that Gq activation of the perisomatic PV and CCK basket cells through designer receptor hM3D and $\alpha 1A$ adrenoreceptors generates stereotyped patterns of IPSCs in the BLA principal neurons, which oppositely modulate the formation of conditioned fear memory. In the first chapter, I focus on a Gq-dependent mechanism of generating repetitive IPSC bursts in the PV interneurons, and how this phasic firing pattern modulates the oscillatory activity in the BLA. I next investigated the role of $\alpha 1A$ noradrenergic activation of PV interneurons in the formation of fear memory with selective re-expression of $\alpha 1A$ adrenoreceptors in the BLA PV cells in a global $\alpha 1A$ knockout and found that $\alpha 1A$ adrenergic signaling enhanced the expression of fear

memory. In the second chapter, I focus on a rhythmic pattern of IPSCs generated by $\alpha 1A$ noradrenergic Gq activation in CCK interneurons. I further show that rescue of CCK interneuron mediated rhythmic IPSCs in the $\alpha 1A$ knockout suppresses fear memory acquisition and expression. Overall, these studies aim to improve our understanding of subtype-specific noradrenergic modulation of BLA neural circuitry in molecularly defined cell types and promote the development of advanced treatment strategies for fear and anxiety-related mental health disorders.

2. Chapter 2: Methods

2.1 Animals

Mice were maintained in an AALAC-approved, temperature-controlled animal facility on a 12-h light/dark cycle with food and water provided *ad libitum*. PV-Cre (Cat. 017320), CCK-ires-Cre (Cat. 012706) and *adra1A* KO mice (Cat. 005039) were purchased from Jackson Laboratories and bred in-house to establish colonies. Heterozygous GAD67-eGFP mice were purchased from Riken BioResource center (Tamamaki et al., 2003) and back-crossed for more than 5 generations with wildtype C57BL/6 mice. All procedures were approved by the Tulane Institutional Animal Care and Use Committee and were conducted in accordance with Public Health Service guidelines for the use of animals in research.

2.2 Intracerebral virus injection

Four- to 6-week-old male mice were anesthetized by intraperitoneal injection of ketamine/xylazine (100 mg/kg) and placed in a stereotaxic frame (Narishige, SR-6N). The scalp was cut along the midline and the skull was exposed. Two burr holes were perforated above the BLA with a Foredom drill (HP4-917). Mice were then injected bilaterally with 350 nl of virus into the BLA (AP: -0.8, ML: 3.05, DV: 4.4) through a 33-gauge Hamilton syringe (10 μ l) connected to a micropump (World Precision Instrument, UMP-2) and controller (Micro4) at a flow rate of 100 nl per minute. After waiting for 5 minutes following virus injection to minimize virus spread up the needle track, the

injection needle was then slowly retracted from the brain. After surgery, the scalp was sealed with Vetbound, a triple antibiotic ointment was applied, and an analgesic (Buprenorphine, 0.05 mg/kg) was injected I.P.

For cloning of Cre-dependent hDlx AAV virus, we amplified the hM3D-mCherry and mCherry coding sequence from the plasmid pAAV-hSyn-DIO-hM3D(Gq)-mCherry (a gift from Bryan Roth, Addgene # 44361) (Krashes et al., 2011) and pAAV-hSyn-DIO-mCherry (also a gift from Bryan Roth, Addgene # 50459) and cloned into pAAV-hDlx-Flex-GFP vector backbone (a gift from Gorden Fishell, Addgene #83895) (Dimidschstein et al., 2016) at AccI and NheI cloning sites. The coding sequence of adra1A was synthesized from Bio Basic Inc. and cloned into a pAAV-hDlx-Flex backbone. AAV virus from Vigene Biosciences Company was further packaged in AAVdj serotype. All hDlx AAV viruses were diluted to the range of 10^{11} to 10^{12} viral genome per ml with virus dilution buffer containing 350 mM NaCl and 5% D-Sorbitol in PBS.

2.3 Fear conditioning and retrieval

3 weeks after virus injection, mice were single housed and handled for more than 5 days before undergoing a fear conditioning paradigm with the Video Fear Conditioning System in a sound attenuated chamber (MED Associates, Inc.). Each chamber is equipped with a metal stainless-steel grid connected to a shock generator (ENV414S Aversive Stimulator). The fear conditioning paradigm consisted of 7 exposures to a continuous tone (7 kHz, 80 db, 30 s duration) as the conditioned stimulus (CS), each of which was co-terminated with an unconditioned aversive stimulus (US) consisting of electric foot shocks (0.7 mA, 2 s duration). The CS-US stimuli were presented at a

randomized intertrial interval (ITI, 30-180 s, average = 110 s) in one context, context A. Twenty four hours later, on day 2, mice were tested for fear retention in a different context, context B, with a planar floor and a black plastic hinged A-frame insert. During fear memory retrieval, five presentations of CS alone were delivered with an inter-stimulus interval of 60 s. Behavior was recorded with an infrared camera and analyzed with Video Freeze software (Med Associates, Inc.). Mice were considered to be exhibiting freezing behavior if no movement other than respiration was detected for ≥ 2 s. Chambers were cleaned with either 70% ethanol or 3% acetic acid before each session of fear conditioning or fear memory retrieval.

2.4 Histology

Perfusion and cryosectioning: two weeks after AAV virus injection, *adralA* KO, PV-Cre, CCK-ires-Cre, PV-Cre::*adralA* KO, and CCK-ires-Cre::*adralA* KO were deeply anesthetized with ketamine/xylazine (300mg/kg) and perfused transcardially with 10 ml ice-cold PBS (pH 7.4) followed by 20 ml 4% paraformaldehyde (PFA) in PBS. Brains were dissected out, postfixed for 3 hours in 4% PFA in PBS, and cryopreserved with 30% sucrose in PBS for 24 hours at 4°C until the brain sunk to the bottom of the container. Coronal sections (45 μ m) were cut on a cryostat (Leica) and harvested in 24-well plates filled with PBS.

Confocal imaging: Sections from virus-injected PV-Cre, CCK-ires-Cre, PV-Cre::*adralA* KO, and CCK-ires-Cre::*adralA* KO mice containing the BLA were selected, rinsed with PBS (3 x 5 mins), and mounted on gel-coated slides. Confocal images were acquired with a Nikon A1 confocal microscope to capture the DAPI (excitation 405 nm,

emission 450 nm), GFP (excitation 488 nm, emission 525 nm), and mCherry (excitation 561 nm, emission 595 nm) signals. For the analysis of colocalization, z stack pictures were imaged under a 40x oil-immersion objective with a step increment of 1.5 μm . The number of BLA cells containing colocalized markers were first quantified from merged maximal intensity images from different channels, and then confirmed in z-stack images with ImageJ (NIH).

X-gal staining: Sections from *adra1A* KO mice were rinsed with PBS (3 x 5 min) and incubated in a β -gal staining solution (Roche, Ref # 11828673001) overnight. After β -gal staining, sections were then rinsed in PBS (3 x 5 min), mounted on gel-coated glass slides, coverslipped with Permount mounting medium (Fisher Scientific), and allowed to air dry. Bright-field imaging was performed in a Zeiss Axio Scanner and processed and analyzed with ImageJ (NIH). For fluorescence confocal imaging, brain sections were rinsed with PBS (3 x 5 min), mounted on gel coated coverslips, and then imaged first on the confocal microscope (Nikon A1) before incubating them in the β -gal staining solution. After staining with X-gal, the slices were rinsed with PBS (3 x 5 mins) and the same regions previously imaged using fluorescence confocal imaging were then re-imaged for the X-gal signal with excitation and emission wavelengths of 638 and 700 nm (Levitsky et al., 2013), respectively. The images were then processed and quantified with ImageJ software to determine the ratio of β -gal-positive cells to fluorescent cells with the same procedure described above.

2.5 Brain slice electrophysiology

Slice preparation: Coronal brain slices containing the BLA were collected from male mice for *ex vivo* electrophysiological recordings. Mice (6 to 9 weeks) were decapitated in a restraining plastic cone (DecapiCone, Braintree Scientific) and the brains were dissected and immersed in ice-cold, oxygenated cutting solution containing the following (in mM): 252 sucrose, 2.5 KCl, 26 NaHCO₃, 1 CaCl₂, 5 MgCl₂, 1.25 NaH₂PO₄, 10 glucose (Barsy et al., 2017). The brains were trimmed and glued to the chuck of a Leica VT-1200 vibratome (Leica Microsystems) and 300 µm-thick coronal slices were sectioned. Slices were transferred to a holding chamber containing oxygenated recording artificial cerebrospinal fluid (aCSF) containing (in mM): 126 NaCl, 2.5 KCl, 1.25 NaH₂PO₄, 1.3 MgCl₂, 2.5 CaCl₂, 26 NaHCO₃, and 10 glucose. They were maintained in the holding chamber at 34°C for 30 min before decreasing the chamber temperature to ~20°C.

Patch clamp electrophysiology: Slices were bisected down the midline and hemi-slices were transferred one-at-a-time from the holding chamber to a submerged recording chamber mounted on the fixed stage of an Olympus BX51WI fluorescence microscope equipped with differential interference contrast (DIC) illumination. The slices in the recording chamber were continuously perfused at a rate of 2 ml/min with recording aCSF maintained at 32-34°C and continuously aerated with 95% O₂/5% CO₂. Whole-cell patch clamp recordings were performed in putative principal neurons in the BLA. Glass pipettes with a resistance of 1.6-2.5 MΩ were pulled from borosilicate glass (ID 1.2mm, OD 1.65mm) on a horizontal puller (Sutter P-97) and filled with an intracellular patch

solution containing (in mM): 110 CsCl, 30 potassium gluconate, 1.1 EGTA, 10 HEPES, 0.1 CaCl₂, 4 Mg-ATP, 0.3 Na-GTP, 4 QX-314; pH was adjusted to 7.25 with CsOH and the solution had a final osmolarity of ~ 290 mOsm. DNQX, APV, TTX, Prazosin, Propranolol, WB4101, A61603, CNO, and NE were delivered at the concentrations indicated via the perfusion bath. Slices were pre-incubated in aCSF containing ω -agatoxin (0.5 μ M, 30 min), ω -conotoxin (0.5 μ M, 30 min), or YM 254890 (10 μ M, 20 min) to block P/Q-type calcium channels, N-type calcium channels and G $\alpha_{q/11}$ activity, respectively (Owen et al., 2013; Takasaki et al., 2004). The same solution as that used for the aCSF was used in the patch pipettes (1.6-2.5 M Ω) for loose-seal extracellular recording of action potentials, which were performed in the I = 0 mode on the patch clamp amplifier. For current clamp recordings, an intracellular patch solution was used containing (in mM): 130 potassium gluconate, 10 HEPES, 10 phosphocreatine Na₂, 4 Mg-ATP, 0.4 Na-GTP, 5 KCl, 0.6 EGTA; pH was adjusted to 7.25 with KOH and the solution had a final osmolarity of ~ 290 mOsm. Series resistance was normally below 10 M Ω immediately after break through the membrane and was continuously monitored. Cells were discarded when the series resistance exceeded 20 M Ω . Data were acquired using a Multiclamp 700B amplifier, a Digidata 1440A analog/digital interface, and pClamp 10 software (Molecular Devices). Recordings were filtered at 2 KHz for IPSC recordings and at 10 KHz for action potential recordings and sampled at 50 KHz. Data were analyzed with MiniAnalysis software (SynptoSoft, NJ) and Clampfit 10 (Molecular Devices).

2.6 Local field potential recordings in the BLA and frontal cortex

(The extracellular local field potential and EEG recordings were done in collaboration with Eric Teboul and Jamie Maguire at Tufts University.)

2.6.1 Field potential recording *in vivo*

LFP recordings were performed in awake, freely behaving C57BL/6J and PV-Cre mice, acquired using prefabricated headmounts (Pinnacle Technology, #8201). Frontal cortex EEG and BLA LFP recordings were acquired through a stainless-steel EEG screw and insulated LFP depth electrode implanted over the frontal cortex and in the ipsilateral BLA, respectively. Animals were tethered to the apparatus and EEG and LFP were recorded at 4KHz and amplified 100 times. All mice were left to habituate to the recording chamber for at least 30 minutes while tethered before recording. In PV-Cre animals expressing BLA PV hM3D, baseline (first intraperitoneal saline injection) and treatment conditions (I.P. injection of saline and CNO (5mg/kg, dissolved in saline)) were recorded for 60 minutes each. In cannulated C57 mice, baseline (first intra-BLA infusion of saline) and treatment conditions (intra-BLA infusion of saline, NE, WB4101, and WB4101 + NE) were recorded for 30 minutes each.

2.6.2 Extracellular field data analysis

LFP and EEG data were band-pass filtered (1-300 Hz, Chebyshev Type II filter), and spectral analysis was performed in MATLAB using publicly accessible custom-made scripts developed by Pantelis Antonoudiou utilizing the fast Fourier transform (Frigo and Johnson 2005). Briefly, recordings were separated into 5 second bins with 50%

overlapping segments. The power spectral density for positive frequencies was obtained by applying a Hann window to eliminate spectral leakage. The mains noise (58-60 Hz band) was removed from each bin and replaced using the PCHIP method. Values 3 times larger or smaller than the median were considered outliers and replaced with the nearest bin. Processed spectral data were then imported to Python for resampling into one-minute bins and normalization to baseline. Finally, normalized, resampled data were imported to GraphPad Prism for statistical analysis.

2.6.3 Cannula fabrication and intra-BLA infusions

Intra-BLA drug infusion cannulas were fabricated in-house using 27G and 30G syringe needles. Twenty-seven gage syringe needles were cut at each end to produce a 10 mm plastic base and 5 mm barrel. Thirty gage syringe needle barrels were cut to 17 mm from the plastic base (including the 1 mm bit of adhesive at the base of the barrel) to create the internal cannula and inserted through the guide cannula to protrude an extra 2 mm to produce a clean syringe barrel opening, barrels were initially cut an extra 1-2 mm longer, and shaved back to the desired length using a Dremel rotary tool (Dremel 3000) with a ¼ inch 120-grit sanding band attachment.

Intra-BLA infusions were performed using a 25 µL Hamilton syringe mounted to an automated micro-infusion pump (Harvard Apparatus, The Pump 11 Elite Nanomite), and connected to the internal cannula needle via a plastic tubing. Intra-BLA infusions of 300 nL norepinephrine (9.88 mM) and WB4101 (10 µM) were administered at a rate of 0.2 µL/min. After infusion, the needle was left to sit for an extra minute to allow for sufficient diffusion and minimize backflow upon removal from the brain.

2.7 Statistical analysis

To investigate the IPSCs induced by Gq activation of perisomatic inhibitory interneurons in the BLA principal cells with or without the agonists and antagonists, the normalized frequency and amplitude of the baseline recording immediately before drug application were compared to the peak or plateau (for NE-induced IPSCs from PV neurons) of drug-induced responses. Statistical comparisons were conducted in Prism 6.0 (GraphPad, La Jolla, CA) with a paired or unpaired Student's *t* test or with a one- or two-way analysis of variance (ANOVA) followed by a *post hoc* Dunnett's test as appropriate ($p < 0.05$ with a two-tailed analysis was considered significant).

To study the effects of rescue of $\alpha 1A$ signaling in the BLA interneurons on fear conditioning, the percentages of time freezing during CS presentations were compared between the control mCherry group and the experimental $\alpha 1A$ re-expression or hM3D expression groups during fear conditioning (day 1) or fear memory retrieval (day 2) with Prism 6.0 using repeated measures Two-Way ANOVA ($p < 0.05$ with a two-tailed analysis was considered significant).

To study the effects of PV Gq signaling on BLA-frontal cortex gamma oscillations *in vivo*, statistical comparisons of normalized values after treatments with different drugs within subjects were conducted with paired Student's *t* tests with Prism 6.0 ($p < 0.05$ with a two-tailed analysis was considered significant).

3. Chapter 3: Oscillatory switch in emotional brain state by neuromodulation-induced burst firing in parvalbumin interneurons of the basolateral amygdala

3.1 Abstract

Network orchestration of behavioral states involves coordinated oscillations within and between brain regions. The network communication between the basolateral amygdala (BLA) and the medial prefrontal cortex (PFC) plays a critical role in fear expression. However, a mechanistic understanding of how amygdalar networks are organized to mediate transitions between brain and behavioral states remains largely unknown. Neuromodulatory systems play an essential role in regulating behavioral states. Here, we examine the role of Gq-mediated neuromodulation in coordinating network and behavioral states using combined chemogenetics, patch clamp and field potential recordings, and genetic manipulations. We demonstrate that activation of Gq-signaling in the BLA via the designer receptor hM3D and the $\alpha 1A$ adrenoreceptor stimulates a previously unknown burst-firing pattern of activity in parvalbumin (PV)-positive interneurons that, in turn, generates bursts of inhibitory postsynaptic currents (IPSCs) in BLA principal neurons and shifts the pattern of activity of the principal neurons from tonic to phasic. Consistent with a critical role for tonic PV neuron activity in generating gamma-frequency (30-120 Hz) network oscillations, the PV neuron Gq-induced transition from tonic to phasic activity suppressed amygdalo-frontal gamma oscillations *in vivo*. The BLA PV interneuron hM3D- and $\alpha 1A$ receptor-induced suppression of BLA gamma oscillatory power also facilitated fear memory recall, consistent with the

association of fear expression with decreased gamma. Thus, our data reveal a PV neuron-specific neuromodulatory mechanism in the BLA that mediates the transition to a fear-associated brain network state via a shift in PV neuron activity pattern that disrupts amygdalo-frontal gamma oscillations.

3.2 Introduction

Animals constantly switch between different behavioral and brain states to adapt to an ever-changing environment. Accompanying brain state switches are prominent changes in population neuronal activities (Lee & Dan, 2012), which can be detected by changes in the oscillations of the local field potentials that are shaped by the activity of inhibitory interneurons (Bocchio et al., 2017; Buzsáki et al., 2012). The subcortical neuromodulatory systems that convey stimulus and emotional salience are key mediators of brain state transitions (Lee & Dan, 2012) and significantly modulate neural circuit oscillations. Mounting evidence shows that inhibitory interneurons are major targets for neuromodulation and are activated by multiple neuromodulators, like norepinephrine, serotonin, and acetylcholine, via their cognate GPCRs coupled to Gq signaling pathways (Wester & McBain, 2014; Zaghera & McCormick, 2014). Thus, Gq-triggered neuromodulatory activation of inhibitory interneurons may be critical for orchestrating the changes in neural circuit oscillation that lead to switches in the network operational states of the brain.

The BLA is a medial temporal lobe structure that is critical for emotional memory processing and that displays a switch in its oscillatory state during the encoding of fear and safety. Specifically, it has been shown that presentation of conditioned safety signals

(i.e., not associated with aversive stimulation like foot shock) promotes an increase in gamma power in the BLA, while exposure of the animals to a conditioned fear stimulus (i.e., that predicts an aversive stimulus) suppresses BLA gamma oscillations (Bocchio & Capogna, 2014; Stujenske et al., 2014). Thus, changes in gamma oscillation in the BLA may serve as a simplified index of the emotional state of the animal. Numerous studies have highlighted an essential role for PV fast spiking interneurons in the neural circuit generation of gamma oscillations (Bartos et al., 2007; Buzsáki et al., 2012; Cardin et al., 2009; Sohal et al., 2009). These fast-spiking interneurons are a main source of basket cell innervation of the perisomatic region of the BLA principal neurons that control BLA population activity and neural oscillations (Freund & Katona, 2007; Ryan et al., 2012; Vereczki et al., 2016; Veres et al., 2017; Woodruff & Sah, 2007a). Moreover, the PV cells are reliably activated by robust glutamatergic synaptic inputs (Andrási et al., 2017; Fuchs et al., 2007), and they fire tonic, phase-locked single action potentials during gamma oscillation cycles (Bartos et al., 2007; Hájos et al., 2004). In addition to the glutamatergic inputs, ascending neuromodulatory signals (e.g., noradrenergic inputs) acting on GPCRs also tune PV cell activity to execute brain state-dependent behavioral tasks (Garcia-Junco-Clemente et al., 2019; Polack et al., 2013), providing a potential cellular mechanism of the modulatory control of these cells, like during stressful fear conditioning, that switches the operational mode of BLA neural circuits to regulate emotional processing. However, despite the critical role of neuromodulation in the processing of BLA-dependent fear memories, the effect of neuromodulatory regulation of PV interneurons on the BLA oscillatory neural output and fear learning remained poorly understood.

Here, we tested the role of Gq neuromodulation of PV interneurons in BLA neural output and fear memory formation. Our findings revealed a novel cellular mechanism of PV interneuron regulation of BLA neural circuit oscillations and fear learning. Stimulation of Gq signaling through either chemogenetic manipulation or $\alpha 1A$ adrenoceptor activation triggered a phasic firing pattern in PV interneurons that generated synchronized repetitive bursts of IPSCs in the postsynaptic BLA principal neurons. Gq activation in amygdala slices transformed tonic action potentials into a burst firing pattern in the PV cells, which drove phasic firing in the principal cells, and it suppressed BLA gamma oscillations in vivo. Selective rescue of $\alpha 1A$ adrenergic signaling in BLA PV interneurons in a global $\alpha 1A$ adrenoceptor knockout mouse restored norepinephrine-induced burst generation in PV neurons and facilitated fear memory retrieval. Our data demonstrate a novel cellular and molecular mechanism for the modulation by emotionally salient signals of neural circuit oscillations and fear memory expression by stimulating burst firing activity in fast-spiking PV cells.

3.3 Experimental design

In this chapter, we conducted four sets of experiments to address the role of neuromodulation of PV interneurons in BLA neural output and fear learning: 1) Whole-cell or loose-seal patch clamp recordings and neuropharmacological treatments in acute brain slices. Brain slices were pre-incubated in the recording chamber with control artificial cerebrospinal fluid or receptor antagonists for ≥ 10 minutes. Norepinephrine, adrenoceptor agonist, clozapine-N-oxide (CNO), or serotonin was then co-applied in the perfusion bath for 5 minutes. Spontaneous IPSCs were recorded and analyzed for

changes in frequency, amplitude, and decay time constant for 10-20 minutes following drug applications. 2) In vivo recordings of brain oscillations. After recovery from stereotaxic surgery (1-3 weeks), electroencephalographic recordings were conducted in the frontal cortex simultaneously with local field potential recordings in the BLA in awake behaving mice. CNO was injected IP or NE was infused directly into the BLA with or without adrenoceptor antagonist, and drug-induced changes in oscillations in the frontal cortex and BLA were measured for 10-30 minutes. 3) Histochemical analyses of α 1A adrenoceptor distribution. The *adra1A* knockout, *GAD67-eGFP::adra1A* KO, and AAV-injected *PV-Cre::adra1A* KO mice were perfused and stained for β -galactosidase activity. The bright field or fluorescent X-gal signals were then imaged and analyzed to reveal the localization of α 1A receptors in the BLA. 4) Behavioral analysis of the effects of α 1A adrenergic activation of PV interneurons on fear conditioning. The freezing behavior during fear acquisition and retrieval were compared between the *adra1A* knockout mice with or without selective re-expression of α 1A adrenoceptors or expression of hM3d designer receptors in the BLA PV interneurons.

3.4 Results

3.4.1 Gq activation in BLA PV interneurons stimulates repetitive bursts of IPSCs

To investigate the function of Gq activation in PV interneurons in the modulation of BLA neural output, a conditional AAV virus was injected bilaterally into the BLA of *PV-Cre* mice to express a Gq-coupled designer receptor activated exclusively by designer drug (DREADD) in a Cre-specific manner in PV interneurons (Fig. 3A-C). Two weeks after viral delivery of the Gq-DREADD to PV interneurons in the BLA, whole-cell

voltage clamp recordings were performed in putative BLA principal neurons in slices of amygdala in the presence of glutamate AMPA-receptor (DNQX, 20 μ M) and NMDA-receptor antagonists (APV, 40 μ M) in order to isolate inhibitory postsynaptic currents (IPSCs). Notably, Gq-DREADD activation selectively in PV interneurons in slices with bath application of CNO (5 μ M) induced highly stereotyped phasic bursts of IPSCs. The repetitive IPSC bursts showed an accelerating intra-burst frequency, which peaked at over 50 Hz and generated an inward shift in the baseline holding current due to extensive summation (Fig. 3D, E). We observed multiple types of phasic bursts with varying amplitudes, durations, and acceleration rates (Fig. 3D), but similar repetitive bursting characteristics, suggesting they were generated by different presynaptic PV interneurons. The PV-mediated repetitive IPSC bursts were of relatively long duration (mean: 3.63 ± 0.26 s) and recurred at a low frequency (mean: 0.032 ± 0.001 Hz; inter-burst interval range: 20 to 80 s) (Fig. 3F) and continued for >20 min after CNO was washed from the recording chamber. Consistent with synaptic output from PV interneurons mediated exclusively by P/Q-type calcium channels, and not N-type calcium channels (Chu et al., 2012; Freund & Katona, 2007; Wilson et al., 2001), we found that the CNO-induced IPSC bursts were totally abolished by the selective P/Q-type calcium channel blocker ω -agatoxin (0.5 μ M), but not by the N-type calcium channel blocker ω -conotoxin (1 μ M) (Fig. 4A-D).

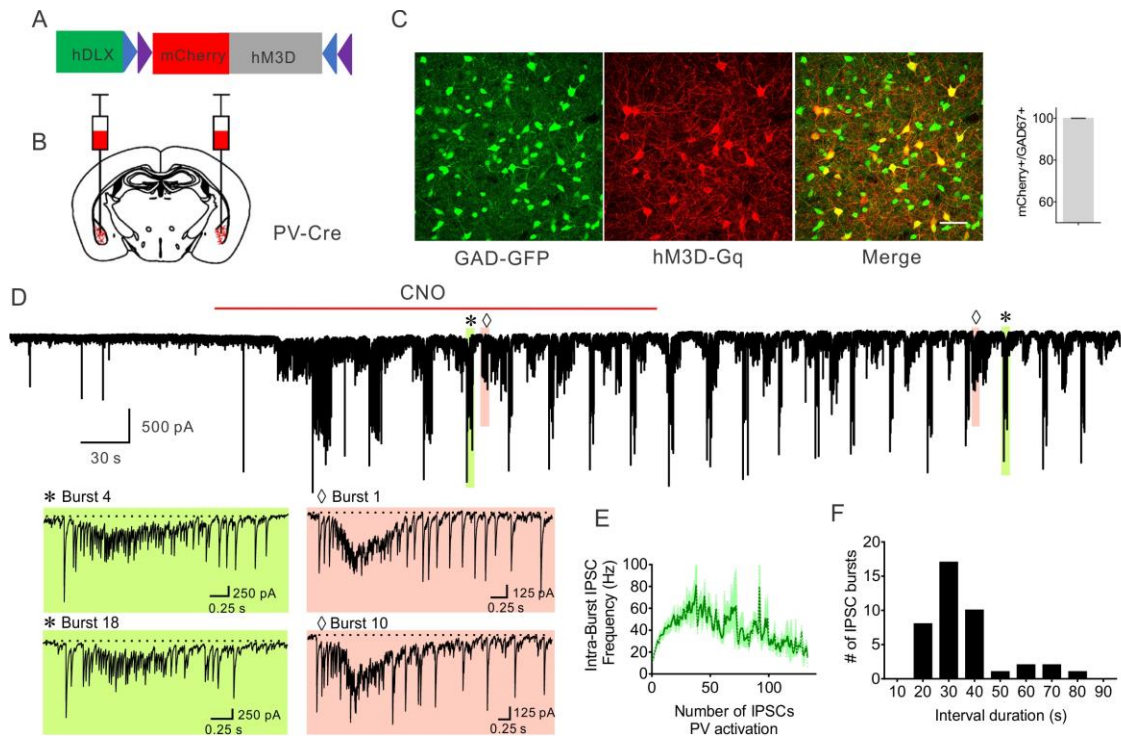


Figure 3. Gq activation of PV interneurons generates repetitive IPSC bursts

(A, B) Schematic diagrams of bilateral injection of conditional AAV virus expressing Gq-coupled DREADD (hM3D) in the BLA of PV-Cre mice. (C) Expression of Gq-DREADD in PV interneurons, which exclusively colocalize with Gad67-positive GABAergic interneurons (10 sections from 4 animals, 278 cells, ratio=99.81%). (D) A representative recording showing the generation of phasic IPSC bursts in a BLA principal neuron by selective Gq activation in PV interneurons with bath application of CNO. Asterisks (*) and diamonds (◇) designate recording segments that were expanded below to illustrate different stereotyped IPSC bursts (color coded) at two successive time points. The dashed lines show the depressed baseline holding current due to the summation of high-frequency IPSCs in each burst. (E) Mean (+/- SEM) of instantaneous intra-burst IPSC frequency over the course of the IPSC bursts. (F) An interevent interval histogram showing the distribution of the phase duration of repetitive IPSC bursts (41 bursts from 12 cells).

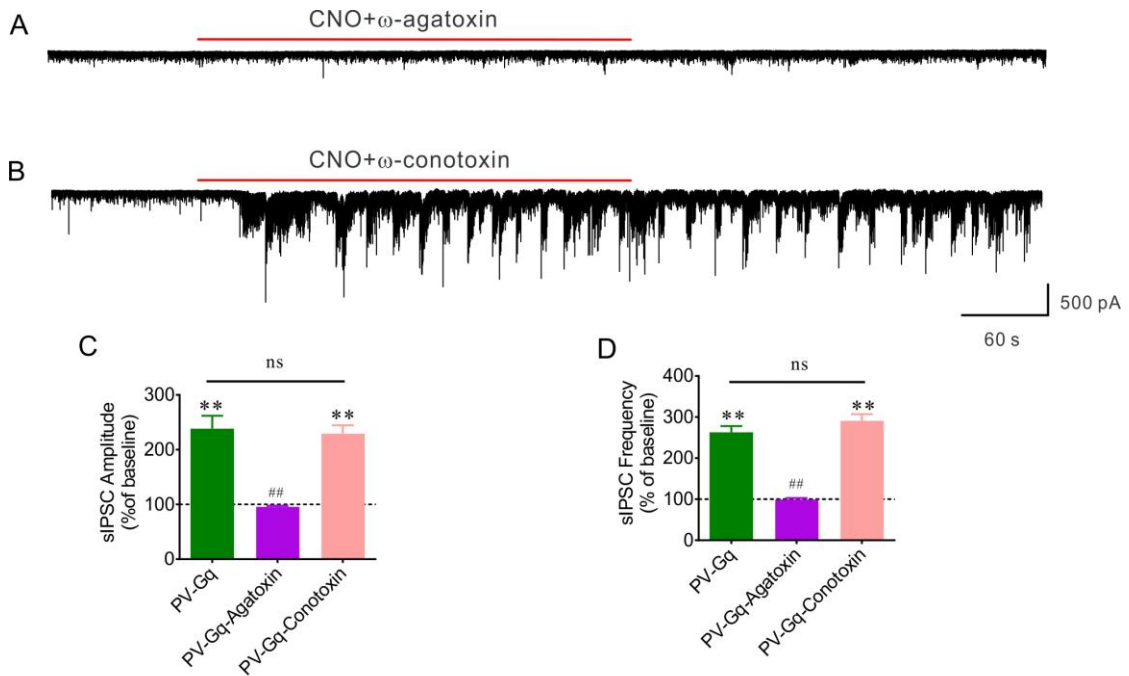


Figure 4. IPSC bursts mediated by Gq activation of PV cells are sensitive to P/Q-type calcium channel blockade

(A, B) Representative recordings of PV interneuron-mediated repetitive IPSC bursts in a BLA principal neuron, which were blocked by pre-treatment of the slice with the P/Q-type calcium channel blocker ω -agatoxin, but were unaffected by pre-incubation of the slice in the N-type calcium channel blocker ω -conotoxin. (C, D) Mean change in sIPSC amplitude and frequency in response to Gq activation in PV interneurons, which was blocked by ω -agatoxin and insensitive to ω -conotoxin. (PV-Gq: 12 cells from 5 mice; PV-Gq-Agatoxin: 7 cells from 3 mice; PV-Gq-Conotoxin: 7 cells from 3 mice) (IPSC amplitude: Paired *t* test, PV-Gq vs. baseline: $p = 0.0001$; PV-Gq-Conotoxin vs. baseline: $p = 0.0001$; **, $p < 0.01$; One-Way ANOVA, $F(2, 23) = 13.86$, $p = 0.0001$; Dunnett's multiple comparisons test, PV-Gq vs. PV-Gq-Agatoxin: $p < 0.0001$; PV-Gq vs. PV-Gq-Conotoxin: $p = 0.93$; ## $p < 0.01$) (IPSC frequency: Paired *t* test, PV-Gq vs. baseline: $p < 0.0001$; PV-Gq-Conotoxin vs. baseline: $p < 0.0001$; **, $p < 0.01$; One-Way ANOVA, $F(2, 23) = 42.83$, $p < 0.0001$; Dunnett's multiple comparisons test, PV-Gq vs. PV-Gq-Agatoxin: $p < 0.0001$; PV-Gq vs. PV-Gq-Conotoxin: $p = 0.93$; ## $p < 0.01$).

To confirm that the Gq-DREADD-induced IPSC bursts were mediated by the excitation of PV interneurons through Gq signaling, we blocked the Gq protein activation with a selective $G\alpha_{q/11}$ inhibitor YM-254890 (10 μ M), which blocks the switch of $G\alpha_q$ from the GDP- to GTP-bound state (Takasaki et al., 2004). We found that CNO-induced IPSC bursts were completely eliminated in the Gq blocker (Fig. 5A-D). In addition, blocking spike activity with tetrodotoxin (TTX, 0.5 μ M) also abolished the PV-mediated IPSC bursts (Fig. 5A-D), which demonstrated the dependence of Gq-induced IPSC bursting in the principal neurons on Gq activation in the presynaptic PV interneuron somata/dendrites. Because bath application of CNO, which creates a stable drug concentration over minutes and presumably generates a continuous activation of the PV interneurons, induced a phasic synaptic output, we next tested whether sustained PV neuron excitation independent of Gq activation is also sufficient to generate the repetitive IPSC bursting pattern in the principal cells using photoactivation of the PV neurons with channelrhodopsin (ChR2). Two weeks after AAV delivery of Cre-dependent ChR2 to PV interneurons in PV-Cre mice, continuous photostimulation of BLA PV interneurons in amygdala slices with blue light induced a tonic increase in IPSCs that was phase-locked to the light stimulation (Fig. 5E, F). These results together suggest that Gq signaling is required to activate the PV interneurons to generate the phasic pattern of inhibitory synaptic output.

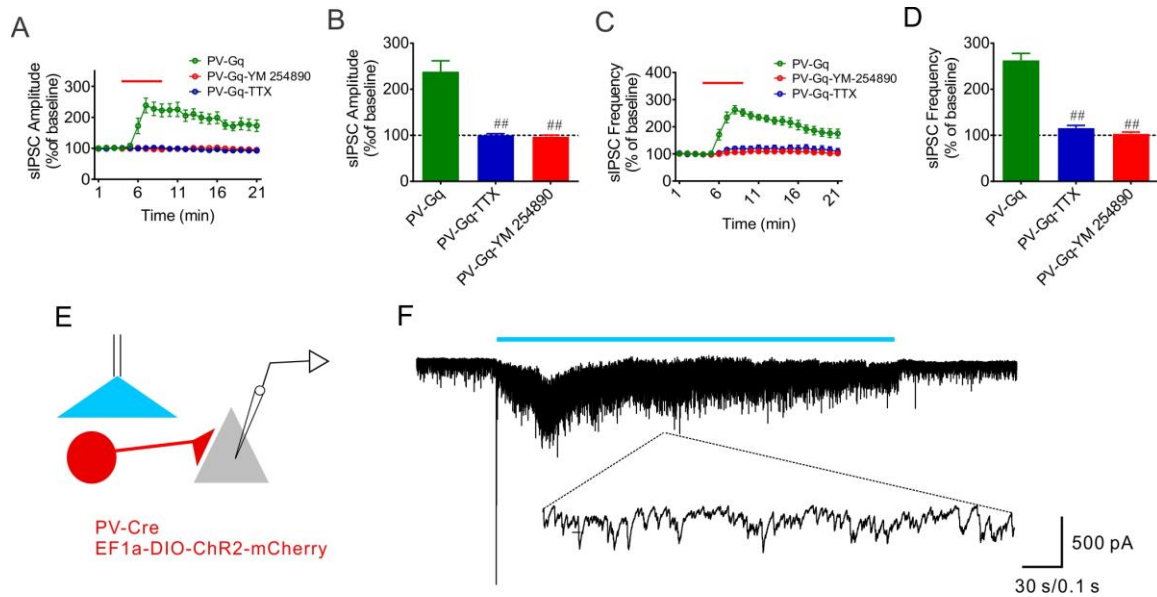


Figure 5. Gq-dependent IPSC burst generation in PV interneurons

(A, B) Time course and mean change in sIPSC amplitude with Gq activation in PV interneurons. The CNO-induced increase in sIPSC amplitude was completely blocked by the sodium channel blocker TTX (8 cells from 4 mice), and the selective $G\alpha_{q/11}$ inhibitor YM-254890 (9 cells from 4 mice). One-Way ANOVA, $F(2, 26) = 24.05$, $p < 0.0001$, Dunnett's multiple comparisons test, PV-Gq vs. PV-Gq-TTX, $p < 0.0001$, PV-Gq vs. PV-Gq-YM 254890, $p < 0.0001$, ###, $p < 0.01$. (C, D) Mean change in sIPSC frequency with Gq activation in PV interneurons over time (C, 1-min bins) and after 3-5 min of CNO application (D). One-Way ANOVA, $F(2, 26) = 65.30$, $p < 0.0001$, Dunnett's multiple comparisons test, PV-Gq vs. PV-Gq-TTX, $p < 0.0001$, PV-Gq vs. PV-Gq-YM 254890, $p < 0.0001$, ###, $p < 0.01$. (E, F) Schematic diagram of recording from BLA principal neurons after transduction and light activation of channelrhodopsin (ChR2) in BLA PV interneurons. (F) Representative recording of the response of a BLA principal neuron to activation of PV interneurons by continuous photostimulation (blue line), which generated a tonic increase in IPSCs. Bottom: Expanded trace showing the tonic generation of IPSCs.

The repetitive bursting pattern of IPSCs in the BLA principal neurons suggests that the presynaptic PV interneurons fire phasic action potential bursts with Gq activation. To directly test this, extracellular loose-seal patch clamp recordings of PV interneurons were performed in slices from PV-Cre mice after AAV delivery of the Cre-dependent Gq-DREADD to the BLA. Similar to the pattern of IPSC bursts in the principal neurons, the PV cells responded to CNO (5 μ M) by firing repetitive accelerating bursts of action potentials that recurred at a low frequency (0.034 ± 0.005 Hz, $n = 9$ cells) in the presence of the glutamate receptor antagonists DNQX and APV (Fig. 6A-C). Further blockade of inhibitory synaptic transmission with picrotoxin (50 μ M) did not affect the pattern of action potential bursts stimulated by CNO in the PV interneurons ($n=3$, data not shown), suggesting that the bursting activity in the PV cells is mediated by an intrinsic, rather than a circuit, mechanism. In paired recordings of synaptically connected PV and principal neurons ($n=5$ pairs), we found that the action potential bursts in the PV neurons were time-locked to one of the subtypes of IPSC bursts in the principal neurons (Fig. 6A), confirming that the different subtypes of Gq-induced IPSC bursts in the principal neurons were generated by different presynaptic PV interneurons. Moreover, we observed that the action potentials within the bursts of PV cells were time-locked with individual IPSCs in the corresponding IPSC bursts of the principal cells (Fig. 6A). Therefore, Gq activation drives a repetitive bursting pattern of action potentials in BLA PV interneurons to deliver phasic inhibitory synaptic inputs to the BLA principal neurons.

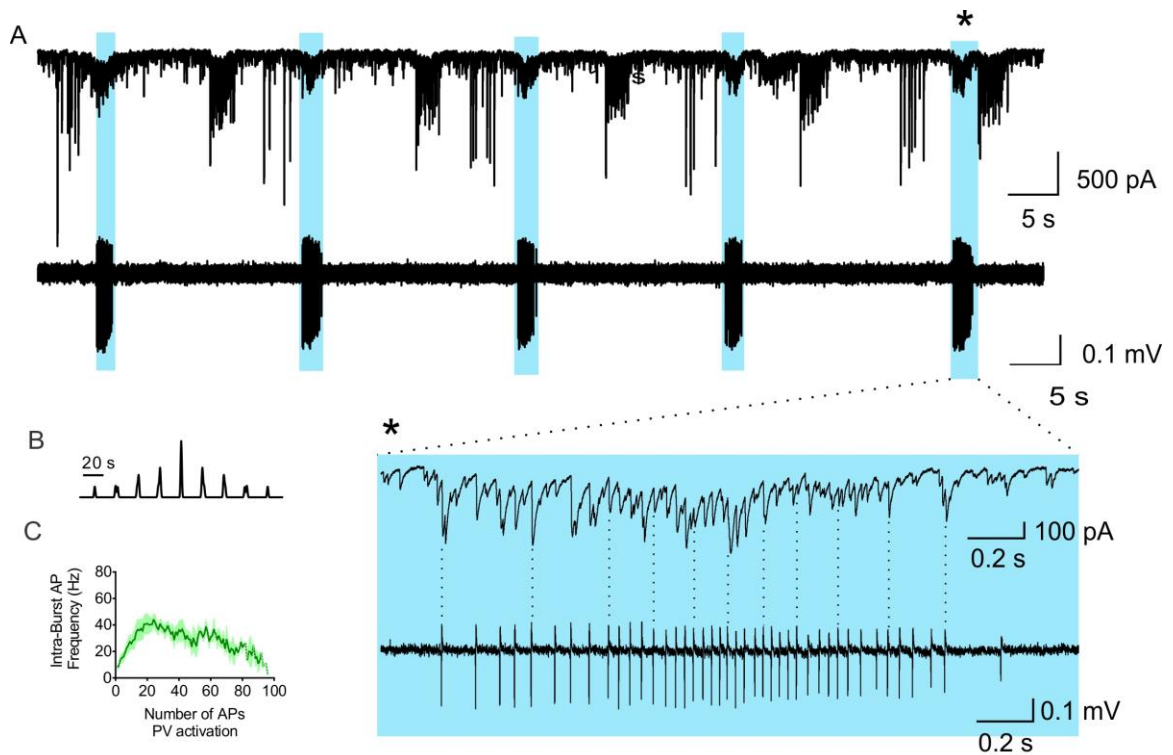


Figure 6. Rhythmic burst firing activity induced by Gq activation of PV interneurons

(A) A representative paired recording showing repetitive IPSC bursts recorded in a BLA principal neuron with whole-cell recording and associated action potential bursts recorded in a PV interneuron with loose-seal recording. Correlated activities are labeled with blue shaded bars and the bursts marked with an asterisk were expanded to show the time-locked IPSCs and action potentials. (B) Autocorrelation diagram showing the rhythmicity of the action potential bursts in the PV interneuron shown in (A). (C) Mean instantaneous intra-burst frequency (\pm SEM) of action potentials in a PV interneurons.

Perisomatic PV interneurons innervate hundreds of principal neurons to effectively control spike timing and population neural output (Andrási et al., 2017; Freund & Katona, 2007; Holmgren et al., 2003; Vereczki et al., 2016; Woodruff & Sah, 2007a), raising the question of whether PV-mediated phasic IPSC bursts are synchronized between neighboring BLA principal neurons. To test this, we first examined the synchrony of the Gq-induced IPSC bursts with paired recordings from adjacent BLA principal neurons (distance within 40 μm) following CNO activation of Gq-DREADD in PV interneurons (Fig. 7A). Interestingly, CNO application induced similar responses in both cells in most of the paired recordings (Fig. 7B). Moreover, we found that the CNO-induced recurrent IPSC bursts were synchronized between each pair at two different levels: 1) bursts that were synchronized between two cells were synchronous at each repetition, and 2) the individual IPSCs within synchronized bursts showed a high level of synchronization (Fig. 7B), which is consistent with each specific subtype of IPSC burst generated by action potential bursts in a single corresponding presynaptic PV interneuron. Dividing the total number of PV-mediated IPSC bursts by the number of synchronized bursts, we calculated one BLA principal neuron receives on average 4.1 different IPSC bursts from presumably a corresponding number of different presynaptic PV interneurons, and 67.7% of the bursts are synchronized between the pairs of recorded principal cells (16 recorded pairs from 5 animals) (Fig. 7C).

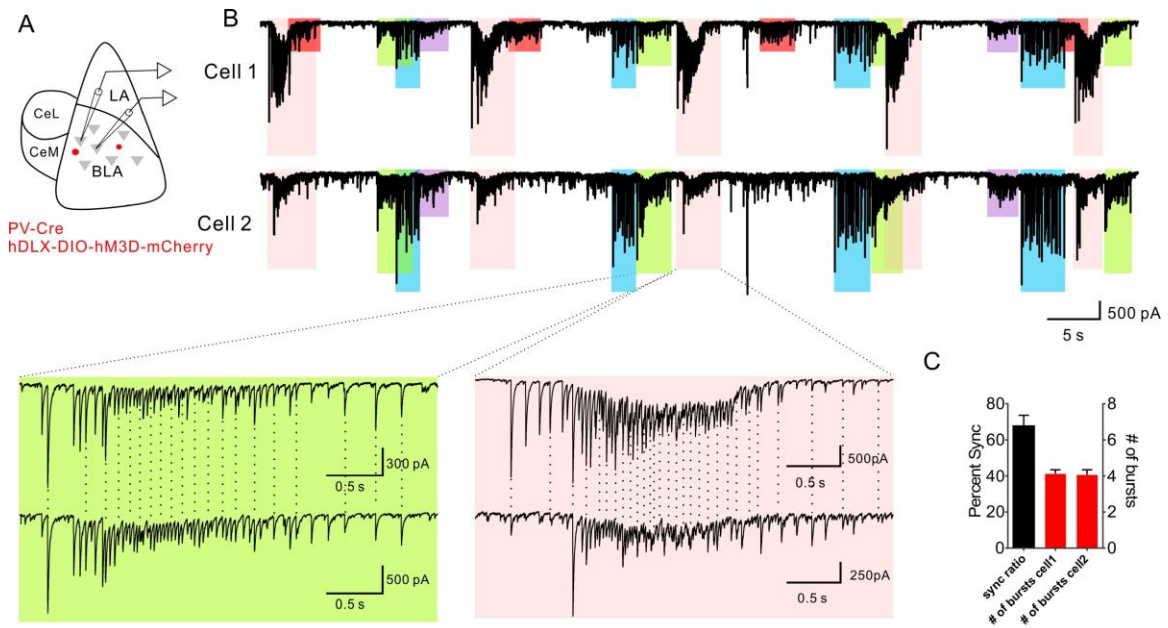


Figure 7. Synchronized PV-Gq-activated IPSC bursts in paired recordings of BLA principal neurons

(A) Schematic showing paradigm of paired recordings of adjacent BLA principal neurons in Gq-DREADD-injected PV-Cre mice. (B) Representative recordings showing synchronized bursts of IPSCs in a pair of BLA principal neurons, Cell 1 and Cell 2. Different colored boxes represent different IPSC bursts repeated over the course of the recording; the same-colored boxes in the two recordings indicate bursts that were synchronized between the two cells. The red-colored bursts in Cell 1 were the only IPSC bursts not associated with a synchronous IPSC burst in Cell 2. Bottom: Expanded traces of two different, color-coded IPSC bursts from each cell. The dashed vertical lines show the high synchronicity between the two cells of the individual IPSCs that make up each of the bursts. (C) The mean ratio of synchronized bursts to total bursts, and the total number of different subtypes of bursts induced in pairs of principal cells by Gq activation of PV interneurons (16 pairs from 6 mice).

3.4.2 Norepinephrine stimulates PV neuron-mediated repetitive IPSC bursts

Having established the role of Gq signaling in driving repetitive phasic synaptic outputs from PV interneurons in the BLA, we next examined if activation of native Gq-coupled GPCRs in PV interneurons generates similar bursts of IPSCs in BLA principal neurons. Norepinephrine (NE) is an arousal neuromodulator and the release of NE is significantly increased during stressful conditions (McIntyre et al., 2002). In addition, alpha1 adrenoreceptors couple to Gq. Thus, we tested whether NE also activates PV interneurons to generate phasic IPSC bursts in BLA principal neurons. Voltage clamp recordings of IPSCs in the presence of glutamate AMPA and NMDA receptor antagonists revealed that NE application (100 μ M) induced a robust increase in spontaneous IPSCs that was characterized by a repetitive bursting pattern that was similar to Gq-DREADD activation in PV neurons (Fig. 8A). Following an initial increase in the frequency of IPSCs that inactivated within 35 s to 135 s, a rhythmic bursting pattern of IPSCs emerged at low frequency (0.028 ± 0.002 Hz) (Fig. 8A-D). The IPSC bursts displayed a fast acceleration of the intra-burst IPSC frequency that reached peak frequencies > 50 Hz (peak frequency = 50 to 133 Hz), lasted for several seconds (duration, 1.58 to 10.55s, mean = 4.88 ± 0.37 s), and gradually tapered off (Fig. 8B, C, E), resembling the repetitive IPSC bursts stimulated by Gq activation in PV interneurons. In some recordings, we observed multiple NE-induced bursts showing different identities, which were considered to be generated from different presynaptic neurons. Individual IPSCs within the bursts showed a fast rise time (10-90%: $1.11 \text{ ms} \pm 0.07 \text{ ms}$) and decay time (tau: $18.94 \text{ ms} \pm 1.04 \text{ ms}$), suggesting that they originated from perisomatic inhibitory interneurons, such as cholecystinin (CCK) or PV basket cells (McGarry & Carter, 2016; Wilson et al.,

2001), which can be distinguished by differential expression of voltage-gated calcium channels and CB1 receptors at their synapses. Double dissociation of NE-induced IPSCs with calcium channel blockers and a cannabinoid receptor agonist showed that while the initial increase in IPSC amplitude was blocked by the N-type calcium channel blocker ω -conotoxin (1 μ M) and a CB1 receptor agonist, WIN 55,212-2 (1 μ M), the repetitive IPSC bursts were not affected by ω -conotoxin (1 μ M) or WIN 55,212-2, but were selectively blocked by the P/Q-type calcium channel blocker ω -agatoxin (0.5 μ M) (Fig. 8A, F, G). Since GABA release from PV interneurons is mediated by calcium influx through P/Q-type calcium channels, while GABA release from CCK interneurons is mediated by N-type channels (Freund & Katona, 2007; Wilson et al., 2001), this indicated that the NE-induced phasic IPSC bursts were generated by GABA release from PV interneuron synapses onto the principal cells. While blocking PV interneuron inputs to the principal cells with the P/Q-type calcium channel antagonist abolished the NE-induced IPSC bursts, it only suppressed the increase in IPSC frequency by about 50%, and blocking CCK basket cell inputs with the CB1 receptor agonist failed to reduce the frequency response further (Fig. 8H, I), which suggested that NE also activates other interneuron inputs to the principal cells, possibly from somatostatin cells. We did not investigate this response further, but focused on the IPSC bursting response.

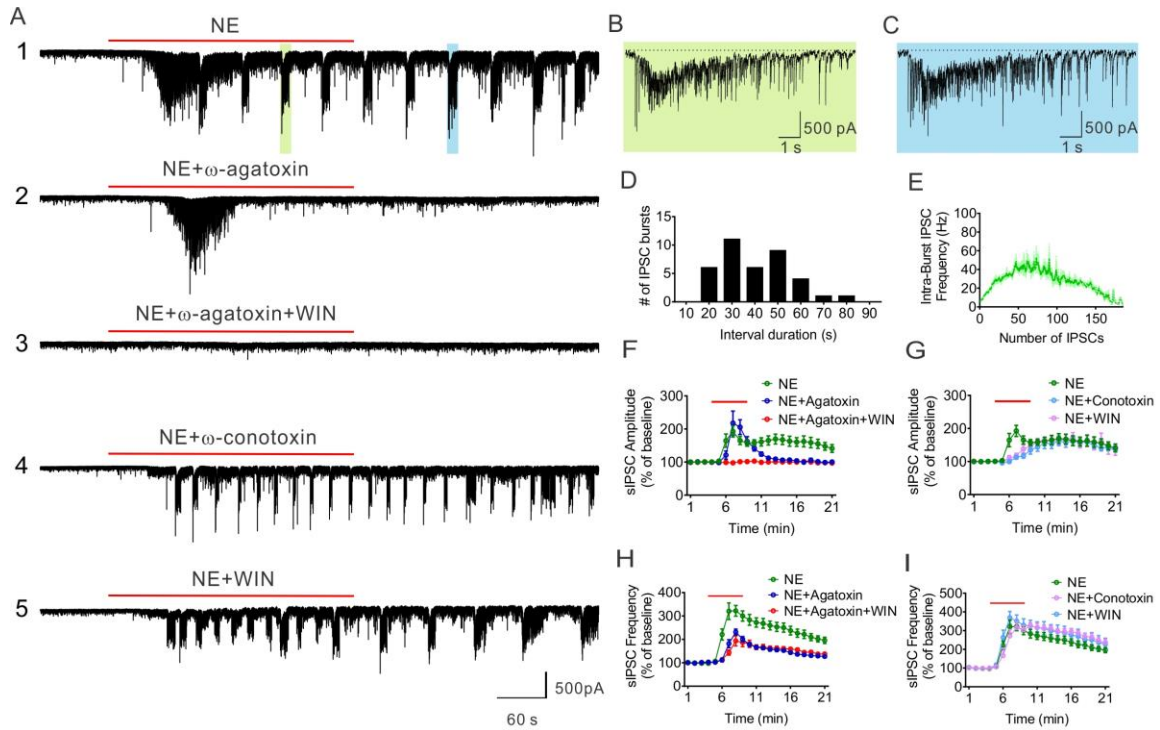


Figure 8. NE activates repetitive IPSC bursts in principal neurons that originate from PV interneurons

(A1-5) Representative recordings showing the effect of different treatments on NE-induced repetitive IPSC bursts in the BLA principal neurons. 1, NE application induced phasic IPSC bursts following an initial increase in IPSCs. 2, Blocking PV neuron-mediated transmission with the P/Q channel blocker ω -agatoxin selectively abrogated the NE-induced repetitive IPSC bursts. 3, The remaining IPSCs insensitive to ω -agatoxin were inhibited by CB1 receptor activation with WIN 55,212-2. 4, Pretreatment of a slice with ω -conotoxin selectively inhibited the NE-induced initial increase of IPSCs, but not the repetitive IPSC bursts. 5, CB1 activation with WIN 55,212-2 blocked the initial IPSC increase but not the repetitive IPSC bursts induced by NE. (B, C) Expanded traces of individual IPSC bursts in A1 (indicated with green and blue shading) showing the fast acceleration in the intra-burst IPSC frequency and resulting depression in the baseline holding current (dashed lines) induced by NE. (D) Histogram of interburst interval showing the distribution of phase durations of NE-induced repetitive IPSC bursts (38 bursts from 16 cells). (E) Mean instantaneous

intra-burst IPSC frequency (+/- SEM) over the course of NE-stimulated accelerating IPSC bursts. (F) Changes in mean IPSC amplitude over time showing the NE-induced plateau increase in sIPSC amplitude was blocked by ω -agatoxin (P/Q blocker), while the peak increase, which corresponds to the NE-induced initial increase in IPSCs shown in (A)2, was unaffected. The ω -agatoxin-insensitive IPSCs were blocked by CB1 receptor activation with WIN 55,212-2, corresponding to the recording in (A)3. (G) Changes in mean IPSC amplitude over time showing that blocking N-type calcium channels and activating CB1 receptors both selectively eliminated the NE-induced initial increase in IPSCs, with little effect on the NE-induced repetitive IPSC bursts, corresponding to the recordings in (A)4 and (A)5. (H) Changes in mean IPSC frequency over time showing that the NE-induced increase in sIPSC frequency was suppressed by blocking P/Q-type calcium channels, and the residual frequency response was not further blocked by CB1 activation. (I) Changes in mean IPSC frequency over time showing that blocking N-type calcium channels with conotoxin and activating CB1 receptors with WIN had little effect on the NE-induced increase in sIPSC frequency, indicating a minor contribution of CCK interneurons to the overall increase in IPSC frequency in response to NE.

To test directly whether NE activates repetitive bursts of action potentials in PV interneurons, extracellular loose-seal recordings of PV interneurons were performed in slices from PV-Cre animals crossed with Ai14 reporter mice, in which the PV interneurons express red fluorescent protein tdTomato. Application of NE induced repetitive bursts of accelerating action potentials in these neurons that recurred at regular intervals of tens of seconds (0.03 ± 0.006 Hz), which were similar to the NE-induced IPSC bursts in the principal neurons (Fig. 9A-C) and to the spike bursts generated in PV neurons by Gq-DREADD activation (see Fig. 6). Overall, these data suggest that the activation of PV interneurons by NE generates repetitive IPSC bursts that are similar to those stimulated by chemogenetic activation of PV interneurons.

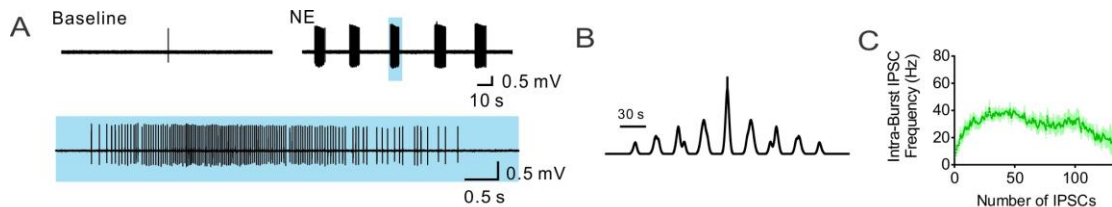


Figure 9. NE induces rhythmic burst firing activity in PV interneurons

(A) Representative loose-seal extracellular recording showing the NE-stimulated repetitive bursts of action potentials in a PV interneuron. A burst of action potentials indicated by the blue box was expanded to show the accelerating intra-burst IPSC frequency. (B) Autocorrelation showing the rhythmicity of NE-induced AP bursts in the PV interneuron shown in (A). (C) Mean instantaneous intra-burst action potential frequency (\pm SEM) over the course of PV action potential bursts induced by NE.

To determine whether the NE-induced IPSC bursts are mediated by activation of a Gq-coupled adrenoceptor, we first tested for the adrenoceptor dependence of the NE-induced increase in IPSCs. Whereas the β adrenoceptor antagonist propranolol (10 μ M) had no effect on the bursts, the NE-induced IPSC bursts were abolished by the broad-spectrum α 1 adrenoceptor antagonist prazosin (10 μ M) (data not shown). The NE-induced increase in IPSCs was also abolished by the α 1A adrenoceptor-selective antagonist WB4101 (1 μ M) and mimicked by the α 1A adrenoceptor-selective agonist A61603 (2 μ M) (Fig. 10A-E). These results suggest an α 1A adrenoceptor dependence of the NE stimulation of inhibitory synaptic inputs to the BLA principal interneurons. Consistent with the α 1A adrenoceptor as a Gq-coupled GPCR, blocking Gq activation with the $G\alpha_{q/11}$ inhibitor YM-254890 eliminated all NE-induced IPSCs (Fig. 10A-E). In addition, blocking spiking activity with TTX also inhibited the NE-induced increase in IPSCs (Fig. 10A-E). Therefore, similar to the chemogenetically-induced phasic IPSC bursts, the NE-induced repetitive IPSC bursts were mediated by Gq activation in presynaptic PV interneurons.

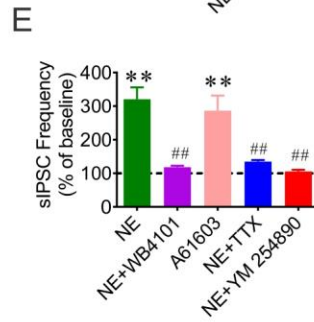
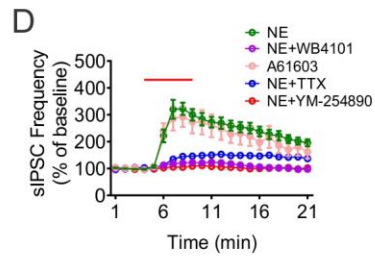
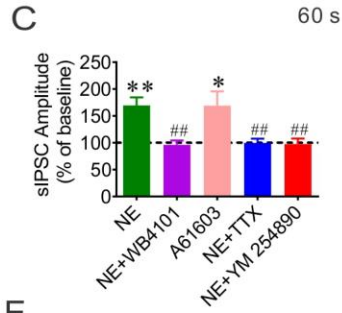
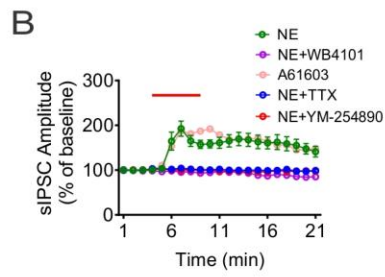
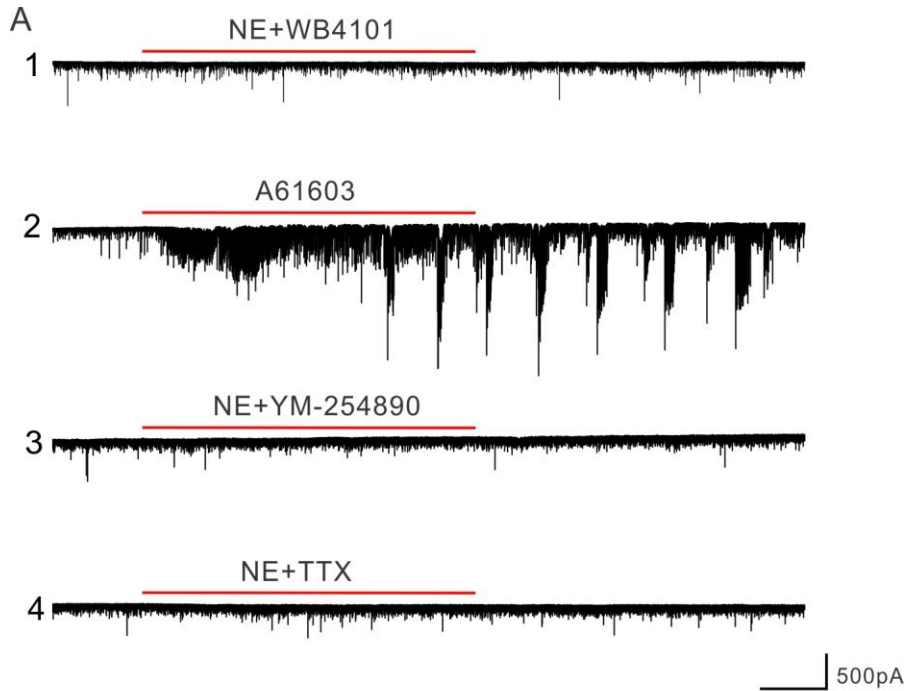


Figure 10. $\alpha 1A$ adrenoreceptor-dependent NE stimulation of IPSC bursts

(A) Representative traces showing NE-induced facilitation of sIPSCs depends on activation of presynaptic interneurons through Gq-coupled $\alpha 1A$ adrenoreceptors. (1) The selective $\alpha 1A$ adrenoreceptor antagonist WB4101 blocked NE-stimulated sIPSCs. (2) The $\alpha 1A$ adrenoreceptor agonist A61603 induced a similar effect as NE, repetitive bursts of IPSCs following the initial increase of IPSCs. (3) Blocking Gq activity with YM-254890 eliminated the NE-induced IPSC increase. (4, Blocking neural activation with TTX prevented the NE facilitation of sIPSCs in BLA principal neurons. (B, C) Mean change in sIPSC amplitude over time in response to NE (16 cells from 5 mice), NE + $\alpha 1A$ receptor antagonist WB4101 (7 cells from 4 mice), NE + $\alpha 1A$ receptor agonist A61603 (10 cells from 4 mice), NE + TTX (10 cells from 5 mice), NE + Gq antagonist YM-254890 (8 cells from 3 mice); Paired *t* test, NE vs. baseline, $p = 0.0003$, A61603 vs. baseline, $p = 0.023$, *, $p < 0.05$, **, $p < 0.01$; One-Way ANOVA, Dunnett's multiple comparisons test, $F(4, 46) = 6.22$, $p = 0.0034$, NE vs. NE + WB4101, $p = 0.0098$, NE vs. A61603, $p > 0.99$, NE vs. NE + TTX, $p = 0.0052$, NE vs. NE + YM-254890, $P = 0.0078$, ##, $p < 0.01$; values at time = 13 min were used to compare ω -agatoxin-sensitive IPSCs. (D, E) Time course and mean change in sIPSC frequency. The NE-induced increase in sIPSC frequency was blocked by the $\alpha 1A$ adrenoceptor antagonist WB4101 and was mimicked by the $\alpha 1A$ adrenoceptor agonist A61603. Blocking either spiking activity with TTX or Gq activation with YM-254890 eliminated NE induced increase in sIPSC frequency. (NE: 16 cells from 5 mice; NE + WB4101: 7 cells from 4 mice; NE + A61603: 10 cells from 4 mice; NE + TTX: 10 cells from 5 mice; NE + YM-254890: 8 cells from 3 mice) (paired *t* test, NE vs. baseline, $p < 0.0001$, A61603 vs. baseline: $p = 0.0027$; one-way ANOVA, $F(6, 70) = 16.34$, $p < 0.0001$, Dunnett's multiple comparisons test, NE vs. NE + WB4101: $p = 0.0003$; NE vs. NE + A61603: $p = 0.81$; NE vs. NE + TTX: $p = 0.0002$; NE vs. NE + YM-254890: $p < 0.0001$). ** $p < 0.01$, ##, $p < 0.01$.

It has been reported that the commercial antibodies against $\alpha 1$ adrenoreceptors are not specific (Jensen et al., 2008). Therefore, to test whether PV interneurons in the BLA express $\alpha 1A$ adrenoreceptors, we took advantage of a global $\alpha 1A$ adrenoreceptor knockout mouse line (*adra1A* KO) to look at the distribution of the receptor indirectly. In this model, a *lacZ* gene cassette is placed in frame with the first exon of the *adra1A* gene, which allows the visualization of $\alpha 1A$ adrenoreceptor expression by histochemical staining for β -galactosidase activity with X-gal (Rokosh & Simpson, 2002). We found the *adra1A* gene to be expressed at high levels in the cortex, hippocampus, amygdala, and hypothalamus (Fig. 11A). In the BLA, we observed a sparse distribution of X-gal-stained cells, which was suggestive of labeled interneurons. To test for the inhibitory interneuron identity of the X-gal-stained cells, the *adra1A* KO mouse was crossed with a *GAD67-eGFP* mouse line, in which all inhibitory interneurons in the BLA express GFP (Tamamaki et al., 2003), and we performed confocal imaging analysis of X-gal and GFP co-staining (Levitsky et al., 2013). In order to combine the β -galactosidase histochemistry with confocal fluorescence imaging without occlusion of the GFP signal, we performed repeated confocal imaging at the same location to track GFP-positive cells before and after the X-gal staining. The sparsely distributed X-gal-labeled cells showed a 98.37% overlap with GFP-labeled GABAergic cells (Fig. 11B, C). We next injected a Cre-dependent AAV virus expressing mCherry into the BLA of PV-Cre mice crossed with the *adra1A* KO mouse (*PV-Cre::adra1A* KO) and examined the ratio of co-labeled PV interneurons and X-gal-labeled neurons. Two weeks after virus injection, we observed most of the labeled PV interneurons to be positive for X-gal (84.7%) (Fig. 11D, E).

Together, these data demonstrated that the $\alpha 1A$ adrenoreceptors are selectively expressed in BLA interneurons, including in most of the PV interneurons.

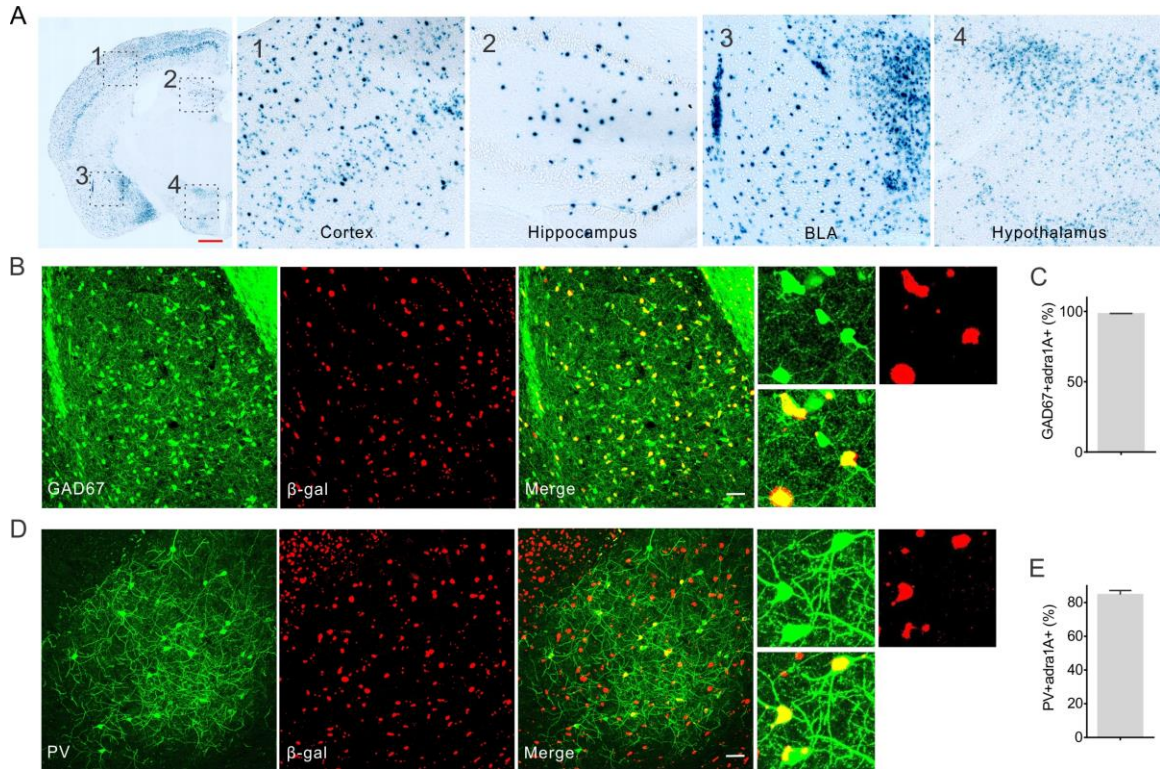


Figure 11. Expression of $\alpha 1A$ adrenoreceptors in BLA PV interneurons

(A) Staining of β -galactosidase showing the expression of $\alpha 1A$ adrenoreceptors in *adra1A* KO mice. (1-4) High-magnification images of areas indicated by dashed boxes showing the cortex (1), the hippocampus (2), the basolateral amygdala (3), and the hypothalamus (4). Scale bar, 500 μ m. (B) Colocalization of the β -gal signal with GFP expression in GABA interneurons in the BLA. Scale bar, 50 μ m. (C) Percentage of total GAD67-positive cells in the BLA that were positive for β -gal ($98.4 \pm 0.18\%$, $N=302$ cells, 3 sections from 2 animals). (D) Colocalization of the β -gal signal with GFP expression in PV interneurons labelled by injection of Cre-dependent virus in PV-Cre mice. Scale bar, 50 μ m. (E) Percentage of GFP-labelled PV interneurons that were positive for β -gal ($84.7 \pm 2.46\%$, $N= 134$ cells, 6 sections from 2 animals).

Multiple neurotransmitter receptors couple to $G_{\alpha_{q/11}}$ to enhance neuronal excitability, suggesting that other neuromodulators may also induce similar phasic IPSC bursts when acting on PV interneurons. Thus, we tested the effect of serotonin, another neuromodulator that has been shown to regulate BLA neural circuit activity via the Gq-coupled 5-HT_{2A} receptor (Jiang et al., 2009), on IPSC bursts in the BLA principal neurons. With the blockade of glutamatergic and CCK basket cell-mediated transmission with DNQX (20 μ M), APV (40 μ M), and the CB1 receptor agonist WIN 55,212-2 (1 μ M), we found that serotonin (100 μ M) also induced repetitive bursts of IPSCs that were blocked by the P/Q calcium channel blocker, ω -agatoxin (0.5 μ M), and by MDL 100907 (1 μ M), an antagonist of the 5HT_{2A} receptor (Fig. 12A-E). These data suggested, therefore, that serotonin also stimulates a phasic synaptic output from PV interneurons and suggest that Gq activation in PV interneurons can serve as a general cellular mechanism for different neuromodulators to regulate BLA neural circuits under different emotional states.

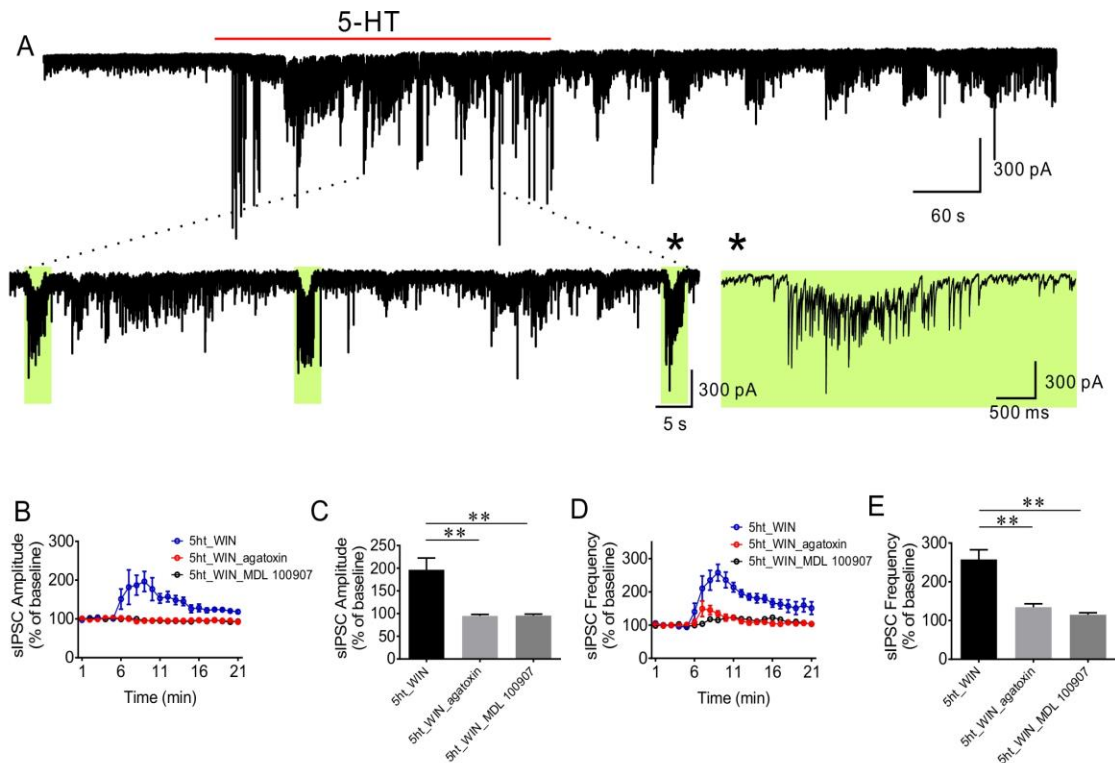


Figure 12. Serotonin 5-HT_{2A} receptor activation of IPSC bursts

(A) A representative recording of serotonin (5-HT, 100 μ M)-induced repetitive IPSC bursts in a BLA principal neuron in the presence of glutamate receptor antagonists, DNQX and AP5, and CB1 receptor agonist WIN 55,212-2. Green boxes show three repetitions of 5-HT-induced bursts. The last repetition was expanded to show the accelerating frequency of intra-burst IPSCs and the negative shift in the baseline due to the progressive summation of high-frequency IPSCs. (B, C) Mean change in sIPSC amplitude over time (B) and after 3-5 min (C) of bath application of 5-HT. The 5-HT-induced IPSC bursts were blocked by ω -agatoxin and the Gq-coupled 5HT_{2A} receptor antagonist MDL 100907 (1 μ M) (5-HT+WIN: 5 cells from 3 mice; 5-HT + WIN + Agatoxin: 5 cells from 3 animals; 5-HT + WIN + MDL 100907: 5 cells from 2 mice; one-way ANOVA, $F(2, 12) = 14.77$, $p = 0.0006$, Dunnett's multiple comparisons test, 5-HT+WIN vs. 5-HT + WIN + Agatoxin: $p = 0.0009$; 5-HT+WIN vs. 5-HT + WIN + MDL 100907: $p = 0.001$). (D, E) Mean change in sIPSC frequency (D) and after 3-5 min (E) in 5-HT. (One-Way ANOVA, $F(2, 12) = 24.86$, $p < 0.0001$, Dunnett's multiple comparisons test, 5-HT+WIN vs. 5-HT + WIN + Agatoxin: $p = 0.0002$; 5-HT+WIN vs. 5-HT + WIN + MDL 100907: $p < 0.0001$). ** $p < 0.01$.

3.4.3 Gq activation of PV cells alters the firing pattern of PV interneurons and principal neurons

PV interneurons are critically involved in the generation of gamma oscillations by firing tonic action potentials, which are precisely phase-locked to the gamma oscillatory cycle (Bartos et al., 2007; Hájos et al., 2004). As Gq activation of PV interneurons generated phasic action potentials with a rapidly accelerating intra-burst frequency, we tested whether the burst firing pattern interferes with tonic activity in PV cells and if so, whether Gq signaling in the PV cells modulates gamma oscillation in the BLA. To address this, we performed extracellular recordings in the loose-seal patch clamp configuration in PV interneurons after injection of the Cre-dependent Gq-DREADD-expressing AAV in the BLA of PV-Cre animals. To increase the probability of recording spontaneous firing activity in the PV interneurons, the extracellular potassium concentration was increased from 2.5 mM to 7.5 mM. Strikingly, in all the PV interneurons that displayed spontaneous tonic firing (n=7, range: 9.7 to 32.2 Hz, mean: 18.56 ± 3.4 Hz), instead of superimposing on the baseline tonic spiking activity, the action potential bursts induced by CNO dominated and transformed the tonic firing pattern of PV cells into a phasic pattern (Fig. 13A, B), suggesting that Gq activation in the PV interneurons switches the operational mode of the PV cells from tonic to phasic.

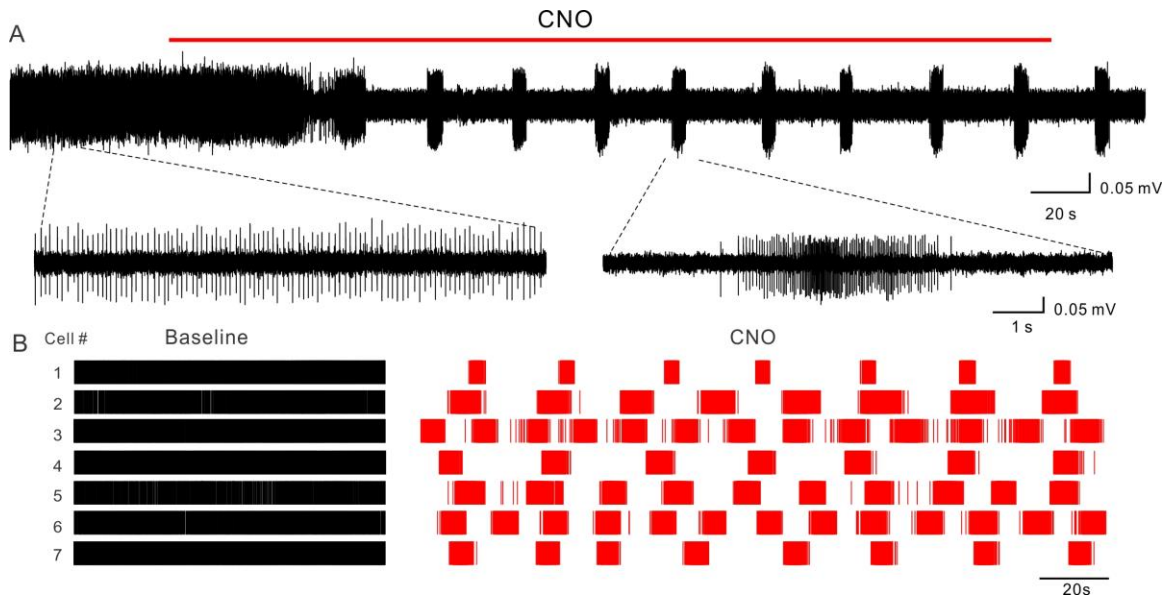


Figure 13. *Gq* activation switches the firing pattern of PV interneurons from tonic to phasic

(A) A representative recording showing that chemogenetic activation of PV interneurons switches the firing pattern of PV cells from tonic to phasic. Below: Traces were expanded to show the tonic firing in the baseline and burst firing after CNO application. (B) Raster plots of spiking activity in recordings from 7 PV interneurons that show the transformation of tonic spiking to phasic spiking by CNO.

To explore the effect of PV-mediated phasic IPSC bursts on the firing pattern of BLA principal neurons, we chemogenetically activated the PV interneurons with the Gq-DREADD and recorded from BLA principal neurons in brain slices in the whole-cell current-clamp recording configuration. The membrane potential of the principal cells was held above threshold with positive current injection to elicit tonic action potential firing at a frequency of 2-5 Hz, which is the range of spontaneous spiking activity observed *in vivo* (Herry et al., 2008; Woodruff & Sah, 2007a). Consistent with the shift in the baseline holding current caused by the summation of accelerating IPSCs within the bursts, activation of repetitive IPSC bursts with CNO application induced prominent oscillatory hyperpolarizations of the membrane potential that dramatically shifted the firing pattern of the principal cells from tonic to phasic, characterized by slowly oscillating spike bursts at $0.035 \pm 0.006\text{Hz}$ (Fig. 14A, B). Together, these data reveal a novel regulatory role of fast spiking interneurons in controlling the BLA neural output pattern in response to Gq activation.

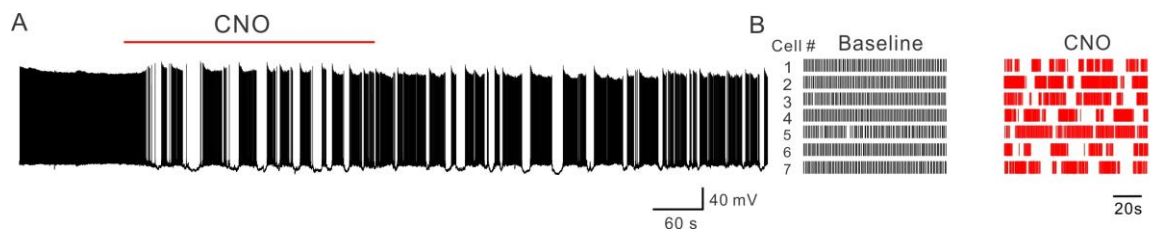


Figure 14. Gq activation of PV interneurons transforms the activity of BLA principal neurons

(A) A representative current clamp recording from a principal neuron showing that Gq-activation in PV cells transforms the firing pattern of a BLA principal neuron from tonic to phasic. (B) Raster plots of spiking activity in recordings from 7 principal neurons that show the transformation of tonic spiking to phasic spiking by CNO.

3.4.4 Gq activation in BLA PV neurons promotes state switches in amygdalo-frontal networks *in vivo*

As Gq-induced burst firing activity interferes with the tonic firing in the PV cells that is critical for the generation of gamma oscillations, we next tested the effect of Gq activation of PV interneurons on neural network oscillations *in vivo*. PV-Cre animals virally transduced to express hM3D in BLA PV interneurons were implanted with paired LFP recording electrodes in the BLA and ipsilateral frontal cortical (FrC) electroencephalogram (EEG) recording screws to monitor mesoscale network activity changes (Fig. 15A, C).¹ Activation of hM3D in BLA PV interneurons with intraperitoneal (I.P.) injection of 5 mg/kg (1 mg/ml) CNO (Fig. 15B) significantly desynchronized gamma-frequency oscillations (separated into 30-70 Hz “slow” and 70-120 Hz “fast” gamma oscillations) in the BLA compared to I.P. saline injection (Fig. 15E-H). CNO administration also resulted in PFC gamma desynchrony in the frontal EEG recording similar to that in the BLA (Fig. 15E-H), which suggested a potential role for BLA PV Gq signaling in desynchronizing amygdalo-frontal networks. Interestingly, similar fast gamma suppression among amygdalo-frontal networks has been reported during conditioned fear expression (Stujenske et al., 2014), suggesting a possible BLA PV-Gq-mediated neuromodulatory control of fear memory formation.

¹ *The extracellular local field potential and EEG recordings in vivo were done in collaboration with Eric Teboul and Jamie Maguire at Tufts University.*

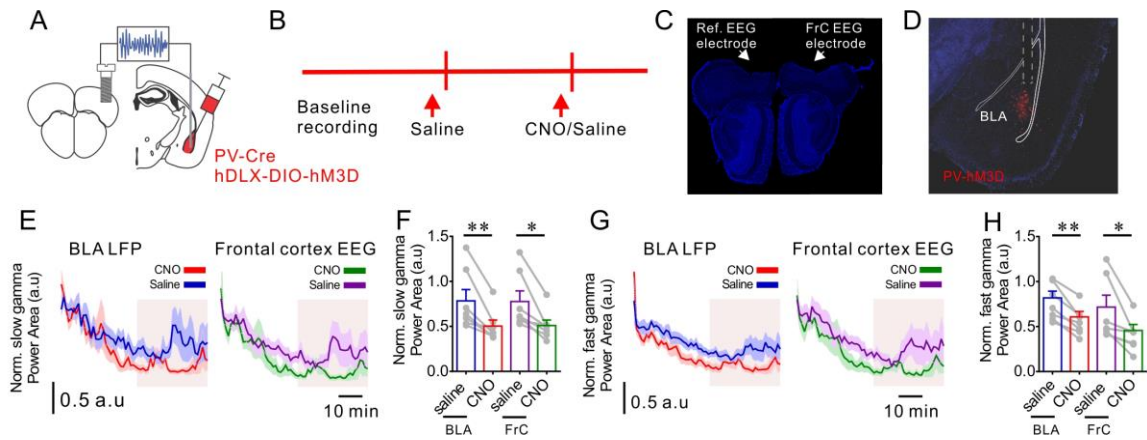


Figure 15. *Gq* signaling in BLA PV interneurons desynchronizes gamma oscillations in amygalo-frontal circuits in vivo.

(A) Schematic illustrating combined *in vivo* EEG recording in the frontal cortex and LFP recording in the BLA, as well as hM3D-expressing virus injection in the BLA of PV-Cre mice. (B) Experimental timeline for EEG and LFP recording of baseline activity and after I.P. injection of saline followed by saline or CNO followed by saline (counterbalanced). (C) Representative image showing the placement of the reference and EEG recording screws on the frontal cortex (marked by the arrows). (D) Representative image showing the LFP recording electrode placement and hM3D distribution in the BLA. (E) Normalized slow gamma power (to baseline) over time in the BLA and the frontal cortex (FrC). (F) Mean (+/- SEM) normalized BLA and FrC slow gamma power for respective analysis windows shown in (E). Paired *t* test, Saline vs CNO, $p = 0.0086$ (BLA), $p = 0.014$ (FrC), *, $p < 0.05$, **, $p < 0.01$. (G) Normalized fast gamma power (to baseline) over time in the BLA and the frontal cortex. (H) Mean (+/- SEM) normalized BLA and FrC fast gamma power for respective analysis windows shown in (G). Paired *t* test, Saline vs CNO, $p = 0.0019$ (BLA), $p = 0.027$ (FrC). Values normalized to baseline. *, $p < 0.05$, **, $p < 0.01$. au = arbitrary units.

We next tested whether BLA α 1A adrenoceptor activation similarly modulates amygdalo-frontal network state transitions by injecting wild-type mice intra-BLA with adrenoceptor analogs and performing paired local field potential recordings in the BLA and ipsilateral frontal EEG recordings (Fig. 16A).¹ Consistent with the effect of chemogenetic activation of PV interneurons on BLA-PFC gamma oscillations, intra-BLA infusion of 9.88 mM NE (0.2 μ L) reduced the power of slow and fast gamma oscillations in both the BLA and frontal EEG recordings (Fig. 16B-I), and this effect was abolished by intra-BLA pretreatment with the α 1A-selective adrenoceptor antagonist WB4101 (10 μ M; 0.2 μ L) (Fig. 16B-I). These data indicate that, like hM3D activation of PV interneurons, α 1A adrenoceptor-dependent noradrenergic signaling in BLA also desynchronizes gamma oscillations in amygdalo-frontal networks.

¹ *The extracellular local field potential and EEG recordings in vivo were done in collaboration with Eric Teboul and Jamie Maguire at Tufts University.*

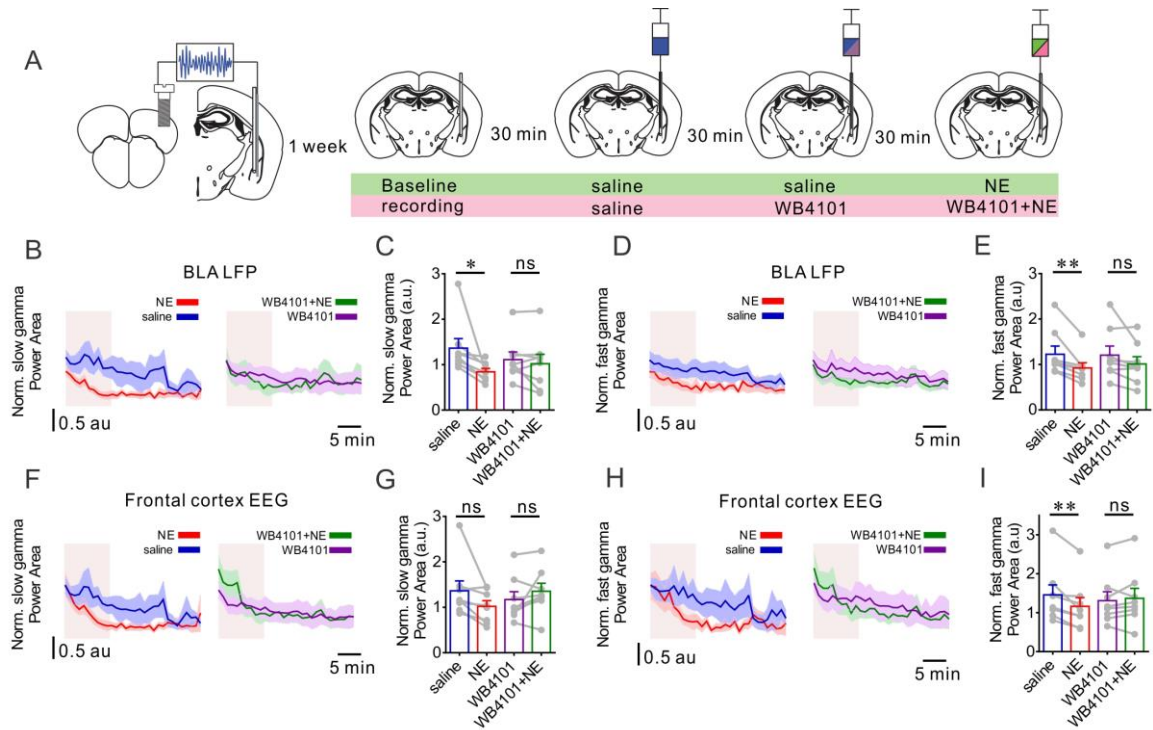


Figure 16. Noradrenergic activation of BLA Gq signaling desynchronizes gamma oscillations in amygdalo-frontal circuits *in vivo*.

(A) Schematic illustrating experimental paradigm combining *in vivo* BLA LFP recording, frontal cortex (FrC) EEG recording, and intra-BLA adrenoceptor agonist/antagonist or vehicle microinfusion. After baseline recording for 30 min, saline was administered twice in the BLA to control for the effect of infusion on LFP. The same three-infusion design is maintained in the $\alpha 1A$ antagonist group. (B) Normalized BLA slow gamma power over time from experiments with intra-BLA infusion of NE and NE + $\alpha 1A$ antagonist WB4101. (C) Mean (+/- SEM) normalized BLA slow gamma power for respective analysis windows in the shaded area shown in (B). Paired *t* test, NE vs. saline, $p = 0.039$, WB4101 + NE vs. WB4101, $p = 0.35$, * $p < 0.05$, ns, not significant. (D) Normalized BLA fast gamma power over time from experiments with intra-BLA infusion of NE and NE + $\alpha 1A$ antagonist WB4101. (E) Mean (+/- SEM) normalized BLA fast gamma power for respective analysis windows in the shaded area shown in (D). Paired *t* test, NE vs. saline, $p = 0.0099$, WB4101 + NE vs. WB4101, $p = 0.099$, ** $p < 0.01$, ns, not significant. (F) Normalized FrC slow gamma power over time from experiments with

*intra-BLA infusion of NE and NE + α 1A antagonist WB4101. (G) Mean (+/- SEM) normalized FrC slow gamma power for respective analysis windows in the shaded area shown in (F). Paired t test, NE vs. saline, $p = 0.067$, WB4101 + NE vs. WB4101, $p = 0.19$, ns, not significant. (H) Normalized FrC fast gamma power over time from experiments with intra-BLA infusion of NE and NE + α 1A antagonist WB4101. (I) Mean (+/- SEM) normalized FrC fast gamma power for respective analysis windows in the shaded area shown in (H). Paired t test, NE vs. saline, $p = 0.0061$, WB4101 + NE vs. WB4101, $p = 0.42$, ** $p < 0.01$, ns, not significant.*

3.4.5 α 1A noradrenergic Gq activation of PV interneurons enhances fear memory formation

A decrease in gamma oscillations in the BLA has been associated with a conditioned fear state (Stujenske et al., 2014). As the NE level in the BLA is significantly elevated during stressful conditions (McIntyre et al., 2002) and we found that α 1A noradrenergic activation of PV interneurons induced a reduction in gamma oscillations in the BLA, we next examined whether PV-mediated gamma suppression by α 1A adrenoreceptor activation promotes fear memory formation with selective re-expression of α 1A receptors bilaterally in PV neurons of the BLA of global *adra1A* knockout mice. In the absence of a floxed α 1A adrenoreceptor-expressing animal model, this allowed us to isolate the α 1A noradrenergic signaling to the BLA PV interneurons.

We first tested the effects of α 1A adrenoreceptor global deletion and re-expression in the BLA on the NE-induced IPSC bursts using whole-cell recordings in brain slices. In slices from *adra1A* KO mice, NE and the selective α 1A adrenoreceptor agonist A61603 failed to induce the IPSC bursts seen in principal cells from wild-type mice (Fig. 17A-C), confirming the specific α 1A adrenoreceptor dependence of the NE-induced IPSC burst generation. To selectively re-express α 1A adrenoreceptors in PV interneurons in the BLA, a Cre-dependent AAV virus expressing α 1A-mCherry (AAVdj-hDLX-DIO- α 1A-mCherry) was injected bilaterally into the BLA of PV-Cre::*adra1A* KO mice (Fig. 17A). Activation of α 1A adrenoreceptors specifically re-expressed in PV interneurons from *adra1A* KO mice rescued the NE-induced phasic IPSC bursts, which displayed an accelerating intra-burst IPSC frequency and recurred at a slow frequency (0.032 ± 0.002 Hz) (Fig. 17A-E).

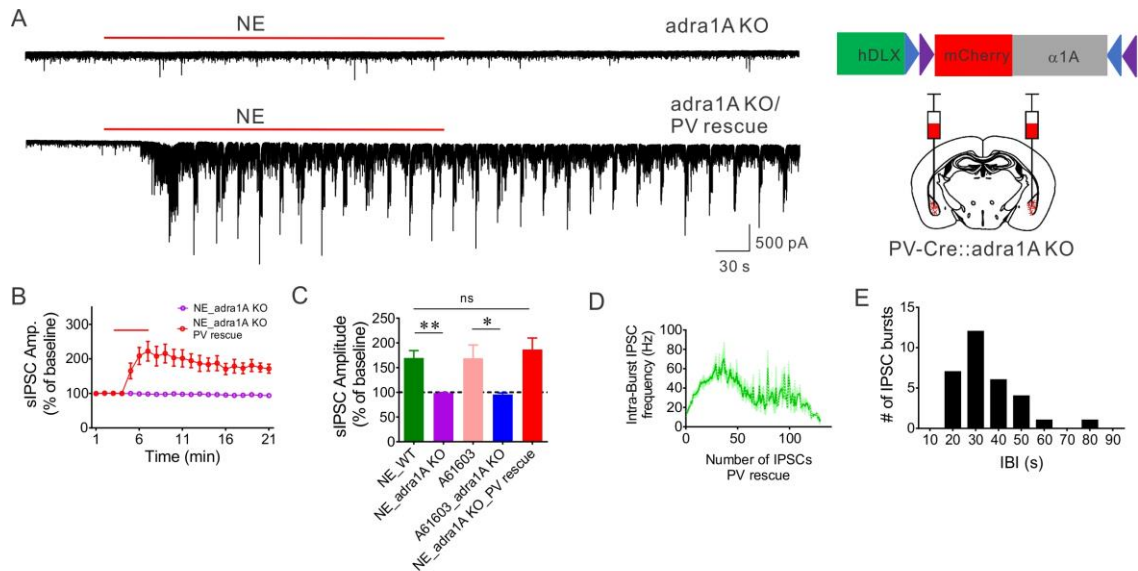


Figure 17. Rescue of Gq signaling in PV interneurons in global *adra1A* KO mice

(A) Representative traces showing that the NE-induced increase in IPSCs is lost in the *adra1A* KO mouse and replacement of the $\alpha 1A$ adrenoceptors in the PV interneurons with AAV viral injection in the BLA (shown on the right) rescued the NE-induced repetitive IPSC bursts. (B) Time course of NE effect on sIPSC amplitude in *adra1A* KO mice with or without virally-mediated re-expression of $\alpha 1A$ adrenoceptors in PV interneurons. (C) Mean change in sIPSC amplitude in BLA principal neurons in response to NE or the $\alpha 1A$ agonist A61603 in slices from wild type (WT) and *adra1A* KO mice. (NE_WT: 16 cells from 5 mice; NE_*adra1A* KO: 9 cells from 4 mice; A61603_WT: 10 cells from 4 mice; A61603_*adra1A* KO: 7 cells from 3 mice; NE_*adra1A* KO_PV rescue: $n = 7$ cells from 3 mice) (Unpaired t test, A61603_WT vs. A61603_*adra1A* KO: $p = 0.039$). * $p < 0.05$; One-Way ANOVA, $F(2, 27) = 7.43$, $p = 0.0025$, Dunnett's multiple comparisons test, NE_WT vs. NE_*adra1A* KO: $p = 0.0046$, NE_WT vs. NE_*adra1A* KO_PV rescue: $p = 0.68$, ** $p < 0.01$. (D) Mean instantaneous intra-burst IPSC frequency (\pm SEM) over the course of the burst. (E) A histogram showing the distribution of the phase duration of NE-induced repetitive IPSC bursts following $\alpha 1A$ adrenoceptor rescue in slices from *adra1A* KO mice.

Having validated the effectiveness of the virus-based rescue of NE-induced repetitive bursts of inhibitory synaptic inputs to the BLA principal cells, we next investigated the role of α 1A noradrenergic engagement of PV cells in the modulation of fear memory formation. Three weeks after α 1A adrenoreceptor re-expression in the BLA with bilateral injection of AAVdj-hDlx-DIO- α 1A-mCherry into the BLA of PV-Cre::adra1A KO mice (Fig. 18A), the mice were subjected to a standard auditory-cued fear conditioning paradigm (Fig. 18B). While we did not observe a significant difference in fear acquisition on day 1 of the fear conditioning, selective rescue of the α 1A noradrenergic signaling bilaterally in the BLA PV interneurons of adra1A KO mice resulted in enhanced fear memory retrieval on day 2 compared with the adra1A KO mice expressing bilateral mCherry alone (Fig. 18C).

Since activation of the Gq-DREADD induced the same IPSC bursting pattern as NE in brain slices, we next tested the effects of Gq-DREADD activation specifically in the PV basket cells on fear memory formation in the α 1A knockout animals. The designer drug CNO (5 mg/kg) was administered I.P. 30 min prior to the beginning of the fear acquisition on day one and again 30 min prior to the beginning of the fear retrieval test on day two (Fig. 18B). Similar to the effects of α 1A adrenoreceptor re-expression on fear memory formation, chemogenetic activation of PV interneurons did not have a significant effect on fear acquisition on day 1, but significantly enhanced fear memory recall on day 2 (Fig. 18D). Therefore, α 1A adrenoreceptor and hM3D activation of Gq-signaling in BLA PV interneurons, which facilitates the generation of repetitive IPSC bursts and decreases gamma oscillations in the BLA and in the amygdalo-frontal network, positively regulates fear memory formation.

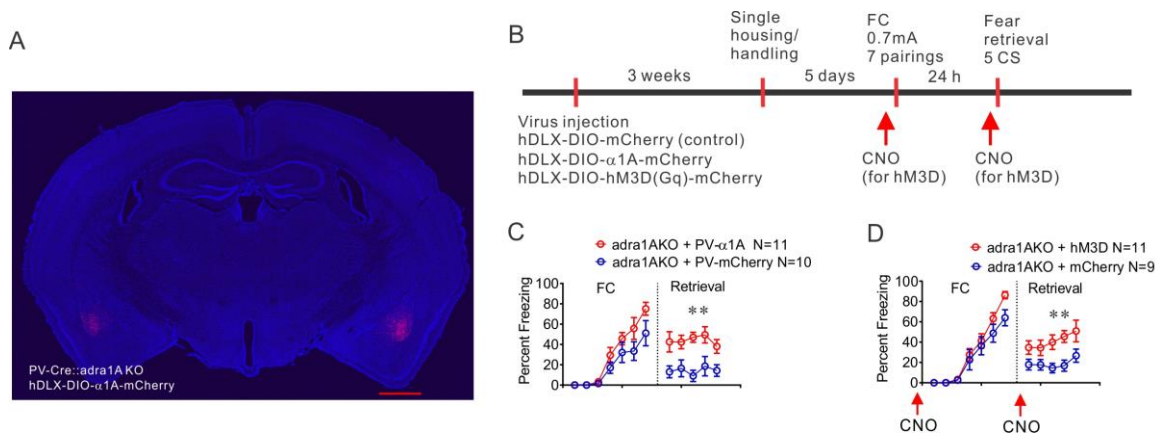


Figure 18. Rescue of Gq signaling in PV interneurons in global adra1A KO mice facilitates the formation of fear memory

(A) Representative image showing expression of α 1A-mCherry fusion protein after bilateral injections of conditional AAV virus in the BLA of PV-Cre::*adra1A* KO mice. Scale bar, 1 mm. (B) Experimental timeline for virus injection and fear conditioning. PV-Cre::*adra1A* KO mice were injected with conditional AAVs expressing Cre-dependent α 1A-mCherry or Gq-DREADD to rescue α 1A adrenoreceptor mediated Gq signaling in BLA PV interneurons. Control PV-Cre::*adra1A* KO mice were injected with conditional AAVs expressing only mCherry. For Gq-DREADD rescue experiments, CNO (5 mg/kg) was administered I.P. 30 min prior to commencement of the fear acquisition and again 30 min prior to commencement of the fear retrieval (red arrows) in both Gq-DREADD and mCherry groups. (C) Replacement of α 1A adrenoreceptors in BLA PV interneurons did not significantly affect the acquisition (Repeated measures Two-Way ANOVA, $F(1, 19) = 3.49$, $p = 0.078$), but facilitated the retrieval of the fear memory (Repeated measures Two-Way ANOVA, $F(1, 19) = 18.47$, $p = 0.0004$). ** $p < 0.01$ compared to control virus-injected PV-Cre::*adra1A* KO group. (D) Rescue of Gq signaling in BLA PV interneurons in *adra1A* KO mice with excitatory DREADD had no significant effect on the fear memory acquisition (Repeated measures Two-Way ANOVA, $F(1, 18) = 2.15$, $p = 0.16$), but enhanced the fear memory retrieval (Repeated measures Two-Way ANOVA, $F(1, 18) = 11.17$, $p = 0.0036$). ** $p < 0.01$ compared to control virus injected PV-Cre::*adra1A* KO group.

3.5 Discussion

Our data revealed a novel cellular mechanism of switching the oscillatory states of the BLA by neuromodulation-dependent burst firing in PV fast spiking interneurons. Upon activation of the Gq-coupled designer receptor hM3D, PV cells generated phasic action potentials to drive synchronized repetitive bursts of inhibitory synaptic inputs to BLA principal neurons. This same Gq-dependent induction of burst firing in PV cells was also found in response to activation of α 1A adrenoreceptors, which are selectively expressed in BLA interneurons, including most of the PV neurons. Furthermore, we showed that activation of Gq signaling through either hM3D or α 1A adrenoreceptors in PV interneurons suppressed *in vivo* gamma oscillations in the BLA, which have been associated with inhibition of fear memory recall. Consistent with this, we found that α 1A noradrenergic signaling specifically in the BLA PV interneurons with re-expression of α 1A adrenoreceptors in the *adra1A* knockout mouse and Gq-DREADD activation in the PV interneurons facilitated the retrieval of conditioned fear (Summarized in Fig. 19).

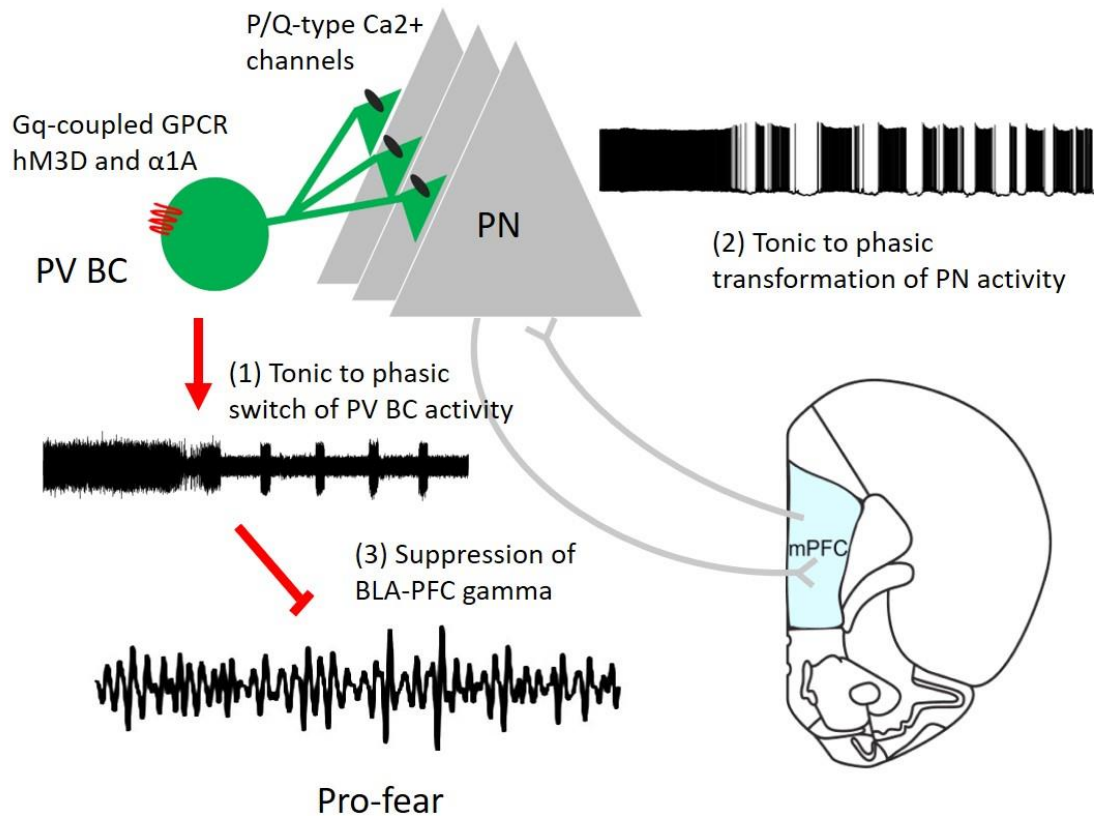


Figure 19. Summary diagram of facilitation of fear expression by PV-Gq modulation of BLA-PFC gamma oscillation

Activation of Gq coupled hM3D and $\alpha 1A$ adrenoreceptors stimulates a repetitive bursting pattern in the PV interneurons, which switches the firing pattern of PV interneurons from tonic into phasic (1). The phasic activity in PV neurons drives repetitive IPSC bursts to the BLA principal neurons, which transforms the activity of principal neurons from tonic to phasic (2), resulting in a suppression of gamma oscillation between BLA and prefrontal cortex through their reciprocal connections (3). In line with a role of desynchronization of BLA-PFC gamma oscillation in promoting the emotional state of fear (Bocchio & Capogna, 2014; Stujenske et al., 2014), Gq activation of PV interneurons via hM3D and $\alpha 1A$ adrenoreceptors facilitates the expression of conditioned fear memory.

In contrast to the canonical electrophysiological property of PV interneurons to fire sustained high-frequency action potentials upon depolarization, we observed these cells to generate bursts of accelerating action potentials in response to Gq activation. In addition to Gq chemogenetic activation with hM3D, we further showed the Gq dependence of this phasic activity with the selective Gq inhibitor YM-254890, which fully eliminated the CNO- and NE-stimulated bursts of IPSCs in the BLA principal neurons. Although the occurrence of repetitive IPSC bursts during continuous perfusion of CNO and NE suggested that inhibitory synaptic connections between PV cells may play a role in the pattern generation, since the PV cells were presumably tonically depolarized in the continuous presence of the agonists, however, the bursts were not suppressed by blocking GABA_A receptors with picrotoxin (in the continuous presence of glutamate receptor blockers) and similar phasic IPSC bursts were not induced with sustained photostimulation of the PV neurons. Thus, our data reveal an important role of Gq neuromodulation in changing the operational mode of PV neurons and indicate that Gq signaling is capable of activating alternating excitation and inhibition cycles in the PV cells non-synaptically via an intrinsic bursting mechanism. It will be of interest with future experiments to dissociate the interacting signaling pathways that give rise to this Gq-induced oscillatory firing pattern in the PV cells.

Parvalbumin interneurons are critically involved in the generation of field gamma oscillations in the cortex, hippocampus, and the BLA (Bartos et al., 2007; Buzsáki et al., 2012; Cardin et al., 2009; Sohal et al., 2009). These cells are reliably recruited by robust glutamatergic synaptic inputs and fire tonic single action potentials that are phase-locked to the field gamma cycles. Our results show that activation of Gq signaling transforms the

tonic firing of the PV cells into burst firing. As would be predicted from changing the tonic pattern important for gamma generation, we found that Gq activation of PV cells *in vivo*, through either chemogenetic manipulation or $\alpha 1A$ adrenoreceptor activation, decreased the power of gamma oscillation in the BLA. Since emotional arousal triggers NE release in the BLA, our results provide a cellular mechanism for the modulation of emotional processing during changes in brain state.

The PV interneurons are basket cells in the BLA that selectively target the perisomatic region of hundreds of principal neurons to control BLA output. Paired recordings from neighboring principal neurons (<40 μm) revealed that a large percentage of the PV-mediated bursts of IPSCs are synchronized. In addition, we showed that the PV-mediated IPSC bursts transformed the firing pattern of the principal neurons from tonic to phasic. Given the long phase interval (20-60 s) of these synchronized IPSC bursts in the principal neurons, we expected to see a slow oscillation in the BLA, falling in the infra-slow oscillation bandwidth, after activation of Gq signaling with NE or CNO. However, we did not see a significant change in slow oscillations (0.01-0.1Hz) in the BLA with *in vivo* field potential recordings. This could be due to the lack of a laminar organization in the BLA and difficulties distinguishing slow oscillations from background drift and noise. It will be interesting in the future to test for changes in infra-slow oscillations with Gq activation of PV interneurons in more regularly organized cortical areas such as the hippocampus and neocortex.

What is the role of decreased gamma oscillations in the BLA induced by Gq activation, in particular by $\alpha 1A$ adrenoreceptors, in PV interneurons in fear processing, when there is a surge of NE? With genetic re-expression of $\alpha 1A$ adrenoreceptors in PV

interneurons bilaterally in the BLA of *α1A* global knockout mice, we looked at the specific contribution of $\alpha 1A$ receptor signaling in the PV interneurons during fear conditioning and found that $\alpha 1A$ noradrenergic activation of the PV cells significantly enhanced the retrieval of fear memory. Moreover, animals with restoration of PV-mediated bursts of IPSCs via Gq-coupled DREADD activation showed similar enhancement of fear recall compared to controls. Thus, the patterned output from BLA PV cells by Gq activation is important in promoting the fear state of the BLA. Interestingly, the power of gamma oscillation, in particular the high band gamma (70-120 Hz), has been found to serve as an index for the fear and safety state of the BLA (Stujenske et al., 2014). Stujenske et al. (2014) demonstrated that whereas safety conditions promoted an increase in BLA high gamma, conditioned fear enhanced local theta and gamma coupling and reduced high gamma power in the BLA (Stujenske et al., 2014). In line with this observation, our results support a link between a decreased BLA gamma oscillation and increased fear retrieval that are both mediated by Gq activation in PV cells, and underscore the important role of Gq neuromodulation of PV cells in switching the oscillatory state of the BLA to regulate the emotional state of the animal.

The $\alpha 1$ adrenergic signaling in the BLA has attracted a lot of interest recently due to the promise of prazosin for the treat of some symptoms of PTSD (Giustino & Maren, 2018; Hendrickson & Raskind, 2016; Singh et al., 2016). One important corollary of our findings is the $\alpha 1A$ subtype-specific noradrenergic modulation of BLA PV interneurons. Consistent with a previous study in juvenile rats showing $\alpha 1A$ -dependent noradrenergic facilitation of GABA release in the BLA (Braga et al., 2004), our findings with pharmacological and genetic manipulation of $\alpha 1$ adrenoreceptors demonstrate that the

NE-induced facilitation of inhibitory synaptic inputs to the BLA principal cells is mediated by selective activation of $\alpha 1A$ adrenoreceptors in local presynaptic interneurons. Moreover, we observed the distribution of $\alpha 1A$ adrenoreceptors is restricted to GAD67-eGFP positive interneurons, including most of the PV interneurons. We also found evidence for $\alpha 1$ adrenoreceptor expression in the BLA principal cells, albeit not the $\alpha 1A$ subtype of receptors (data not shown), which would also be blocked with systemic antagonist administration. Therefore, our findings in PV neurons provides valuable histological data for the understanding of $\alpha 1$ noradrenergic signaling in the BLA, which may help in the development of cell type- and receptor subtype-specific therapeutics for the treatment of pathologies of excitation-inhibition balance, including anxiety disorders, autism spectrum disorders, and epilepsy.

Despite thousands of genes in the mammalian genome that encode G protein-coupled receptors, there are only four main classes of G proteins that transduce and converge extracellular stimuli onto downstream signaling cascades (Pierce et al., 2002). Thus, different neuromodulators acting on their cognate Gq-coupled receptors can have a similar influence on neuronal activity through activation of the same signaling pathway. Similar to the Gq chemogenetic activation of PV interneurons, we showed that activation of Gq-coupled $\alpha 1A$ adrenoreceptors and 5-HT_{2A} serotonergic receptors also generated repetitive bursts of IPSCs in the BLA principal neurons. Interestingly, acetylcholine also drives repetitive IPSC bursts in pyramidal neurons of the frontal cortex, possibly through Gq-coupled M1 muscarinic receptors (Kondo & Kawaguchi, 2001), although whether this response is also mediated by PV interneuron activation is not known. Notably, PV interneurons are also activated by neuropeptides like CCK through G protein-coupled

CCK_B receptors both in the hippocampus and BLA (Chung & Moore, 2007; Chung & Moore, 2009; Földy et al., 2007; Lee et al., 2011), and the IPSCs induced by CCK_B activation of PV interneurons appear to be tonic. Although the CCK_B receptors are classically coupled to Gq signaling pathways, however, it has been shown at least in hippocampal PV cells, CCK_B receptor induced excitation is mediated through a Gi/o-coupled signaling pathway involving the mobilization of internal calcium stores and opening of transient receptor potential (TRP) channels (Lee et al., 2011). Thus, neuromodulatory excitation of PV interneurons via different G protein mechanisms may induce distinct output patterns. This implies that the patterned bursts of IPSCs may serve as a fundamental functional output of PV interneurons following activation of Gq-coupled receptors by different neuromodulators.

In conclusion, our findings provide a cellular mechanism for the switch in the oscillatory state of the BLA that controls fear expression via neuromodulation of inhibitory neural circuits. Thus, during emotional arousal, PV fast spiking interneurons transition to a bursting pattern of activity with Gq activation, which dampens gamma oscillations in the BLA and facilitates fear memory formation. Interestingly, chemogenetics proved to be an invaluable approach in our study to examine the endogenous cell type-specific regulation of neural network activity and behavioral states, since the cellular, network, and behavioral effects of PV interneuron stimulation were dependent specifically on Gq activation, and not on, for example, simple excitation of the PV cells (e.g., by optogenetic stimulation).

4. Chapter 4: Neuromodulatory activation of CCK interneurons in the BLA stimulates patterned perisomatic inhibition to restrain fear learning

4.1 Abstract

Norepinephrine release in the basolateral amygdala (BLA) during emotional arousal plays essential roles in the processing of fear. However, the cell type-specific noradrenergic modulation of the fear circuit in the BLA has not been fully resolved. Here, using patch clamp recordings, Cre-dependent DLX intersectional targeting, and genetic manipulations, I demonstrate that NE activates cholecystinin (CCK)-positive interneurons to generate synchronized trains of rhythmic CB1-sensitive IPSCs (~ 4 Hz) in the BLA principal neurons through Gq-coupled $\alpha 1A$ adrenoreceptors expressed in the majority of the CCK interneurons in the BLA. This Gq-dependent mechanism of noradrenergic activation of CCK interneurons is generalizable to chemogenetic Gq manipulation and other neuromodulators, like serotonin. I further tested the role of the noradrenergic activation of CCK interneurons in fear learning with $\alpha 1A$ adrenoreceptor re-expression in a global *adra1A* knockout mouse. Restoration of $\alpha 1A$ noradrenergic signaling specifically in the CCK interneurons restored the NE-induced rhythmic IPSCs in the principal neurons and decreased fear memory acquisition and recall. Thus, my data reveal an inhibitory role of $\alpha 1A$ noradrenergic signaling in fear learning through activation of patterned perisomatic inhibitory inputs from CCK interneurons. In comparison with the facilitatory effect of $\alpha 1A$ noradrenergic activation of BLA PV cells

on fear memory retrieval, this suggests that NE may fine-tune associative fear learning by balancing the contribution of different patterns of perisomatic inhibition.

4.2 Introduction

Adaptive fear learning is an essential survival mechanism for animals to avoid stimuli that predict danger. However, unrestrained excessive fear learning is maladaptive, leading to the development of fear-related mental disorders. It remains unclear how the nervous system fine tunes the level of fear learning during stressful encounters to achieve optimal emotional memories. The basolateral amygdala is a cortical-like structure that plays essential roles in the emotional processing of fear (Capogna, 2014; Duvarci & Pare, 2014; Herry & Johansen, 2014; McGaugh, 2004). While the plastic changes at glutamatergic synapses on BLA principal neurons have been causally linked to the encoding of associative fear memories (Johansen et al., 2011; Krabbe et al., 2018), accumulating evidence suggests this process is tightly gated by local inhibitory GABAergic interneurons through inhibition or disinhibition (Krabbe et al., 2018; Krabbe et al., 2019; Wolff et al., 2014). Thus, differential engagement of antagonistic inhibitory neural circuits in the BLA may serve as a controller to modulate the level of fear acquisition.

The GABAergic inhibitory interneurons in the BLA can be classified into two main groups according to a morpho-functional classification, dendritic inhibitory and perisomatic inhibitory interneurons (McDonald, 2020; Spampanato et al., 2011). The dendritic inhibitory interneurons, such as the somatostatin-positive interneurons, project their axons to the distal dendrites of the principal cells to regulate synaptic integration

(Muller et al., 2007). In comparison, the perisomatic interneurons, including the cholecystokinin (CCK)-positive and parvalbumin (PV)-positive basket cells, predominantly innervate the soma and the proximal dendrites of the principal neurons and are thought to control the principal neuron spike timing and synchronization (Freund & Katona, 2007; Veres et al., 2017; Woodruff & Sah, 2007a). Whereas the PV cells are reliably activated by their robust glutamatergic inputs, the CCK cells receive less glutamatergic synapses and are more regulated by subcortical neuromodulatory signals (Andrási et al., 2017; Freund & Katona, 2007). Moreover, the type 1 cannabinoid receptors (CB1Rs) are selectively and abundantly expressed on the terminals of CCK basket cells (Katona et al., 2001; Yoshida et al., 2011), and, as a result, the CCK BC-mediated inhibitory transmission is strongly inhibited by cannabinoid signaling (Varga et al., 2010; Vogel et al., 2016; Yoshida et al., 2011). Although the function of the CCK basket cells in the regulation of fear has been indirectly extrapolated from manipulation of CB1 signaling (Atsak et al., 2015; Campolongo et al., 2009; Di et al., 2016; Morena et al., 2016), little is known about the role of the activity of these cells driven by neuromodulatory signals in the regulation of fear memory formation.

Emotional salience facilitates memory formation, a phenomenon largely mediated by noradrenergic signaling in the basolateral amygdala (McGaugh, 2004). The BLA receives a robust noradrenergic innervation from the locus coeruleus (LC) (Giustino & Maren, 2018), and stressful stimuli, like foot shocks, strongly stimulate the release of NE in the BLA (McIntyre et al., 2002). In addition to the converging evidence showing that activation of the β adrenoreceptors boosts BLA principal neuronal activity (Giustino et al., 2020; McCall et al., 2017) and enhances the consolidation of fear (McGaugh, 2004),

NE has also been found to facilitate inhibitory synaptic transmission through $\alpha 1A$ adrenoreceptors in the BLA of juvenile rats (Braga et al., 2004), which may be due to the activation of regular spiking interneurons in the BLA (Kaneko et al., 2008). Behaviorally, the functional role of $\alpha 1$ adrenoreceptor tested with the general $\alpha 1$ antagonist prazosin in the regulation of fear memory formation is controversial (Ferry et al., 1999; Gazarini et al., 2013; Lazzaro et al., 2010; Lucas et al., 2019), possibly due to the lack of highly selective antagonists for the three different $\alpha 1$ subtypes and cell type-specific manipulations. Therefore, it remains to be determined whether and how NE modulates defined inhibitory circuits in the BLA to regulate fear memory formation.

My previous data showed that NE stimulates two types of dissociable perisomatic inhibitory synaptic activity in the BLA principal neurons. While the PV interneurons are responsible for the generation of repetitive bursts of IPSCs in the BLA principal neurons (see Chapter 3), the other type of IPSCs are sensitive to the blockade of CCK basket cell-specific N-type calcium channels and activation of CB1 receptors, suggesting an origin in the CCK basket cells. Here, I tested the role of BLA CCK interneurons in the noradrenergic modulation of inhibitory synaptic transmission and fear learning by combining brain slice electrophysiology, intersectional viral targeting, and genetic manipulations. I found a Gq-dependent mechanism by which $\alpha 1A$ noradrenergic activation of CCK interneurons generates synchronized trains of rhythmic CB1-sensitive IPSCs ($\sim 4\text{Hz}$) in the principal neurons. Moreover, while the CCK interneuron-mediated rhythmic IPSCs were lost in a global *adra1A* knockout, I found that selective re-expression of $\alpha 1A$ adrenoreceptors in the BLA CCK interneurons restored NE-stimulated rhythmic IPSCs in the principal neurons and decreased fear memory formation. Taken

together, my data reveal a previously undefined role of CCK interneurons in the noradrenergic modulation of fear learning.

4.3 Experimental design

In this chapter, I investigated the role of α 1A adrenergic activation of CCK interneurons in fear conditioning with three sets of experiments: 1) Whole-cell patch clamp recordings and neuropharmacological treatments in acute brain slices. Brain slices were pre-incubated in the recording chamber with control artificial cerebrospinal fluid or receptor antagonists for ≥ 10 minutes. Norepinephrine, adrenoceptor agonist, clozapine-N-oxide (CNO), or serotonin was then co-applied in the perfusion bath for 5 minutes. Spontaneous IPSCs were recorded and analyzed for changes in frequency, amplitude, and decay time constant for 10-20 minutes following drug applications. 2) Histochemical analyses of α 1A adrenoceptor distribution in the CCK interneurons. Virus-injected CCK-ires-Cre::adra1A KO mice were perfused and stained for β -galactosidase activity. The bright field or fluorescent X-gal signals were then imaged and analyzed to reveal the localization of α 1A receptors in the BLA. 3) Behavioral analysis of the effects of α 1A adrenergic activation of CCK interneurons on fear conditioning. The freezing behavior during fear acquisition and retrieval were compared between the adra1A knockout mice with or without selective re-expression of α 1A adrenoceptors or expression of hM3D designer receptors in the BLA CCK interneurons.

4.4 Results

4.4.1 NE stimulates synchronized rhythmic perisomatic inhibitory synaptic inputs to BLA principal neurons by activating CCK basket cells

In addition to the PV interneuron-mediated repetitive bursts of inhibitory postsynaptic currents (see Chapter 3), NE stimulated another pattern of IPSCs in the BLA principal neurons through α 1A adrenergic activation of the presynaptic interneurons, which were insensitive to P/Q-type calcium channel blockade. After blocking the glutamatergic transmission with DNQX (20 μ M) and APV (40 μ M) and the PV-mediated inhibitory input with selective P/Q-type calcium channel blocker ω -agatoxin (0.5 μ M), NE (100 μ M) induced multiple singular inactivating trains of IPSCs in the principal neurons that had a rhythmic instantaneous intra-burst frequency of \sim 4 Hz (range: 2.17 to 5.30 Hz, mean: 3.91 Hz) and a duration of \sim 70 s (range: 36.88 to 134.75 s, mean: 71.01 s) (Fig. 20A, B). These multiple IPSC trains were abrogated by blocking neural spiking activity with TTX (0.5 μ M) (Fig. 20C), and showed varying amplitudes and inter-event frequency, and they sometimes overlapped with one another (Fig. 20A), and were considered to be generated from activation of different presynaptic interneurons. As with NE-stimulated repetitive IPSC bursts from PV interneurons (see Chapter 3), the trains of IPSCs were blocked by the α 1A adrenoceptor WB4101 (1 μ M) and mimicked by the α 1A adrenoceptor agonist A61603 (2 μ M) (Fig. 20C). Furthermore, pre-incubation of the slices with the selective $G\alpha_q$ inhibitor YM-254890 (10 μ M) totally abolished these NE-induced IPSCs (Fig. 20C). Taken together, these data suggested that NE activates

BLA local interneurons through Gq-coupled $\alpha 1A$ adrenoreceptors to drive trains of rhythmic IPSCs in the BLA principal neurons.

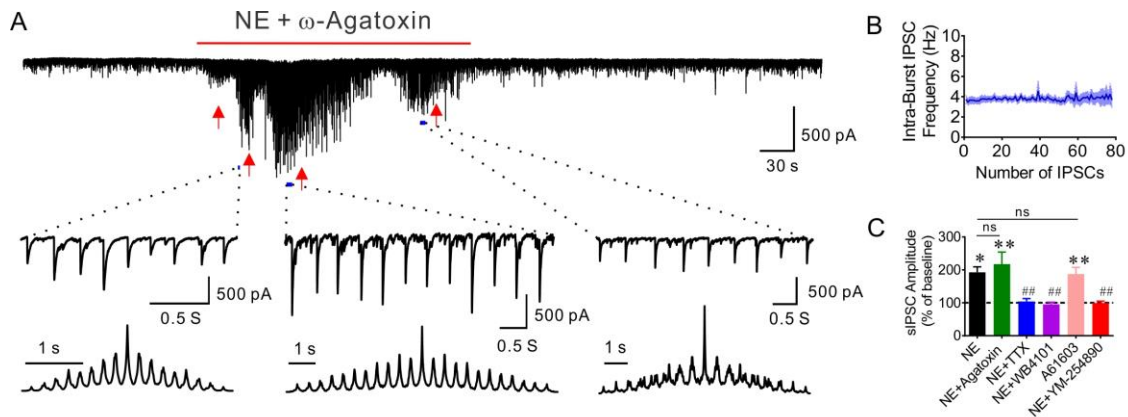


Figure 20. NE stimulates trains of rhythmic IPSCs in the BLA principal neurons

(A). A representative recording showing multiple trains of rhythmic IPSCs induced by NE in the presence of the P/Q-type calcium channel blocker ω -agatoxin. Red arrows delineate different IPSC trains, which were expanded to show the regularity of the IPSC events within each train, with the corresponding autocorrelational graphs beneath each expanded train. (B). Mean (\pm SEM) instantaneous frequency of NE-induced IPSCs throughout the course of the trains. (C). Mean change in amplitude of NE-induced IPSCs. The NE-induced increase of IPSC amplitude (16 cells from 5 mice) was not affected by blocking P/Q-type calcium channels with ω -agatoxin (10 cells from 4 mice), but was eliminated by blocking neural activity with the sodium channel blocker TTX (10 cells from 5 mice). The NE-induced rhythmic IPSCs were blocked and mimicked, respectively, by the α 1A adrenoreceptor antagonist WB4101 (7 cells from 4 mice) and agonist A61603 (10 cells from 4 mice). Inhibition of Gq activation abrogated the NE-induced increase of IPSC amplitudes (8 cells from 3 mice). Paired *t* test, NE vs. baseline, $p=0.01$, NE + Agatoxin vs. baseline, $p<0.0001$, A61603 vs. baseline, $p = 0.0024$, *, $p < 0.05$, **, $p < 0.01$; One-Way ANOVA, $F (5, 55) = 7.145$, $p < 0.0001$; Dunnett's multiple comparisons test, NE vs. NE+Agatoxin, $p = 0.79$, NE vs. NE+TTX, $p = 0.0053$, NE vs. NE+WB4101, $p = 0.0068$, NE vs. A61603, $p = 0.99$, NE vs. NE+YM-254890, $p = 0.0066$, values at the peak of IPSC amplitude increase (time = 7 min in all the treatments) were used to compare ω -agatoxin-insensitive IPSCs. ##, $P < 0.01$.

The IPSCs in the trains displayed a fast rise time ($1.40 \text{ ms} \pm 0.05 \text{ ms}$, $n = 11$ bursts in 5 mice) and fast decay time ($18.43 \text{ ms} \pm 1.16 \text{ ms}$, $n=11$ bursts in 5 mice), a characteristic of perisomatic inhibition originated from basket cells (Barsy et al., 2017; Wilson et al., 2001), which comprise the CCK and PV positive interneurons in the BLA. Consistent with my previous finding that the NE-induced IPSC trains are sensitive to N-type calcium channel blockade with ω -conotoxin ($1 \text{ } \mu\text{M}$) and CB1 receptor activation with WIN 55,212-2 ($1 \text{ } \mu\text{M}$), I observed these IPSCs underwent transient and complete depolarization-induced suppression of inhibition (DSI) that was totally reversed by a CB1 receptor antagonist, AM251 ($10 \text{ } \mu\text{M}$) (Fig. 21A-C). As the CCK basket cells exclusively utilize the N-type calcium channels for GABA release and the CB1 receptors are selectively expressed on the CCK, but not the PV axon terminals (Fig. 21A-C) (Freund & Katona, 2007; Katona et al., 2001; Wilson et al., 2001; Yoshida et al., 2011), these data collectively indicated that NE activates CCK interneurons to generate a rhythmic pattern of IPSCs in the BLA principal neurons.

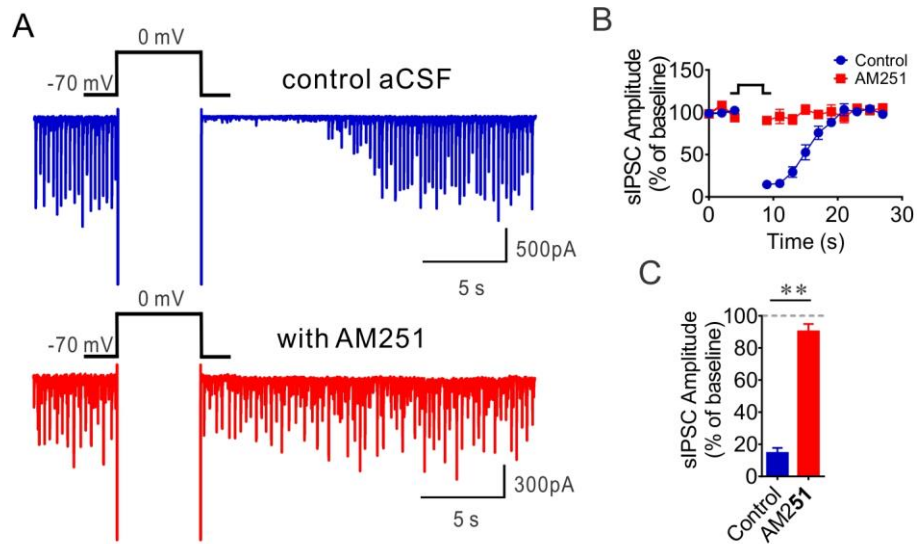


Figure 21. NE-induced IPSC trains undergo transient and complete DSI

(A). Representative recording traces showing ω -agatoxin-isolated IPSCs underwent transient and complete depolarization-induced suppression of inhibition (DSI, top), which was reversed by CB1 receptor antagonist, AM251 (bottom). (B, C). Time course (B) and mean change of IPSC amplitude (C) showing the DSI in NE-induced IPSCs (8 cells from 3 mice) that were blocked by CB1 receptor antagonist, AM251 (3 cells from 2 mice). Unpaired *t* test, control vs. AM251, $p < 0.0001$, **, $P < 0.01$.

As the perisomatic basket cells innervate hundreds of principal neurons through their extensive arborizations, I examined if the activity-dependent NE-induced IPSC trains were synchronized between BLA principal neurons. To address this question, I conducted paired recordings in adjacent BLA principal neurons and monitored the response of each cell in the pair simultaneously to NE after blocking PV interneuron inputs with ω -agatoxin (Fig. 22A, B). Interestingly, NE application induced similar responses in both cells in most of the paired recordings (Fig. 22C). Moreover, I found that the NE-induced IPSC trains were synchronized between each pair, and that the individual IPSCs within the synchronous trains also showed a high level of synchronization (Fig. 22D). These data suggested that NE might modulate the synchronous neural output from the BLA by activating perisomatic basket cells to generate synchronous trains of inhibitory synaptic signals.

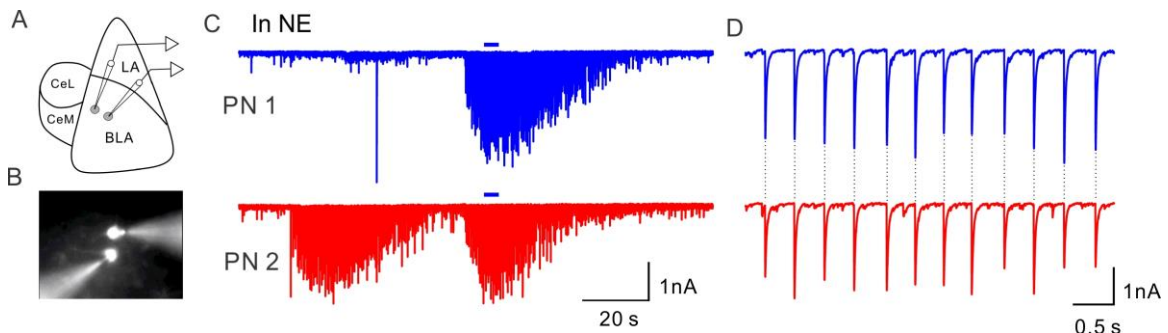


Figure 22. NE-induced IPSC trains are synchronized between BLA principal neurons

(A, B). Schematic diagram and fluorescent image showing dual recording in two adjacent BLA principal neurons. Alexa488 dye was included in the patch solution to visualize the recorded neurons. (C). Representative traces showing NE-induced responses in a pair of recorded BLA principal neurons. (D). Synchronized trains of rhythmic IPSCs were expanded (segment designated by blue bar above traces) to show that the individual IPSCs in the two principal neurons cells were synchronized (marked with dashed lines).

4.4.2 Expression of $\alpha 1A$ adrenoreceptors on the BLA CCK interneurons

To test whether CCK interneurons express the $\alpha 1A$ adrenoreceptors that mediate the NE-induced CB1-sensitive IPSC trains, I first labeled the CCK interneurons by injection of intersectional hDLX virus (hDLX-DIO-mCherry) in the BLA of the CCK-ires-Cre mouse line (Fig. 23A, B). Consistent with previous literature (Dimidschstein et al., 2016; Liu et al., 2020), injection of a Cre-dependent hDLX virus selectively labeled CCK interneurons in the BLA, as $98.2 \pm 1.5\%$ of the mCherry labeled cells are colocalized with the interneuron marker GAD-GFP (Fig. 23C, D).

I next examined whether the $\alpha 1A$ adrenoreceptors are expressed in BLA CCK interneurons. As the commercial antibodies against the $\alpha 1$ adrenoreceptors are not specific (Jensen et al., 2008), I indirectly looked at the $\alpha 1A$ adrenoreceptor distribution with β -gal staining in a global *adra1A* knockout mouse line, which has the *adra1A* open reading frame replaced by a *lacZ* gene cassette (Rokosh & Simpson, 2002). Two weeks after injection of DLX virus in the BLA of the CCK-ires-Cre::*adra1A* KO to label the CCK interneurons, I stained the β -galactosidase with X-gal to reveal the cells that express the $\alpha 1A$ adrenoreceptors. A majority of the labeled CCK interneurons (74.5%, Fig. 23E, F) were positive for X-gal. Thus, my data provide histological evidence for the $\alpha 1A$ adrenoreceptor-dependent rhythmic IPSC generation through activation of CCK interneurons.

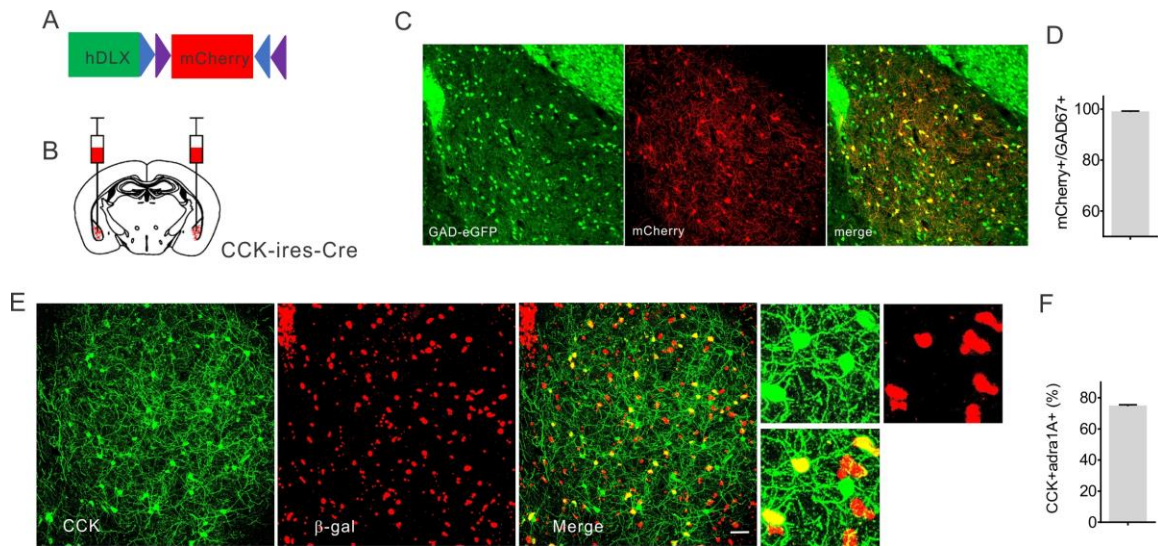


Figure 23. Expression of $\alpha 1A$ adrenoreceptors in BLA CCK interneurons

(A, B). Schematic diagram showing injection of Cre-dependent intersectional DLX-mCherry virus into the BLA of CCK-ires-Cre interneurons. (C). Expression of mCherry was colocalized with Gad67-eGFP, which labels all GABAergic interneurons in the BLA. (D). Quantification of the colocalization of CCK-mCherry and Gad67-eGFP. ($98.2 \pm 1.5\%$, $N=430$ cells). (E). Representative images showing that most of the CCK interneurons labeled with mCherry co-expressed β galactosidase. (F). Quantification of the colocalization of CCK-mCherry and b-gal. ($74.5 \pm 1.99\%$, $N= 145$ cells).

4.4.3 Gq activation of CCK interneurons drives the rhythmic trains of IPSCs in the BLA

Having established the role of CCK interneurons in the generation of the NE-induced trains of IPSCs through activation of Gq-coupled $\alpha 1A$ adrenoreceptors, I next examined if selective chemogenetic Gq activation of CCK interneurons is sufficient to stimulate the same pattern of IPSCs to the BLA principal neurons. To specifically express the Gq-coupled designer receptor hM3D in the CCK interneurons, I bilaterally injected Cre-dependent hDLX AAV virus (AAVdj-hDLX-DIO-hM3D-mCherry) in the BLA of CCK-ires-Cre animals (Dimidschstein et al., 2016; Liu et al., 2020) (Fig. 24A, B). Two weeks after viral injection, I observed that the expression of Gq-mCherry was also restricted to the interneurons of the BLA (Fig. 24C). Notably, whole-cell voltage clamp recordings in BLA slices from virus-injected animals showed that selective activation of Gq-DREADDs in the CCK interneurons with CNO (5 μ M) predominantly induced a similar pattern of rhythmic IPSCs (2.74 to 7.37 Hz, mean = 4.01 Hz, Fig. 24D-G) in the principal neurons. Consistent with the double dissociation of two NE-induced patterns of IPSCs with calcium channel blockers, the IPSCs generated by Gq activation in CCK interneurons were eliminated by blocking N-type calcium channels with ω -conotoxin (1 μ M), while they were unaffected by blockade of the P/Q-type calcium channels with ω -agatoxin (0.5 μ M) (Fig. 24D, H, I). Moreover, similar to the NE-induced trains of IPSCs, the CCK interneuron-mediated IPSCs also underwent transient and complete DSI, which was totally reversed by the CB1 receptor antagonist AM251 (10 μ M) (Fig. 24J-L). Collectively, these results confirmed the specificity of the pharmacological manipulation of CCK basket cell-mediated synaptic release and demonstrated that Gq activation of

CCK cells is both necessary and sufficient for inducing NE-mediated inactivating trains of IPSCs.

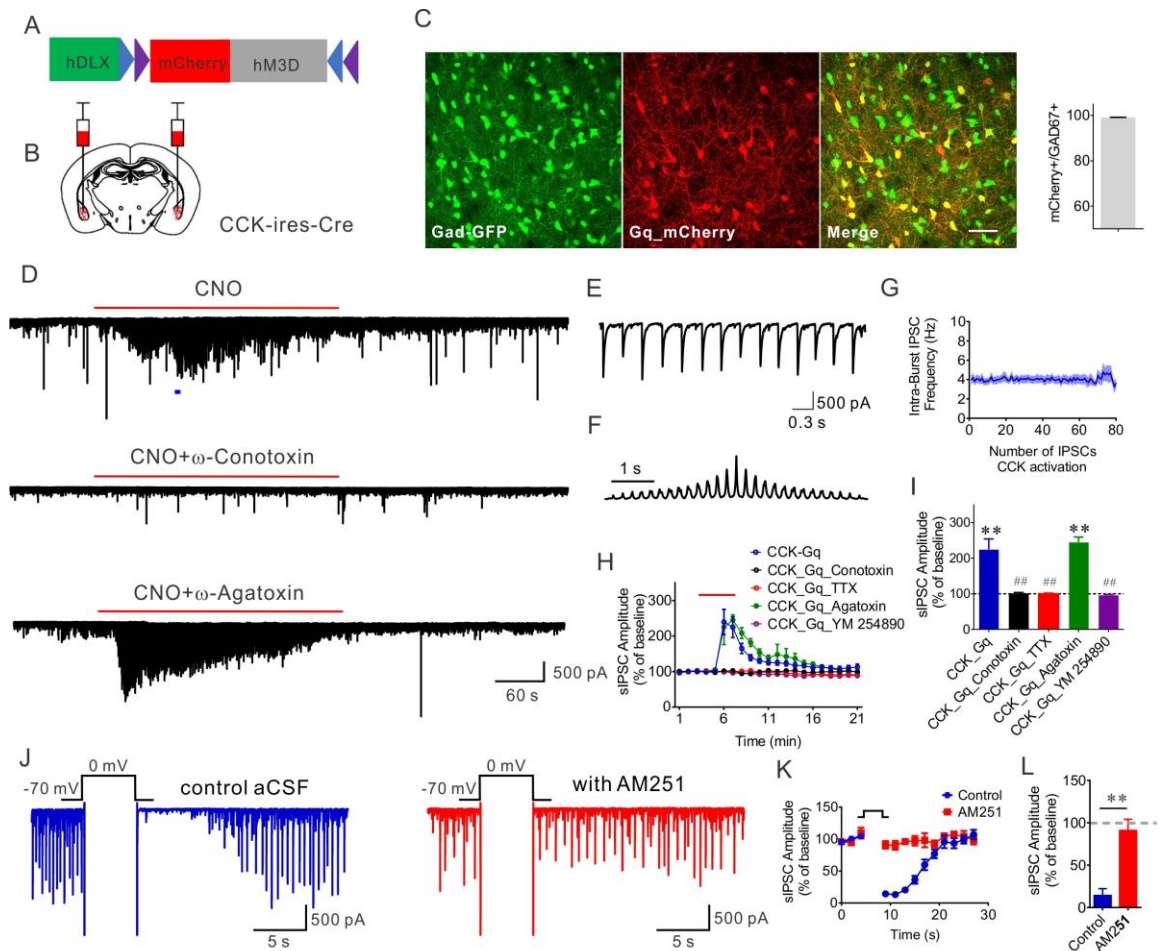


Figure 24. Chemogenetic activation of BLA CCK interneurons stimulates IPSCs in the BLA principal neurons

(A, B) Schematic diagram showing injection of Cre dependent intersectional DLX-DIO-hM3D(Gq) virus into the BLA of the CCK-ires-Cre mouse. (C) Representative images and quantification of colocalization of hM3D-mCherry and Gad67-GFP in the BLA ($98.82 \pm 0.56\%$, 1722 cells). (D) Representative recordings showing that Gq activation of CCK interneurons in the BLA stimulated trains of IPSCs (top trace), which were blocked with the N-type calcium channel blocker ω -conotoxin (middle

trace), and were unaffected by the P/Q-type calcium channel blocker ω -agatoxin (bottom trace). (E, F) Expanded trace from recording in D (E) and autocorrelational graph (F) showing the rhythmicity of CNO-induced IPSCs. (G) Mean (\pm SEM) instantaneous frequency of CNO-induced trains of IPSCs showing constant IPSC frequency throughout the trains. (H, I) Time course and mean change in sIPSC amplitude mediated by Gq activation in CCK interneurons. The CNO-induced increase in sIPSC amplitude (10 cells from 4 mice) was blocked by the N-type calcium channel antagonist ω -conotoxin (6 cells from 2 mice), the sodium channel blocker TTX (6 cells from 2 mice), and the selective $G\alpha_{q/11}$ inhibitor YM-254890 (5 cells from 3 mice), but not by the P/Q-type calcium channel antagonist ω -agatoxin (5 cells from 2 mice). Paired *t* test, CCK-Gq vs. baseline, $p = 0.0022$; CCK-Gq-Agatoxin vs. baseline, $p = 0.0006$, **, $p < 0.01$; One way ANOVA, $F(4, 27) = 11.62$, $P < 0.0001$; Dunnett's multiple comparisons test, CCK-Gq vs. CCK-Gq-Conotoxin, $p = 0.0007$; CCK-Gq vs. CCK-Gq-TTX, $p = 0.0006$; CCK-Gq vs. CCK-Gq-Agatoxin, $p = 0.91$; CCK-Gq vs CCK-Gq-YM-254890, $p = 0.0008$, ##, $p < 0.01$. (J) Representative recordings showing that the CCK interneuron-mediated IPSCs underwent transient and complete DSI. (K, L) Average time course and mean change in the amplitude of CNO-induced rhythmic IPSCs by depolarization of the postsynaptic principal neurons (9 cells from 4 mice). The transient suppression of IPSC amplitude is reversed completely by CB1 receptor antagonist, AM251 (5 cells from 2 mice). Unpaired *t* test, control vs. AM251, $p < 0.0001$, **, $p < 0.01$.

As Gq activation of CCK interneurons in the BLA mimicked the NE-induced rhythmic trains of IPSCs, I questioned whether this Gq mechanism could also be applied to other neuromodulators if their cognate Gq-coupled receptors are expressed in CCK interneurons. Strikingly, bath application of serotonin (5-HT, 100 μ M) to ω -agatoxin (0.5 μ M)-treated BLA slices in the presence of the ionotropic glutamate receptor antagonists DNQX (20 μ M) and AP-5 (40 μ M) stimulated multiple inactivating trains of rhythmic IPSCs similar to NE (2.55 to 7.35 Hz, mean = 4.37 Hz, Fig. 25A, B). Moreover, blockade of neural activation with TTX (0.5 μ M) and CCK-mediated inhibitory transmission with the CB1 agonist WIN 55,212-2 (1 μ M) totally abrogated the 5-HT-induced IPSC trains, indicating that the 5-HT-induced IPSCs also originate from activation of CCK interneurons (Fig. 25C, D). Additionally, pretreatment of slices with the selective 5HT2C antagonist RS102221 (10 μ M) or the Gq inhibitor YM-254890 (10 μ M) eliminated the 5-HT-induced increase of IPSCs (Fig. 25C, D). Thus, activation of Gq signaling in the CCK interneurons and the resulting rhythmic output of IPSCs could serve as a general mechanism for different neuromodulators to regulate neural circuit activity in the BLA.

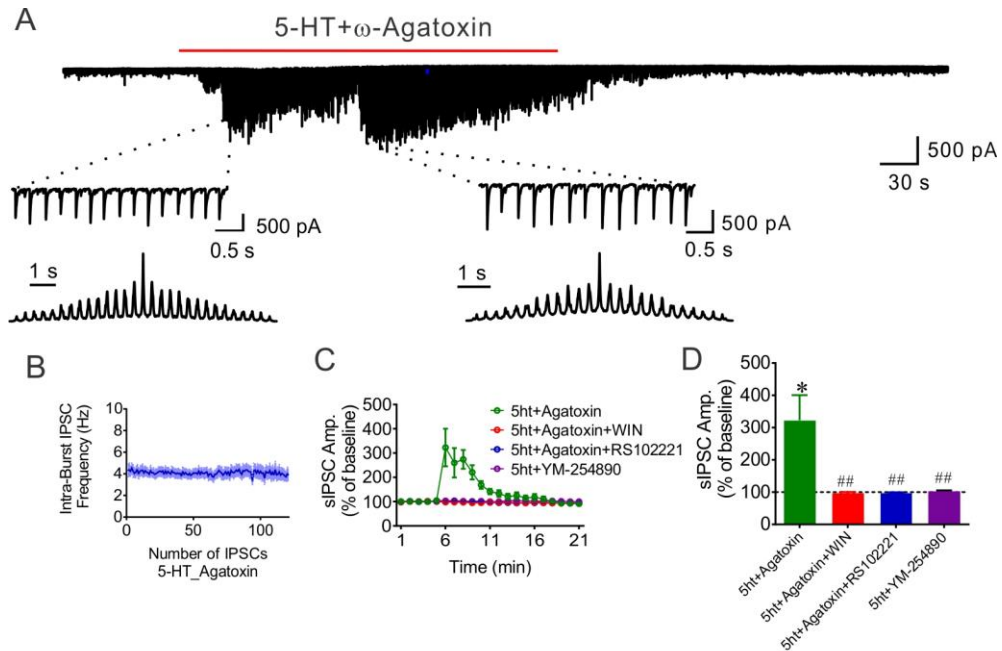


Figure 25. Serotonin 5-HT_{2C} receptor activation of rhythmic IPSC trains

(A). A representative trace showing that in the presence of ω -agatoxin, serotonin induced trains of IPSCs similar to those induced by NE application in the BLA principal neurons. Expanded trace (inset) and autocorrelational graph showing the rhythmicity of 5-HT induced IPSCs. (B) Mean (\pm SEM) instantaneous frequency of 5-HT-induced trains of IPSCs, showing the constant intra-train IPSC frequency. (C, D). Time course (C) and mean change in sIPSC amplitude (D) induced by 5-HT activation of CCK interneurons. The 5-HT-induced IPSCs (isolated by ω -agatoxin, 8 cells from 3 mice) were blocked by: CB₁ receptor activation with WIN 55,212-2 (6 cells from 3 mice), the 5HT_{2C} receptor antagonist RS102221 (6 cells from 3 mice), and the Gq protein inhibitor YM-254890 (6 cells from 3 mice). Paired *t* test, 5HT-Agatoxin vs. baseline $p = 0.024$, *, $P < 0.05$; One-way ANOVA, $F(3, 24) = 7.836$, $p = 0.0018$; Dunnett's multiple comparisons test, 5-HT+Agatoxin vs. 5-HT+Agatoxin+WIN, $p = 0.0025$; 5-HT+Agatoxin vs. 5-HT+Agatoxin+RS102221, $p = 0.005$; 5-HT+Agatoxin vs. 5-HT+YM-254890, $p = 0.006$. ##, $p < 0.01$.

4.4.4 Activation of α 1A adrenergic signaling in CCK interneurons suppresses conditioned fear learning

Stressful stimuli trigger a significant increase of NE in the BLA, which plays a key role in the modulation of fear memory formation (Galvez et al., 1996; McGaugh, 2004; Quirarte et al., 1998). To selectively investigate the role of α 1A noradrenergic activation of CCK interneurons and the resulting rhythmic IPSCs in the principal neurons in BLA-dependent fear memory formation, I tested the effects of re-expression of α 1A adrenoreceptors in the BLA CCK interneurons with Cre-dependent hDLX intersectional AAV virus in the global *adra1A* knockout mice in a standard fear conditioning paradigm (Fig. 26A, B).

I first tested the effects of α 1A adrenoreceptor global deletion and re-expression in the BLA on the NE-induced rhythmic trains of IPSCs using whole-cell recordings in brain slices. In slices from *adra1A* knockout mice, NE (100 μ M) and the selective α 1A adrenoreceptor agonist A61603 (2 μ M) failed to induce the facilitation of sIPSC frequency and amplitude seen in principal cells from wild type mice (Fig. 26C, H), confirming the specific α 1A adrenoreceptor dependence of the NE-induced IPSC burst generation. After injection of Cre-dependent, α 1A-expressing hDLX virus (AAVdj-hDLX-DIO- α 1A-mCherry) bilaterally in the BLA of CCK-ires-Cre::*adra1A* KO mice, activation of α 1A adrenoreceptors specifically re-expressed in CCK interneurons from *adra1A* knockout mice rescued the NE-induced rhythmic trains of IPSCs in the BLA principal neurons (n=9 cells from 4 mice, Fig. 26C-H).

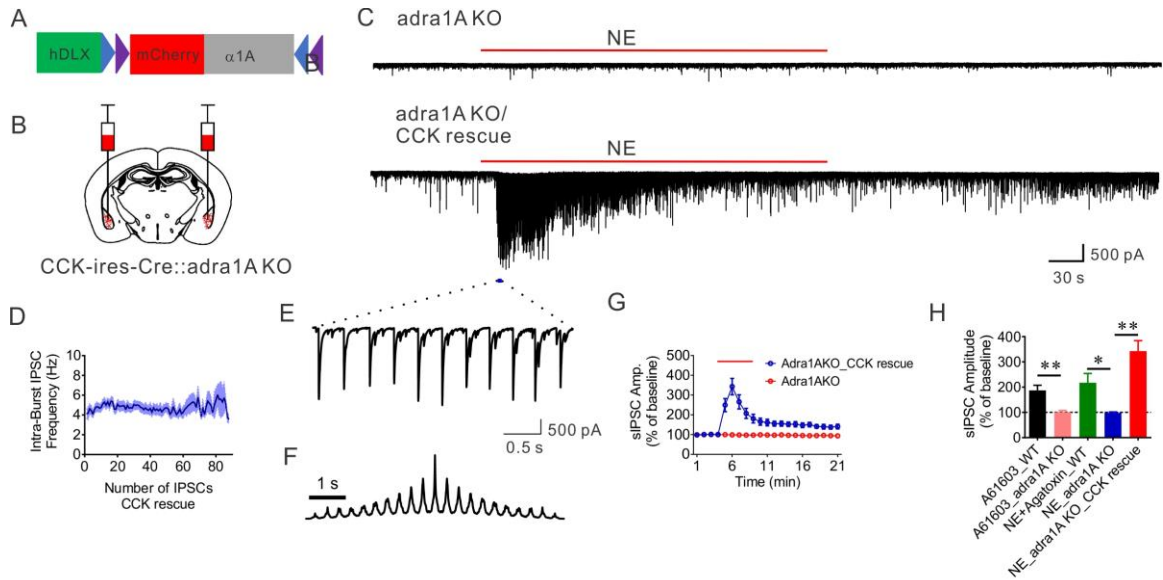


Figure 26. Rescue of $\alpha 1A$ adrenoreceptors in the BLA CCK interneurons restores rhythmic IPSC trains

(A, B). Diagram showing injection of Cre dependent hDLX- $\alpha 1A$ virus into the BLA of CCK-ires-Cre::*adra1A* KO mice. (C). Representative traces showing the lack of response to NE in a BLA principal neuron in a slice from a global *adra1A* KO mouse (Top trace) and that the re-expression of the $\alpha 1A$ adrenoreceptors in the CCK interneurons rescued the NE-induced trains of rhythmic IPSCs (Bottom trace). (D). Mean (\pm SEM) instantaneous frequency of the rescued CCK-mediated IPSCs. (E, F). Expanded trace (E) and autocorrelational graph (F) showing the rhythmicity of the restored CCK-mediated IPSCs. (G). Time course of the NE effect on sIPSC amplitude in *adra1A* KO mice with or without virally-mediated re-expression of $\alpha 1A$ adrenoreceptors in CCK interneurons. (H). Mean change in sIPSC amplitude in BLA principal neurons in response to NE or the $\alpha 1A$ agonist A61603 in slices from wild type (WT) and *adra1A* KO mice. (NE+Agatoxin_WT: 10 cells from 4 mice; NE_*adra1A* KO: 9 cells from 4 mice; A61603_WT: 10 cells from 4 mice; A61603_*adra1A* KO: 7 cells from 3 mice; NE_*adra1A* KO_CCK rescue: n = 9 cells from 3 mice) (Unpaired *t* test, A61603_WT vs. A61603_*adra1A* KO: $p = 0.0032$, ** $p < 0.01$; One-Way ANOVA, $F(2, 25) = 13.85$, $p < 0.0001$, Dunnett's multiple comparisons test, NE+Agatoxin_WT vs. NE_*adra1A* KO: $p = 0.0268$, NE_*adra1A* KO vs. NE_*adra1A* KO_CCK rescue: $p < 0.0001$, * $p < 0.05$, ** $p < 0.01$).

Having validated the effectiveness of the virus-based rescue of NE-induced CCK-type inhibitory synaptic inputs to the BLA principal cells, I next investigated the roles of α 1A noradrenergic engagement of CCK basket cells in the modulation of fear memory formation. Three weeks after α 1A adrenoreceptor re-expression with bilateral injection of AAVdj-hDlx-DIO- α 1A-mCherry into the BLA of CCK-ires-Cre::adra1A KO mice (Fig. 27A), the mice were subjected to a standard auditory-cued fear conditioning paradigm (Fig. 27B). Animals with global knockout of α 1A adrenoreceptors did not show a significant difference in fear memory acquisition or retrieval compared with their wildtype littermate controls (Fig. 27C, adra1A WT vs. adra1A KO, fear acquisition, $p=0.13$; fear expression, $p = 0.45$). Selective rescue of the α 1A noradrenergic signaling specifically in the BLA CCK interneurons resulted in impaired fear acquisition and retrieval, which was manifested by less freezing behavior with repetitive pairing of the auditory tone and the foot shock during fear conditioning training (Fig. 27D, $p = 0.018$), and when the animals were presented 24h later with the auditory tone alone (Fig. 27D, $p = 0.0002$). Since activation of the Gq-DREADD induced the same IPSC bursting patterns as NE did in the brain slices, I next tested the effects of the Gq-DREADD-induced rhythmic IPSCs on fear learning in the α 1A knockout animals. The designer drug CNO (5 mg/kg) was administered I.P. 30 min prior to beginning the fear conditioning paradigm. Similar to the effects of α 1A adrenoreceptor re-expression on fear learning, chemogenetic activation of CCK interneurons also inhibited fear acquisition (Fig. 27E, $p = 0.0004$) and retrieval (Fig. 27E, $p = 0.0007$), indicating that the induction of the rhythmic pattern of IPSCs was sufficient to recapitulate the inhibitory effect of α 1A activation of CCK interneurons on fear learning. As activation of α 1A noradrenergic signaling in the BLA

PV interneurons generates repetitive bursts of IPSCs and has been shown to facilitate fear learning (see Chapter 3), these results collectively suggested that the BLA contains two competing perisomatic inhibitory neural circuits that, when activated by Gq signaling during conditioned stimulus presentation, balance the acquisition of learned fear through their different patterns of inhibitory outputs.

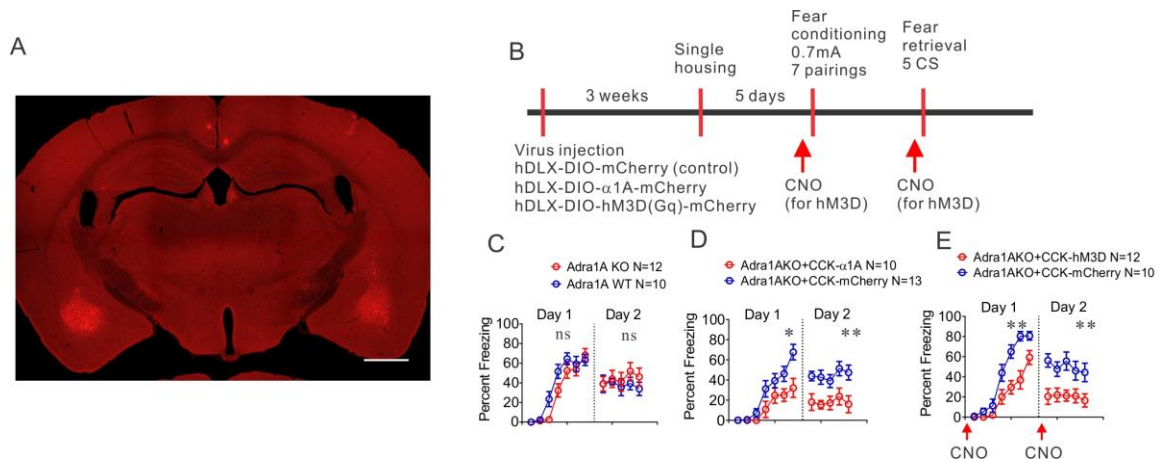


Figure 27. α 1A adrenoreceptors in BLA CCK interneurons suppress fear acquisition

(A). A representative image showing successful bilateral injection of conditional DLX virus to label the BLA CCK interneurons. Scale bar, 1mm. (B). Experimental timeline for virus injection and fear conditioning. CCK-ires-Cre::*adra1A* KO mice were injected with conditional AAVs expressing Cre-dependent α 1A-mCherry or Gq-DREADD to rescue α 1A adrenoreceptor mediated Gq signaling in BLA CCK interneurons. Control CCK-ires-Cre::*adra1A* KO mice were injected with conditional AAVs expressing only mCherry. For Gq-DREADD rescue experiments, CNO (5 mg/kg) was administered I.P. 30 min prior to commencement of the fear acquisition and again 30 min prior to commencement of the fear retrieval (red arrows) in both Gq-DREADD and mCherry groups. (C). Global *adra1A* deletion did not change fear memory acquisition (Repeated measures Two-Way ANOVA, $F(1, 20) = 2.49$, $p = 0.13$) and recall compared to the wildtype littermate controls. (Repeated measures

*Two-Way ANOVA, $F(1, 20) = 0.60, p = 0.45$). (D). Replacement of $\alpha 1A$ adrenoreceptors selectively in BLA CCK interneurons significantly attenuated fear acquisition (Repeated measures Two-Way ANOVA, $F(1, 21) = 6.63, p = 0.018$ compared to control virus-injected CCK-ires-Cre::*adra1A* KO group), and the retrieval of the fear memory (Repeated measures Two-Way ANOVA, $F(1, 21) = 20.73, p = 0.0002$). * $p < 0.05$, ** $p < 0.01$ compared to control virus-injected CCK-ires-Cre::*adra1A* KO group. (M). Rescue of Gq signaling in BLA CCK interneurons in *adra1A* KO mice with excitatory DREADD decreased fear memory acquisition (Repeated measures Two-Way ANOVA, $F(1,20) = 17.69, p = 0.0004$ compared to control virus injected CCK-ires-Cre::*adra1A* KO group), and fear memory retrieval (Repeated measures Two-Way ANOVA, $F(1,20) = 16.26, p = 0.0007$). ** $p < 0.01$ compared to control virus injected CCK-ires-Cre::*adra1A* KO group.*

4.5 Discussion

Although cannabinoid modulation of the inhibitory synaptic transmission mediated by CB1-expressing CCK basket cells has been proposed to regulate the stress-facilitation of fear memory formation (Atsak et al., 2015; Campolongo et al., 2009; Morena et al., 2016), direct investigation of the role of CCK interneuron activity stimulated by stress-related neuromodulators in learned fear has been largely impeded by the lack of cell type-specific genetic tools targeting the CCK interneurons. Here, I demonstrated that the CB1-expressing CCK interneurons are activated by Gq-coupled $\alpha 1A$ adrenergic receptors to generate a rhythmic-patterned inhibitory output to the BLA principal neurons. With an interneuron-specific, Cre-dependent $\alpha 1A$ -expressing hDLX virus, I found that the selective re-expression of $\alpha 1A$ adrenoreceptors in the BLA CCK interneurons of global *adra1A* knockouts and the resulting rescue of rhythmic perisomatic

IPSCs inhibited the acquisition and expression of conditioned fear memory (Summarized in Fig. 28).

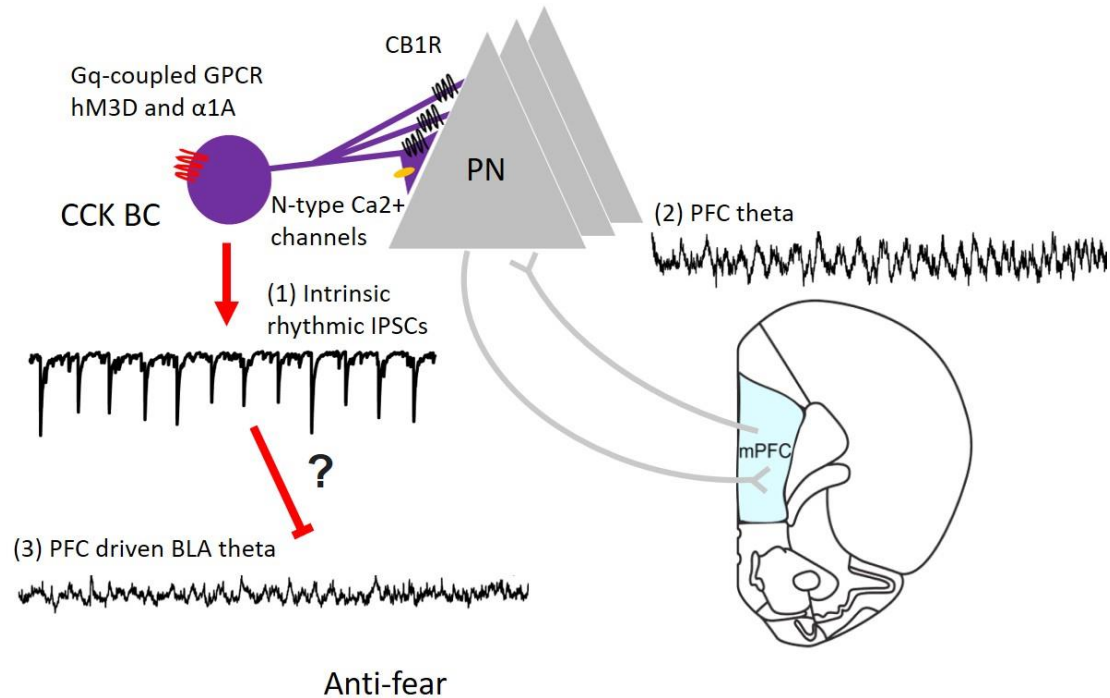


Figure 28. Summary diagram of suppression of fear learning by Gq activation of rhythmic IPSCs from CCK interneurons

NE stimulates a rhythmic pattern (~4Hz) of cannabinoid sensitive IPSCs in BLA principal neurons by Gq dependent $\alpha 1A$ noradrenergic activation of CCK basket cells (1). Activation of Gq signaling through hM3D and $\alpha 1A$ adrenoreceptors in the CCK interneurons suppressed the acquisition and expression of fear. During fear expression, the theta oscillation in the prefrontal cortex (2) entrained the BLA to generate the extrinsic PFC-driven theta (3) (Karalis et al., 2016). It is still not known whether the CCK-mediated rhythmic and synchronized IPSCs in the BLA, which have been shown in the hippocampus to enhance intrinsic theta oscillation (Alger et al., 2014; Nagode et al., 2011; Reich et al., 2005), interfere with the PFC-driven theta in the BLA and impair fear memory formation and retrieval.

Despite the documented role of NE in the facilitation of inhibitory synaptic transmission in the BLA (Braga et al., 2004; Miyajima et al., 2010), knowledge of the identities of the presynaptic interneurons and the patterns of synaptic activity activated by NE is still inconclusive. According to my previous double-dissociation experiments of NE-induced IPSCs with calcium channel blockers and a CB1 receptor agonist, the NE-induced initial inactivating trains of IPSCs are sensitive to inhibition of CCK BC-mediated transmission with N-type calcium channel blockade and CB1 receptor activation, while they are unaffected by blocking PV transmission with a P/Q-type calcium channel blocker. Consistent with this, I found in this study that the ω -agatoxin-insensitive IPSCs induced by NE underwent complete and transient DSI, a process mediated by depolarization-induced retrograde endocannabinoid signaling at CB1-expressing inhibitory synaptic terminals from CCK basket cells, suggesting that presynaptic CCK interneurons are responsible for the generation of the NE-induced IPSC trains. Moreover, as with the α 1A adrenoreceptor-dependent activation of PV interneurons, I found that the NE-induced IPSC trains were also mediated by activation of α 1A adrenoreceptors. To further support the role of CCK interneurons in generating the IPSC trains, I observed that most of the CCK interneurons in the BLA express α 1A adrenoreceptors and that restoration of the α 1A adrenoreceptors specifically in BLA CCK interneurons of the *adra1A* KO mouse rescued the NE-induced IPSC trains. Taken together, these data showed that α 1A noradrenergic activation of CCK interneurons generates the NE-induced trains of IPSCs in the BLA.

In line with the α 1A adrenoreceptors being a classic Gq-coupled GPCR, I found that inhibition of Gq signaling with a selective $G\alpha_{q/11}$ inhibitor YM-254890 eliminated

NE-induced IPSC trains. As signaling from multiple extracellular modulators converges onto the Gq signaling pathway to modulate neuronal excitability, it is possible that other neuromodulators acting on their cognate Gq-coupled receptors on the CCK interneurons may generate similar patterns of inhibitory output. Notably, I found that selective Gq activation of CCK interneurons with the hM3D DREADD generated similar trains of rhythmic IPSCs that were sensitive to N-type calcium channel blockade and underwent complete and transient DSI. Moreover, I showed that 5-HT, another native neuromodulator that plays important roles in regulating BLA activity and emotional processing, also stimulated CB1 sensitive trains of rhythmic IPSCs through the activation of Gq-coupled 5HT2C receptors. Interestingly, in the hippocampal CA1, activation of Gq-coupled M1/3 muscarinic receptors also induced similar rhythmic IPSCs from CCK interneurons at a frequency around 4 Hz that were sensitive to CB1 receptor activation (Alger et al., 2014; Nagode et al., 2011; Nagode et al., 2014). Thus, the generation of trains of rhythmic IPSCs in the principal neurons may serve as the functional output of Gq activation in the CCK interneurons by multiple neuromodulators carrying emotional salience. Whether this stereotyped response to Gq signaling in CCK neurons in the BLA generalizes to other cortical brain structures remains to be tested.

Selective genetic access to the CCK interneurons is hindered by the fact that low levels of CCK or its prohormone are expressed in the principal neurons (Taniguchi et al., 2011). As a result, an intersectional strategy combining Cre-driven recombination and interneuron specificity is required to target the CCK interneurons. Here, I utilized a recently reported GABA neuron-specific hDLX intersectional AAV virus (Dimidschstein et al., 2016; Liu et al., 2020), and was able to successfully target the CCK interneurons

with the expression of mCherry, an excitatory Gq DREADD, and α 1A adrenoreceptors. By re-expressing the α 1A adrenoreceptors in the CCK interneurons bilaterally in the BLA in a global *adra1A* knockout mouse line crossed with CCK-ires-Cre mouse (CCK-ires-Cre::*adra1A* KO), I found that α 1A noradrenergic activation of CCK interneurons by endogenously released NE suppressed the acquisition and expression of conditioned fear. Moreover, this effect was recapitulated by chemogenetic Gq activation of CCK interneurons during fear conditioning and fear retrieval, suggesting an essential role of the patterned rhythmic inhibitory output from CCK interneurons in fear memory formation. My finding of an inhibitory effect of CCK interneuron activation on conditioned fear is consistent with a prior study that showed that 20 Hz optogenetic stimulation of CCK interneurons during CS presentations facilitated fear extinction (Rovira-Esteban et al., 2019). In comparison with a study showing that whole-brain Gq activation of the CCK interneurons promotes fear learning (Whissell et al., 2019), my data provide brain region specificity and suggest that CCK interneurons in other brain areas may have opposite effects to the ones in the BLA.

In the cortex, hippocampus, and BLA, synchronized rhythmic perisomatic inhibition is critically involved in the generation of neural circuit oscillation. It has been well established that the rhythmic IPSCs induced by muscarinic activation of CCK interneurons drives theta oscillations in the CA1 (Alger et al., 2014; Nagode et al., 2011; Reich et al., 2005). As would be predicted from the synchronized rhythmic IPSCs at around 4 Hz, α 1A noradrenergic activation of CCK interneurons should increase the power of theta oscillation in the BLA. Emerging evidence has shown that oscillation at theta frequency in the BLA entrained from the prefrontal cortex is essential for the

expression of learned fear (Bocchio et al., 2017; Karalis et al., 2016), however, I found that the intrinsic CCK-mediated rhythmic bursts at theta frequency in the BLA suppress fear acquisition and expression. One possible explanation for the opposite effects of extrinsic and intrinsic theta oscillation on fear expression is phase interference, by which the intrinsically driven CCK basket cell-mediated rhythmic IPSCs disrupt the timing of the PFC-driven BLA theta oscillations, leading to an inhibition of fear expression. It will be fascinating with future experiments to test the effect of CCK Gq activation on BLA theta oscillations during fear memory retrieval.

CCK-positive GABAergic interneurons are heterogeneous, including both large-somata, CB1-positive basket cells and small-somata, CB1-negative cells that co-express vasoactive intestinal polypeptide (VIP) (Jasnow et al., 2009; Katona et al., 2001; Mascagni & McDonald, 2003; Vogel et al., 2016). As a result, CCK interneurons targeted with injection of DLX virus in the CCK-ires-Cre mice should include cells from both categories. I observed that Gq activation in the entire population of BLA CCK interneurons generated IPSCs in the principal cells that underwent strong DSI, nearly 100%, suggesting the principal neurons receive few, if any, inputs from the CCK-positive, CB1-negative VIP interneurons. This observation is consistent with the characteristic of VIP interneurons in the BLA projecting preferentially to other interneurons (Krabbe et al., 2019; Rhomberg et al., 2018). Functionally, the VIP interneurons have been shown to provide disinhibitory gating to the BLA principal cells and activation of these cells enhanced fear learning (Krabbe et al., 2019). Thus, whereas activation of the VIP interneurons alone facilitated associative fear learning, my findings demonstrated that activation of the whole CCK population, including both CCK basket

cells and CCK/VIP cells, inhibited the acquisition of fear memory. Taken together, my data indicate that CCK basket cells in the BLA restrain fear memory formation by generating rhythmic IPSCs in the principal neurons in response to NE release during fear learning. Whether the effect on fear memory formation is caused by inhibition of fear acquisition, suppression of fear expression, or both will require further studies to separate the effects of Gq activation on fear acquisition and recall.

Compared with the accelerating and repetitive bursts of IPSCs generated by Gq activation of PV interneurons, the CCK interneuron-mediated IPSCs driven by Gq activation exhibited a stable frequency and were clustered in a single train. Strikingly, I observed that the same ligands (CNO and NE) acting on the same receptors (hM3D and α 1A adrenoceptor, respectively) stimulated totally different patterned outputs in CCK and PV interneurons. This cell type-specific response may be generated by different electrophysiological properties and intracellular signaling targets in these two cell types (Armstrong & Soltesz, 2012). As neuromodulators typically work in a fashion of volume transmission to regulate the activity of populations of neurons, this interesting dichotomy of output pattern from the basket cells in response to Gq activation by the same ligand presents a mechanism for neuromodulators to provide precise regulation of their actions in the BLA neural circuits. Opposite to the facilitatory effect of α 1A noradrenergic signaling in PV interneurons on fear learning, activation of CCK interneurons through the same receptor inhibited the acquisition and expression of conditioned fear. This may explain why there was no effect on fear learning of the loss of α 1A adrenoceptors in the global *adra1A* knockout compared to wildtype controls. Overall, the diversified responses to one neuromodulator in PV and CCK interneurons presents a possible mechanism of

how stress can fine tune associative fear learning by balancing the contribution of different patterns of perisomatic inhibition.

In conclusion, I present a cellular mechanism for controlling fear memory formation through a rhythmic inhibitory synaptic output by Gq-coupled $\alpha 1A$ adrenergic activation of CCK interneurons in the BLA. Importantly, Gq signaling mediated by the same receptor in BLA PV interneurons generated a burst-firing pattern and facilitated fear learning. Thus, during emotional arousal, the ascending noradrenergic signaling may titrate the contribution of different patterns of perisomatic inputs to the BLA principal cells to achieve optimized fear memories.

5. Unified discussion

This work presented two sites of noradrenergic neuromodulation that influence the output of BLA neural circuits and the processing of fear. Presynaptic $\alpha 1A$ Gq activation in PV interneurons generates phasic bursts of IPSCs in the principal neurons that are blocked by P/Q-type calcium channel blocker, while $\alpha 1A$ activation in CCK interneurons induced singular rhythmic IPSC trains in the principal neurons that are sensitive to N-type calcium channel blockade and CB1 receptor activation. The $\alpha 1A$ subtype specificity of NE modulation of perisomatic inhibitory synaptic transmission in the BLA is demonstrated by the observations that (1) both CCK- and PV-type IPSCs were blocked and mimicked by $\alpha 1A$ receptor antagonist and agonist, (2) both types of IPSCs were lost in the global $\alpha 1A$ knockout mice, (3) the $\alpha 1A$ adrenoreceptors were selectively expressed in the BLA interneurons, including most of the CCK and PV interneurons, and (4) rescue of $\alpha 1A$ adrenergic signaling in the BLA CCK and PV interneurons in the global $\alpha 1A$ knockout mice selectively restored the CCK- and PV-type IPSCs to the principal neurons. $\alpha 1A$ Gq activation of PV interneurons in the BLA suppressed the BLA-PFC gamma oscillation and switched the network into a fear state. Cell-type specific re-expression of $\alpha 1A$ adrenoreceptors in the global $\alpha 1A$ knockout mice revealed that the patterned perisomatic IPSCs mediated by $\alpha 1A$ adrenergic activation of CCK and PV interneurons oppositely gate fear memory formation (Summarized in Fig. 29).

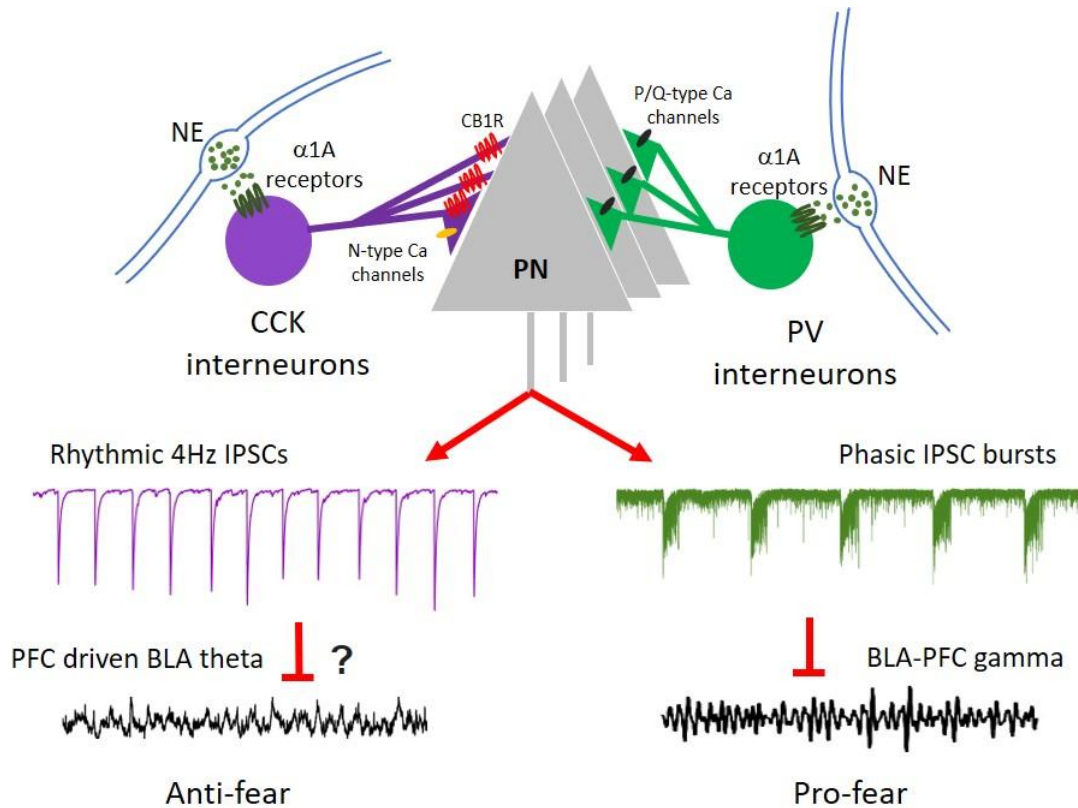


Figure 29. Summary diagram of dissociable roles of NE-stimulated CCK and PV perisomatic inhibition in fear learning

NE release in the BLA during stressful conditions (fear conditioning and fear retrieval) activates the perisomatic targeting CCK and PV interneurons by acting on the Gq-coupled $\alpha 1A$ adrenoreceptors, which generate different patterns of perisomatic inhibitory synaptic outputs to the BLA principal neurons. The switch of the operational mode of PV interneurons to phasic firing by $\alpha 1A$ adrenoreceptors suppresses the BLA-PFC gamma oscillation and facilitates the expression of fear. NE-activation of CCK basket cells generates a rhythmic pattern of IPSCs to the BLA principal neurons and inhibits the acquisition and expression of conditioned fear memory, which may be due to the interference of extrinsic BLA theta oscillation driven by the prefrontal cortex.

To the best of my knowledge, this is the first time to report the repetitive burst firing pattern in the PV fast-spiking interneurons, which are well known to fire high frequency and non-accommodating action potentials upon depolarization (Freund & Katona, 2007; Hu et al., 2014). This burst pattern suggests a Gq-activated oscillatory up and down phase of the membrane potential in the PV interneurons, which could be generated by a circuit or intrinsic mechanism. Interestingly, this firing pattern is not affected by blocking the inhibitory and excitatory synaptic transmission. Although the BLA PV interneurons are known to form a syncytium through electrical synapses (McDonald, 2020; Woodruff & Sah, 2007b), it is also unlikely that the burst firing pattern is mediated by the gap junctions between the PV interneurons as (1) there are multiple IPSCs bursts in the principal neurons that are generated independently, and (2) electrical coupling between PV cells per se would not generate alternating transitions in the oscillatory membrane potential. Thus, the Gq activation may induce an intrinsic pace-making activity in the PV interneurons through activating an oscillatory depolarization, or an oscillatory hyperpolarization superimposed on a stable depolarization, or interaction of oscillatory depolarization and hyperpolarization. Since the selective G α q inhibitor YM-254890 eliminated all PV-mediated IPSC events in the principal neurons, the signaling pathways downstream from G α q activation hence are essential for neural depolarization. Additionally, as the PV-mediated IPSC bursts exhibited a long phase interval (~20 to 60s), it is more likely that turning on and off the G α q-mediated neural activation, rather than activation and inactivation of the ion channels, gives rise to the burst firing at a slow frequency. As the G α q protein activation and inactivation is regulated by the GTPase-activating proteins (GAPs) and guanine nucleotide exchange

factors (GEFs) (Grundmann & Kostenis, 2017; Siderovski & Willard, 2005), it will be interesting with future experiments to test whether these associative proteins are involved in the generation of pace-making activity in the PV interneurons.

Although the CCK basket cells occupy a central position in the integration of the afferent neuromodulatory signals carrying emotional salience and the locally synthesized endocannabinoid signaling, relatively little is known about the role of neuromodulatory activation of the BLA CCK interneurons in the control of fear memory formation. My results demonstrated that α 1A noradrenergic Gq activation of CCK interneurons generated a rhythmic IPSC pattern in the principal neurons. Furthermore, rescue of the α 1A adrenergic signaling in the BLA CCK interneurons in global *adra1A* knockout mice suppressed the acquisition and expression of conditioned fear memory. However, the CCK interneurons represent a heterogeneous population, including at least the small-soma CCK/VIP interneurons and large-soma CCK basket cells (Jasnow et al., 2009; Katona et al., 2001; McDonald, 2020; Vogel et al., 2016). Thus, the inhibitory role of Gq activation of CCK basket cells in fear memory formation shown here is confounded by the activation of other types of CCK-positive interneurons in the CCK-ires-Cre mice, although the VIP interneurons have been shown to facilitate fear memory formation by disinhibiting the BLA principal neurons (Krabbe et al., 2019). As the CB1 receptors are exclusively expressed in the CCK basket cells among the interneuron populations (Katona et al., 2001; Yoshida et al., 2011), a better strategy to interrogate the function of CCK basket cells would be by the intersectional targeting of the CB1-expressing interneurons by applying the Cre-dependent, GABA neuron-selective hDLX virus to mice engineered to express Cre in CB1-expressing neurons. It will be fascinating in the

future to develop a CB1-Cre mouse line and tease apart CCK basket cells to clarify their roles in the operation of neural circuits and emotional processing.

In conclusion, NE exerts a dual modulation on BLA neural circuitry and fear memory formation through activation of different patterns of perisomatic inhibition from PV and CCK basket cells to the principal neurons. This suggests a well-balanced patterned perisomatic output from these basket cells is critical for the acquisition of appropriate fear memories during emotional arousal. A strategy that biases the engagement of these antagonistic perisomatic inhibitory inputs could be potentially used to treat stress- and fear-related mental health disorders.

6. References

- Adolphs, R., Tranel, D., Damasio, H., & Damasio, A. (1994). Impaired recognition of emotion in facial expressions following bilateral damage to the human amygdala. *Nature*, *372*(6507), 669-672. <https://doi.org/10.1038/372669a0>
- Alger, B. E., Nagode, D. A., & Tang, A.-H. (2014). Muscarinic cholinergic receptors modulate inhibitory synaptic rhythms in hippocampus and neocortex [Review]. *Frontiers in Synaptic Neuroscience*, *6*(18). <https://doi.org/10.3389/fnsyn.2014.00018>
- Amano, T., Duvarci, S., Popa, D., & Paré, D. (2011). The Fear Circuit Revisited: Contributions of the Basal Amygdala Nuclei to Conditioned Fear. *The Journal of Neuroscience*, *31*(43), 15481. <https://doi.org/10.1523/JNEUROSCI.3410-11.2011>
- Andrási, T., Veres, J. M., Rovira-Esteban, L., Kozma, R., Vikór, A., Gregori, E., & Hájos, N. (2017). Differential excitatory control of 2 parallel basket cell networks in amygdala microcircuits. *PLOS Biology*, *15*(5), e2001421. <https://doi.org/10.1371/journal.pbio.2001421>
- Armstrong, C., & Soltesz, I. (2012). Basket cell dichotomy in microcircuit function. *The Journal of physiology*, *590*(4), 683-694. <https://doi.org/https://doi.org/10.1113/jphysiol.2011.223669>
- Ascoli, G. A., Alonso-Nanclares, L., Anderson, S. A., Barrionuevo, G., Benavides-Piccione, R., Burkhalter, A., Buzsáki, G., Cauli, B., DeFelipe, J., Fairén, A., Feldmeyer, D., Fishell, G., Fregnac, Y., Freund, T. F., Gardner, D., Gardner, E. P., Goldberg, J. H., Helmstaedter, M., Hestrin, S., Karube, F., Kisvárdy, Z. F.,

- Lambolez, B., Lewis, D. A., Marin, O., Markram, H., Muñoz, A., Packer, A., Petersen, C. C. H., Rockland, K. S., Rossier, J., Rudy, B., Somogyi, P., Staiger, J. F., Tamas, G., Thomson, A. M., Toledo-Rodriguez, M., Wang, Y., West, D. C., Yuste, R., & The Petilla Interneuron Nomenclature, G. (2008). Petilla terminology: nomenclature of features of GABAergic interneurons of the cerebral cortex. *Nature Reviews Neuroscience*, *9*(7), 557-568. <https://doi.org/10.1038/nrn2402>
- Atsak, P., Hauer, D., Campolongo, P., Schelling, G., Fornari, R. V., & Roozendaal, B. (2015). Endocannabinoid Signaling within the Basolateral Amygdala Integrates Multiple Stress Hormone Effects on Memory Consolidation. *Neuropsychopharmacology*, *40*(6), 1485-1494. <https://doi.org/10.1038/npp.2014.334>
- Atsak, P., Roozendaal, B., & Campolongo, P. (2012). Role of the endocannabinoid system in regulating glucocorticoid effects on memory for emotional experiences. *Neuroscience*, *204*, 104-116. <https://doi.org/https://doi.org/10.1016/j.neuroscience.2011.08.047>
- Barsy, B., Szabó, G. G., Andrási, T., Vikór, A., & Hájos, N. (2017). Different output properties of perisomatic region-targeting interneurons in the basal amygdala. *European Journal of Neuroscience*, *45*(4), 548-558. <https://doi.org/https://doi.org/10.1111/ejn.13498>
- Bartos, M., Vida, I., & Jonas, P. (2007). Synaptic mechanisms of synchronized gamma oscillations in inhibitory interneuron networks. *Nature Reviews Neuroscience*, *8*(1), 45-56. <https://doi.org/10.1038/nrn2044>

- Blanchard, D. C., & Blanchard, R. J. (1972). Innate and conditioned reactions to threat in rats with amygdaloid lesions. *Journal of Comparative and Physiological Psychology*, *81*(2), 281-290. <https://doi.org/10.1037/h0033521>
- Bocchio, M., & Capogna, M. (2014). Oscillatory Substrates of Fear and Safety. *Neuron*, *83*(4), 753-755. <https://doi.org/https://doi.org/10.1016/j.neuron.2014.08.014>
- Bocchio, M., Nabavi, S., & Capogna, M. (2017). Synaptic Plasticity, Engrams, and Network Oscillations in Amygdala Circuits for Storage and Retrieval of Emotional Memories. *Neuron*, *94*(4), 731-743. <https://doi.org/https://doi.org/10.1016/j.neuron.2017.03.022>
- Braga, M. F. M., Aroniadou-Anderjaska, V., Manion, S. T., Hough, C. J., & Li, H. (2004). Stress Impairs α 1A Adrenoceptor-Mediated Noradrenergic Facilitation of GABAergic Transmission in the Basolateral Amygdala. *Neuropsychopharmacology*, *29*(1), 45-58. <https://doi.org/10.1038/sj.npp.1300297>
- Breen, A., Blankley, K., & Fine, J. (2017). The efficacy of prazosin for the treatment of posttraumatic stress disorder nightmares in U.S. military veterans. *Journal of the American Association of Nurse Practitioners*, *29*(2). https://journals.lww.com/jaanp/Fulltext/2017/02000/The_efficacy_of_prazosin_for_the_treatment_of.4.aspx
- Burgos-Robles, A., Vidal-Gonzalez, I., & Quirk, G. J. (2009). Sustained Conditioned Responses in Prelimbic Prefrontal Neurons Are Correlated with Fear Expression and Extinction Failure. *The Journal of Neuroscience*, *29*(26), 8474-8482. <https://doi.org/10.1523/jneurosci.0378-09.2009>

- Buzsáki, G., Anastassiou, C. A., & Koch, C. (2012). The origin of extracellular fields and currents — EEG, ECoG, LFP and spikes. *Nature Reviews Neuroscience*, *13*(6), 407-420. <https://doi.org/10.1038/nrn3241>
- Cahill, L., Babinsky, R., Markowitsch, H. J., & McGaugh, J. L. (1995). The amygdala and emotional memory. *Nature*, *377*(6547), 295-296. <https://doi.org/10.1038/377295a0>
- Campolongo, P., Roozendaal, B., Trezza, V., Hauer, D., Schelling, G., McGaugh, J. L., & Cuomo, V. (2009). Endocannabinoids in the rat basolateral amygdala enhance memory consolidation and enable glucocorticoid modulation of memory. *Proceedings of the National Academy of Sciences*, *106*(12), 4888-4893. <https://doi.org/10.1073/pnas.0900835106>
- Capogna, M. (2014). GABAergic cell type diversity in the basolateral amygdala. *Current Opinion in Neurobiology*, *26*, 110-116. <https://doi.org/https://doi.org/10.1016/j.conb.2014.01.006>
- Cardin, J. A., Carlén, M., Meletis, K., Knoblich, U., Zhang, F., Deisseroth, K., Tsai, L.-H., & Moore, C. I. (2009). Driving fast-spiking cells induces gamma rhythm and controls sensory responses. *Nature*, *459*(7247), 663-667. <https://doi.org/10.1038/nature08002>
- Chu, H.-Y., Ito, W., Li, J., & Morozov, A. (2012). Target-Specific Suppression of GABA Release from Parvalbumin Interneurons in the Basolateral Amygdala by Dopamine. *The Journal of Neuroscience*, *32*(42), 14815. <https://doi.org/10.1523/JNEUROSCI.2997-12.2012>

- Chung, L., & Moore, S. D. (2007). Cholecystokinin enhances GABAergic inhibitory transmission in basolateral amygdala. *Neuropeptides*, 41(6), 453-463. <https://doi.org/https://doi.org/10.1016/j.npep.2007.08.001>
- Chung, L., & Moore, S. D. (2009). Cholecystokinin Excites Interneurons in Rat Basolateral Amygdala. *Journal of Neurophysiology*, 102(1), 272-284. <https://doi.org/10.1152/jn.90769.2008>
- Ciocchi, S., Herry, C., Grenier, F., Wolff, S. B. E., Letzkus, J. J., Vlachos, I., Ehrlich, I., Sprengel, R., Deisseroth, K., Stadler, M. B., Müller, C., & Lüthi, A. (2010). Encoding of conditioned fear in central amygdala inhibitory circuits. *Nature*, 468(7321), 277-282. <https://doi.org/10.1038/nature09559>
- Courtin, J., Chaudun, F., Rozeske, R. R., Karalis, N., Gonzalez-Campo, C., Wurtz, H., Abdi, A., Baufreton, J., Bienvenu, T. C. M., & Herry, C. (2014). Prefrontal parvalbumin interneurons shape neuronal activity to drive fear expression. *Nature*, 505(7481), 92-96. <https://doi.org/10.1038/nature12755>
- de Kloet, E. R., Oitzl, M. S., & Joëls, M. (1999). Stress and cognition: are corticosteroids good or bad guys? *Trends in Neurosciences*, 22(10), 422-426. [https://doi.org/https://doi.org/10.1016/S0166-2236\(99\)01438-1](https://doi.org/https://doi.org/10.1016/S0166-2236(99)01438-1)
- Di, S., Itoga, C. A., Fisher, M. O., Solomonow, J., Roltsch, E. A., Gilpin, N. W., & Tasker, J. G. (2016). Acute Stress Suppresses Synaptic Inhibition and Increases Anxiety via Endocannabinoid Release in the Basolateral Amygdala. *The Journal of Neuroscience*, 36(32), 8461-8470. <https://doi.org/10.1523/jneurosci.2279-15.2016>

- Dimidschstein, J., Chen, Q., Tremblay, R., Rogers, S. L., Saldi, G.-A., Guo, L., Xu, Q., Liu, R., Lu, C., Chu, J., Grimley, J. S., Krostag, A.-R., Kaykas, A., Avery, M. C., Rashid, M. S., Baek, M., Jacob, A. L., Smith, G. B., Wilson, D. E., Kosche, G., Kruglikov, I., Rusielewicz, T., Kotak, V. C., Mowery, T. M., Anderson, S. A., Callaway, E. M., Dasen, J. S., Fitzpatrick, D., Fossati, V., Long, M. A., Noggle, S., Reynolds, J. H., Sanes, D. H., Rudy, B., Feng, G., & Fishell, G. (2016). A viral strategy for targeting and manipulating interneurons across vertebrate species. *Nature Neuroscience*, *19*(12), 1743-1749. <https://doi.org/10.1038/nn.4430>
- Duvarci, S., & Pare, D. (2014). Amygdala Microcircuits Controlling Learned Fear. *Neuron*, *82*(5), 966-980. <https://doi.org/https://doi.org/10.1016/j.neuron.2014.04.042>
- Duvarci, S., & Paré, D. (2007). Glucocorticoids Enhance the Excitability of Principal Basolateral Amygdala Neurons. *The Journal of Neuroscience*, *27*(16), 4482-4491. <https://doi.org/10.1523/jneurosci.0680-07.2007>
- Faber, E. S. L., Delaney, A. J., Power, J. M., Sedlak, P. L., Crane, J. W., & Sah, P. (2008). Modulation of SK Channel Trafficking by Beta Adrenoceptors Enhances Excitatory Synaptic Transmission and Plasticity in the Amygdala. *The Journal of Neuroscience*, *28*(43), 10803-10813. <https://doi.org/10.1523/jneurosci.1796-08.2008>
- Fadok, J. P., Krabbe, S., Markovic, M., Courtin, J., Xu, C., Massi, L., Botta, P., Bylund, K., Müller, C., Kovacevic, A., Tovote, P., & Lüthi, A. (2017). A competitive inhibitory circuit for selection of active and passive fear responses. *Nature*, *542*(7639), 96-100. <https://doi.org/10.1038/nature21047>

- Ferry, B., Roozendaal, B., & McGaugh, J. L. (1999). Involvement of α 1-adrenoceptors in the basolateral amygdala in modulation of memory storage. *European Journal of Pharmacology*, 372(1), 9-16. [https://doi.org/10.1016/S0014-2999\(99\)00169-7](https://doi.org/10.1016/S0014-2999(99)00169-7)
- Földy, C., Lee, S. Y., Szabadics, J., Neu, A., & Soltesz, I. (2007). Cell type-specific gating of perisomatic inhibition by cholecystokinin. *Nature Neuroscience*, 10(9), 1128-1130. <https://doi.org/10.1038/nn1952>
- Frances Davies, M., Tsui, J., Flannery, J. A., Li, X., DeLorey, T. M., & Hoffman, B. B. (2004). Activation of α 2 Adrenergic Receptors Suppresses Fear Conditioning: Expression of c-Fos and Phosphorylated CREB in Mouse Amygdala. *Neuropsychopharmacology*, 29(2), 229-239. <https://doi.org/10.1038/sj.npp.1300324>
- Freund, T. F. (2003). Interneuron Diversity series: Rhythm and mood in perisomatic inhibition. *Trends Neurosci*, 26(9), 489-495. [https://doi.org/10.1016/s0166-2236\(03\)00227-3](https://doi.org/10.1016/s0166-2236(03)00227-3)
- Freund, T. F., & Katona, I. (2007). Perisomatic Inhibition. *Neuron*, 56(1), 33-42. <https://doi.org/10.1016/j.neuron.2007.09.012>
- Fuchs, E. C., Zivkovic, A. R., Cunningham, M. O., Middleton, S., LeBeau, F. E. N., Bannerman, David M., Rozov, A., Whittington, M. A., Traub, R. D., Rawlins, J. N. P., & Monyer, H. (2007). Recruitment of Parvalbumin-Positive Interneurons Determines Hippocampal Function and Associated Behavior. *Neuron*, 53(4), 591-604. <https://doi.org/10.1016/j.neuron.2007.01.031>

- Galvez, R., Mesches, M. H., & McGaugh, J. L. (1996). Norepinephrine Release in the Amygdala in Response to Footshock Stimulation. *Neurobiology of Learning and Memory*, *66*(3), 253-257. <https://doi.org/10.1006/nlme.1996.0067>
- Garcia-Junco-Clemente, P., Tring, E., Ringach, D. L., & Trachtenberg, J. T. (2019). State-Dependent Subnetworks of Parvalbumin-Expressing Interneurons in Neocortex. *Cell Reports*, *26*(9), 2282-2288.e2283. <https://doi.org/10.1016/j.celrep.2019.02.005>
- Gazarini, L., Stern, C. A. J., Carobrez, A. P., & Bertoglio, L. J. (2013). Enhanced noradrenergic activity potentiates fear memory consolidation and reconsolidation by differentially recruiting α 1- and β -adrenergic receptors. *Learning & Memory*, *20*(4), 210-219. <https://doi.org/10.1101/lm.030007.112>
- Giltsbach, R., & Hein, L. (2012). Are the pharmacology and physiology of α 2adrenoceptors determined by α 2-heteroreceptors and autoreceptors respectively? *British Journal of Pharmacology*, *165*(1), 90-102. <https://doi.org/10.1111/j.1476-5381.2011.01533.x>
- Giustino, T. F., & Maren, S. (2018). Noradrenergic Modulation of Fear Conditioning and Extinction [Review]. *Frontiers in Behavioral Neuroscience*, *12*(43). <https://doi.org/10.3389/fnbeh.2018.00043>
- Giustino, T. F., Ramanathan, K. R., Totty, M. S., Miles, O. W., & Maren, S. (2020). Locus Coeruleus Norepinephrine Drives Stress-Induced Increases in Basolateral Amygdala Firing and Impairs Extinction Learning. *The Journal of Neuroscience*, *40*(4), 907-916. <https://doi.org/10.1523/jneurosci.1092-19.2019>

- Goosens, K. A., Hobin, J. A., & Maren, S. (2003). Auditory-evoked spike firing in the lateral amygdala and Pavlovian fear conditioning: mnemonic code or fear bias? *Neuron*, 40(5), 1013-1022. [https://doi.org/10.1016/s0896-6273\(03\)00728-1](https://doi.org/10.1016/s0896-6273(03)00728-1)
- Grundmann, M., & Kostenis, E. (2017). Temporal Bias: Time-Encoded Dynamic GPCR Signaling. *Trends in Pharmacological Sciences*, 38(12), 1110-1124. <https://doi.org/https://doi.org/10.1016/j.tips.2017.09.004>
- Guthman, E. M., Garcia, J. D., Ma, M., Chu, P., Baca, S. M., Smith, K. R., Restrepo, D., & Huntsman, M. M. (2020). Cell-type-specific control of basolateral amygdala neuronal circuits via entorhinal cortex-driven feedforward inhibition. *eLife*, 9, e50601. <https://doi.org/10.7554/eLife.50601>
- Haan, L. d., & Hirst, T. R. (2004). Cholera toxin: A paradigm for multi-functional engagement of cellular mechanisms (Review). *Molecular Membrane Biology*, 21(2), 77-92. <https://doi.org/10.1080/09687680410001663267>
- Hájos, N., Pálhalmi, J., Mann, E. O., Németh, B., Paulsen, O., & Freund, T. F. (2004). Spike Timing of Distinct Types of GABAergic Interneuron during Hippocampal Gamma Oscillations *In Vitro*. *The Journal of Neuroscience*, 24(41), 9127-9137. <https://doi.org/10.1523/jneurosci.2113-04.2004>
- Hamm, A. O., & Weike, A. I. (2005). The neuropsychology of fear learning and fear regulation. *International Journal of Psychophysiology*, 57(1), 5-14. <https://doi.org/https://doi.org/10.1016/j.ijpsycho.2005.01.006>
- Haubensak, W., Kunwar, P. S., Cai, H., Ciocchi, S., Wall, N. R., Ponnusamy, R., Biag, J., Dong, H.-W., Deisseroth, K., Callaway, E. M., Fanselow, M. S., Lüthi, A., & Anderson, D. J. (2010). Genetic dissection of an amygdala microcircuit that gates

conditioned fear. *Nature*, 468(7321), 270-276.
<https://doi.org/10.1038/nature09553>

Hefft, S., & Jonas, P. (2005). Asynchronous GABA release generates long-lasting inhibition at a hippocampal interneuron–principal neuron synapse. *Nature Neuroscience*, 8(10), 1319-1328. <https://doi.org/10.1038/nn1542>

Helmstetter, F. J., & Bellgowan, P. S. (1994). Effects of muscimol applied to the basolateral amygdala on acquisition and expression of contextual fear conditioning in rats. *Behav Neurosci*, 108(5), 1005-1009.
<https://doi.org/10.1037//0735-7044.108.5.1005>

Hendrickson, R. C., & Raskind, M. A. (2016). Noradrenergic dysregulation in the pathophysiology of PTSD. *Experimental Neurology*, 284, 181-195.
<https://doi.org/https://doi.org/10.1016/j.expneurol.2016.05.014>

Herry, C., Ciocchi, S., Senn, V., Demmou, L., Müller, C., & Lüthi, A. (2008). Switching on and off fear by distinct neuronal circuits. *Nature*, 454(7204), 600-606.
<https://doi.org/10.1038/nature07166>

Herry, C., & Johansen, J. P. (2014). Encoding of fear learning and memory in distributed neuronal circuits. *Nature Neuroscience*, 17(12), 1644-1654.
<https://doi.org/10.1038/nn.3869>

Holmgren, C., Harkany, T., Svennenfors, B., & Zilberter, Y. (2003). Pyramidal cell communication within local networks in layer 2/3 of rat neocortex. *The Journal of physiology*, 551(Pt 1), 139-153. <https://doi.org/10.1113/jphysiol.2003.044784>

- Hu, H., Gan, J., & Jonas, P. (2014). Fast-spiking, parvalbumin⁺ GABAergic interneurons: From cellular design to microcircuit function. *Science*, *345*(6196), 1255263. <https://doi.org/10.1126/science.1255263>
- Jasnow, A. M., Ressler, K. J., Hammack, S. E., Chhatwal, J. P., & Rainnie, D. G. (2009). Distinct Subtypes of Cholecystokinin (CCK)-Containing Interneurons of the Basolateral Amygdala Identified Using a CCK Promoter-Specific Lentivirus. *Journal of Neurophysiology*, *101*(3), 1494-1506. <https://doi.org/10.1152/jn.91149.2008>
- Jensen, B. C., Swigart, P. M., & Simpson, P. C. (2008). Ten commercial antibodies for alpha-1-adrenergic receptor subtypes are nonspecific. *Naunyn-Schmiedeberg's Archives of Pharmacology*, *379*(4), 409. <https://doi.org/10.1007/s00210-008-0368-6>
- Jiang, X., Xing, G., Yang, C., Verma, A., Zhang, L., & Li, H. (2009). Stress Impairs 5-HT_{2A} Receptor-Mediated Serotonergic Facilitation of GABA Release in Juvenile Rat Basolateral Amygdala. *Neuropsychopharmacology*, *34*(2), 410-423. <https://doi.org/10.1038/npp.2008.71>
- Joëls, M., & de Kloet, E. R. (1992). Control of neuronal excitability by corticosteroid hormones. *Trends in Neurosciences*, *15*(1), 25-30. [https://doi.org/https://doi.org/10.1016/0166-2236\(92\)90345-9](https://doi.org/https://doi.org/10.1016/0166-2236(92)90345-9)
- Johansen, Joshua P., Cain, Christopher K., Ostroff, Linnaea E., & LeDoux, Joseph E. (2011). Molecular Mechanisms of Fear Learning and Memory. *Cell*, *147*(3), 509-524. <https://doi.org/https://doi.org/10.1016/j.cell.2011.10.009>

- Johansen, J. P., Hamanaka, H., Monfils, M. H., Behnia, R., Deisseroth, K., Blair, H. T., & LeDoux, J. E. (2010). Optical activation of lateral amygdala pyramidal cells instructs associative fear learning. *Proceedings of the National Academy of Sciences*, *107*(28), 12692. <https://doi.org/10.1073/pnas.1002418107>
- Kaneko, K., Tamamaki, N., Owada, H., Kakizaki, T., Kume, N., Totsuka, M., Yamamoto, T., Yawo, H., Yagi, T., Obata, K., & Yanagawa, Y. (2008). Noradrenergic excitation of a subpopulation of GABAergic cells in the basolateral amygdala via both activation of nonselective cationic conductance and suppression of resting K⁺ conductance: A study using glutamate decarboxylase 67–green fluorescent protein knock-in mice. *Neuroscience*, *157*(4), 781-797. <https://doi.org/https://doi.org/10.1016/j.neuroscience.2008.09.029>
- Karalis, N., Dejean, C., Chaudun, F., Khoder, S., Rozeske, R. R., Wurtz, H., Bagur, S., Benchenane, K., Sirota, A., Courtin, J., & Herry, C. (2016). 4-Hz oscillations synchronize prefrontal–amygdala circuits during fear behavior. *Nature Neuroscience*, *19*(4), 605-612. <https://doi.org/10.1038/nn.4251>
- Karst, H., Berger, S., Erdmann, G., Schütz, G., & Joëls, M. (2010). Metaplasticity of amygdalar responses to the stress hormone corticosterone. *Proceedings of the National Academy of Sciences*, *107*(32), 14449-14454. <https://doi.org/10.1073/pnas.0914381107>
- Katada, T. (2012). The Inhibitory G Protein G_i Identified as Pertussis Toxin-Catalyzed ADP-Ribosylation. *Biological and Pharmaceutical Bulletin*, *35*(12), 2103-2111. <https://doi.org/10.1248/bpb.b212024>

- Katona, I., & Freund, T. F. (2008). Endocannabinoid signaling as a synaptic circuit breaker in neurological disease. *Nature Medicine*, *14*(9), 923-930. <https://doi.org/10.1038/nm.f.1869>
- Katona, I., Rancz, E. A., Acsády, L., Ledent, C., Mackie, K., Hájos, N., & Freund, T. F. (2001). Distribution of CB1 Cannabinoid Receptors in the Amygdala and their Role in the Control of GABAergic Transmission. *The Journal of Neuroscience*, *21*(23), 9506-9518. <https://doi.org/10.1523/jneurosci.21-23-09506.2001>
- Kim, J. J., & Jung, M. W. (2006). Neural circuits and mechanisms involved in Pavlovian fear conditioning: a critical review. *Neurosci Biobehav Rev*, *30*(2), 188-202. <https://doi.org/10.1016/j.neubiorev.2005.06.005>
- Kim, J. J., Rison, R. A., & Fanselow, M. S. (1993). Effects of amygdala, hippocampus, and periaqueductal gray lesions on short- and long-term contextual fear. *Behav Neurosci*, *107*(6), 1093-1098. <https://doi.org/10.1037//0735-7044.107.6.1093>
- Klüver, H., & Bucy, P. C. (1937). "Psychic blindness" and other symptoms following bilateral temporal lobectomy in Rhesus monkeys. *American Journal of Physiology*, *119*, 352-353.
- Kondo, S., & Kawaguchi, Y. (2001). Slow synchronized bursts of inhibitory postsynaptic currents (0.1–0.3 Hz) by cholinergic stimulation in the rat frontal cortex in vitro. *Neuroscience*, *107*(4), 551-560. [https://doi.org/https://doi.org/10.1016/S0306-4522\(01\)00388-8](https://doi.org/https://doi.org/10.1016/S0306-4522(01)00388-8)
- Krabbe, S., Gründemann, J., & Lüthi, A. (2018). Amygdala Inhibitory Circuits Regulate Associative Fear Conditioning. *Biological Psychiatry*, *83*(10), 800-809. <https://doi.org/https://doi.org/10.1016/j.biopsych.2017.10.006>

- Krabbe, S., Paradiso, E., d'Aquin, S., Bitterman, Y., Courtin, J., Xu, C., Yonehara, K., Markovic, M., Müller, C., Eichlisberger, T., Gründemann, J., Ferraguti, F., & Lüthi, A. (2019). Adaptive disinhibitory gating by VIP interneurons permits associative learning. *Nature Neuroscience*, 22(11), 1834-1843. <https://doi.org/10.1038/s41593-019-0508-y>
- Krashes, M. J., Koda, S., Ye, C., Rogan, S. C., Adams, A. C., Cusher, D. S., Maratos-Flier, E., Roth, B. L., & Lowell, B. B. (2011). Rapid, reversible activation of AgRP neurons drives feeding behavior in mice. *The Journal of Clinical Investigation*, 121(4), 1424-1428. <https://doi.org/10.1172/JCI46229>
- LaBar, K. S., Gatenby, J. C., Gore, J. C., LeDoux, J. E., & Phelps, E. A. (1998). Human amygdala activation during conditioned fear acquisition and extinction: a mixed-trial fMRI study. *Neuron*, 20(5), 937-945. [https://doi.org/10.1016/s0896-6273\(00\)80475-4](https://doi.org/10.1016/s0896-6273(00)80475-4)
- Lang, P. J., Bradley, M. M., & Cuthbert, B. N. (1997). Motivated attention: Affect, activation, and action. In *Attention and orienting: Sensory and motivational processes*. (pp. 97-135). Lawrence Erlbaum Associates Publishers.
- Lazzaro, S. C., Hou, M., Cunha, C., LeDoux, J. E., & Cain, C. K. (2010). Antagonism of lateral amygdala alpha1-adrenergic receptors facilitates fear conditioning and long-term potentiation. *Learning & Memory*, 17(10), 489-493. <https://doi.org/10.1101/lm.1918210>
- LeDoux, J. E. (2014). Coming to terms with fear. *Proceedings of the National Academy of Sciences*, 111(8), 2871. <https://doi.org/10.1073/pnas.1400335111>

- Lee, S.-H., & Dan, Y. (2012). Neuromodulation of Brain States. *Neuron*, 76(1), 209-222.
<https://doi.org/https://doi.org/10.1016/j.neuron.2012.09.012>
- Lee, S. Y., Földy, C., Szabadics, J., & Soltesz, I. (2011). Cell-Type-Specific CCK2 Receptor Signaling Underlies the Cholecystinin-Mediated Selective Excitation of Hippocampal Parvalbumin-Positive Fast-Spiking Basket Cells. *The Journal of Neuroscience*, 31(30), 10993-11002. <https://doi.org/10.1523/jneurosci.1970-11.2011>
- Levitsky, K. L., Toledo-Aral, J. J., López-Barneo, J., & Villadiego, J. (2013). Direct confocal acquisition of fluorescence from X-gal staining on thick tissue sections. *Scientific Reports*, 3(1), 2937. <https://doi.org/10.1038/srep02937>
- Li, H., Penzo, M. A., Taniguchi, H., Kopec, C. D., Huang, Z. J., & Li, B. (2013). Experience-dependent modification of a central amygdala fear circuit. *Nat Neurosci*, 16(3), 332-339. <https://doi.org/10.1038/nn.3322>
- Lissek, S., Rabin, S., Heller, R. E., Lukenbaugh, D., Geraci, M., Pine, D. S., & Grillon, C. (2010). Overgeneralization of conditioned fear as a pathogenic marker of panic disorder. *Am J Psychiatry*, 167(1), 47-55.
<https://doi.org/10.1176/appi.ajp.2009.09030410>
- Liu, X., Dimidschstein, J., Fishell, G., & Carter, A. G. (2020). Hippocampal inputs engage CCK+ interneurons to mediate endocannabinoid-modulated feed-forward inhibition in the prefrontal cortex. *eLife*, 9, e55267.
<https://doi.org/10.7554/eLife.55267>
- Lucas, E. K., Wu, W.-C., Roman-Ortiz, C., & Clem, R. L. (2019). Prazosin during fear conditioning facilitates subsequent extinction in male C57Bl/6N mice.

Psychopharmacology, 236(1), 273-279. <https://doi.org/10.1007/s00213-018-5001-x>

- Lupien, S. J., & McEwen, B. S. (1997). The acute effects of corticosteroids on cognition: integration of animal and human model studies. *Brain Research Reviews*, 24(1), 1-27. [https://doi.org/10.1016/S0165-0173\(97\)00004-0](https://doi.org/10.1016/S0165-0173(97)00004-0)
- Marek, R., Jin, J., Goode, T. D., Giustino, T. F., Wang, Q., Acca, G. M., Holehonnur, R., Ploski, J. E., Fitzgerald, P. J., Lynagh, T., Lynch, J. W., Maren, S., & Sah, P. (2018). Hippocampus-driven feed-forward inhibition of the prefrontal cortex mediates relapse of extinguished fear. *Nature Neuroscience*, 21(3), 384-392. <https://doi.org/10.1038/s41593-018-0073-9>
- Mascagni, F., & McDonald, A. J. (2003). Immunohistochemical characterization of cholecystokinin containing neurons in the rat basolateral amygdala. *Brain Res*, 976(2), 171-184. [https://doi.org/10.1016/s0006-8993\(03\)02625-8](https://doi.org/10.1016/s0006-8993(03)02625-8)
- McCall, Jordan G., Al-Hasani, R., Siuda, Edward R., Hong, Daniel Y., Norris, Aaron J., Ford, Christopher P., & Bruchas, Michael R. (2015). CRH Engagement of the Locus Coeruleus Noradrenergic System Mediates Stress-Induced Anxiety. *Neuron*, 87(3), 605-620. <https://doi.org/10.1016/j.neuron.2015.07.002>
- McCall, J. G., Siuda, E. R., Bhatti, D. L., Lawson, L. A., McElligott, Z. A., Stuber, G. D., & Bruchas, M. R. (2017). Locus coeruleus to basolateral amygdala noradrenergic projections promote anxiety-like behavior. *eLife*, 6, e18247. <https://doi.org/10.7554/eLife.18247>

- McDonald, A. J. (1989). Coexistence of somatostatin with neuropeptide Y, but not with cholecystokinin or vasoactive intestinal peptide, in neurons of the rat amygdala. *Brain Res*, 500(1-2), 37-45. [https://doi.org/10.1016/0006-8993\(89\)90297-7](https://doi.org/10.1016/0006-8993(89)90297-7)
- McDonald, A. J. (2020). Chapter 1 - Functional neuroanatomy of the basolateral amygdala: Neurons, neurotransmitters, and circuits. In J. H. Urban & J. A. Rosenkranz (Eds.), *Handbook of Behavioral Neuroscience* (Vol. 26, pp. 1-38). Elsevier. <https://doi.org/https://doi.org/10.1016/B978-0-12-815134-1.00001-5>
- McDonald, A. J., Mascagni, F., & Zaric, V. (2012). Subpopulations of somatostatin-immunoreactive non-pyramidal neurons in the amygdala and adjacent external capsule project to the basal forebrain: evidence for the existence of GABAergic projection neurons in the cortical nuclei and basolateral nuclear complex. *Front Neural Circuits*, 6, 46. <https://doi.org/10.3389/fncir.2012.00046>
- McGarry, L. M., & Carter, A. G. (2016). Inhibitory Gating of Basolateral Amygdala Inputs to the Prefrontal Cortex. *The Journal of Neuroscience*, 36(36), 9391-9406. <https://doi.org/10.1523/jneurosci.0874-16.2016>
- McGaugh, J. L. (2004). The amygdala modulates the consolidation of memories of emotionally arousing experiences. *Annu Rev Neurosci*, 27, 1-28. <https://doi.org/10.1146/annurev.neuro.27.070203.144157>
- McIntyre, C. K., Hatfield, T., & McGaugh, J. L. (2002). Amygdala norepinephrine levels after training predict inhibitory avoidance retention performance in rats. *European Journal of Neuroscience*, 16(7), 1223-1226. <https://doi.org/https://doi.org/10.1046/j.1460-9568.2002.02188.x>

- Miyajima, M., Ozaki, M., Wada, K., & Sekiguchi, M. (2010). Noradrenaline-induced spontaneous inhibitory postsynaptic currents in mouse basolateral nucleus of amygdala pyramidal neurons: Comparison with dopamine-induced currents. *Neuroscience Letters*, 480(3), 167-172. <https://doi.org/10.1016/j.neulet.2010.06.001>
- Morena, M., Patel, S., Bains, J. S., & Hill, M. N. (2016). Neurobiological Interactions Between Stress and the Endocannabinoid System. *Neuropsychopharmacology*, 41(1), 80-102. <https://doi.org/10.1038/npp.2015.166>
- Morris, J. S., Frith, C. D., Perrett, D. I., Rowland, D., Young, A. W., Calder, A. J., & Dolan, R. J. (1996). A differential neural response in the human amygdala to fearful and happy facial expressions. *Nature*, 383(6603), 812-815. <https://doi.org/10.1038/383812a0>
- Muller, J., Corodimas, K. P., Fridel, Z., & LeDoux, J. E. (1997). Functional inactivation of the lateral and basal nuclei of the amygdala by muscimol infusion prevents fear conditioning to an explicit conditioned stimulus and to contextual stimuli. *Behav Neurosci*, 111(4), 683-691. <https://doi.org/10.1037//0735-7044.111.4.683>
- Muller, J. F., Mascagni, F., & McDonald, A. J. (2007). Postsynaptic targets of somatostatin-containing interneurons in the rat basolateral amygdala. *J Comp Neurol*, 500(3), 513-529. <https://doi.org/10.1002/cne.21185>
- Muller, J. F., Mascagni, F., & McDonald, A. J. (2009). Dopaminergic innervation of pyramidal cells in the rat basolateral amygdala. *Brain Structure and Function*, 213(3), 275-288. <https://doi.org/10.1007/s00429-008-0196-y>

- Nagode, D. A., Tang, A.-H., Karson, M. A., Klugmann, M., & Alger, B. E. (2011). Optogenetic Release of ACh Induces Rhythmic Bursts of Perisomatic IPSCs in Hippocampus. *PLoS One*, 6(11), e27691. <https://doi.org/10.1371/journal.pone.0027691>
- Nagode, D. A., Tang, A.-H., Yang, K., & Alger, B. E. (2014). Optogenetic identification of an intrinsic cholinergically driven inhibitory oscillator sensitive to cannabinoids and opioids in hippocampal CA1 [<https://doi.org/10.1113/jphysiol.2013.257428>]. *The Journal of physiology*, 592(1), 103-123. <https://doi.org/https://doi.org/10.1113/jphysiol.2013.257428>
- Owen, S. F., Tuncdemir, S. N., Bader, P. L., Tirko, N. N., Fishell, G., & Tsien, R. W. (2013). Oxytocin enhances hippocampal spike transmission by modulating fast-spiking interneurons. *Nature*, 500(7463), 458-462. <https://doi.org/10.1038/nature12330>
- Parsons, R. G., & Ressler, K. J. (2013). Implications of memory modulation for post-traumatic stress and fear disorders. *Nature Neuroscience*, 16(2), 146-153. <https://doi.org/10.1038/nn.3296>
- Pavlidis, C., & McEwen, B. S. (1999). Effects of mineralocorticoid and glucocorticoid receptors on long-term potentiation in the CA3 hippocampal field. *Brain Research*, 851(1), 204-214. [https://doi.org/https://doi.org/10.1016/S0006-8993\(99\)02188-5](https://doi.org/https://doi.org/10.1016/S0006-8993(99)02188-5)
- Pavlidis, C., Ogawa, S., Kimura, A., & McEwen, B. S. (1996). Role of adrenal steroid mineralocorticoid and glucocorticoid receptors in long-term potentiation in the

- CA1 field of hippocampal slices. *Brain Research*, 738(2), 229-235.
[https://doi.org/https://doi.org/10.1016/S0006-8993\(96\)00776-7](https://doi.org/https://doi.org/10.1016/S0006-8993(96)00776-7)
- Penzo, M. A., Robert, V., & Li, B. (2014). Fear Conditioning Potentiates Synaptic Transmission onto Long-Range Projection Neurons in the Lateral Subdivision of Central Amygdala. *The Journal of Neuroscience*, 34(7), 2432.
<https://doi.org/10.1523/JNEUROSCI.4166-13.2014>
- Pierce, K. L., Premont, R. T., & Lefkowitz, R. J. (2002). Seven-transmembrane receptors. *Nature Reviews Molecular Cell Biology*, 3(9), 639-650.
<https://doi.org/10.1038/nrm908>
- Polack, P.-O., Friedman, J., & Golshani, P. (2013). Cellular mechanisms of brain state-dependent gain modulation in visual cortex. *Nature Neuroscience*, 16(9), 1331-1339. <https://doi.org/10.1038/nn.3464>
- Quirarte, G. L., Galvez, R., Roozendaal, B., & McGaugh, J. L. (1998). Norepinephrine release in the amygdala in response to footshock and opioid peptidergic drugs. *Brain Research*, 808(2), 134-140. [https://doi.org/https://doi.org/10.1016/S0006-8993\(98\)00795-1](https://doi.org/https://doi.org/10.1016/S0006-8993(98)00795-1)
- Quirarte, G. L., Roozendaal, B., & McGaugh, J. L. (1997). Glucocorticoid enhancement of memory storage involves noradrenergic activation in the basolateral amygdala. *Proceedings of the National Academy of Sciences*, 94(25), 14048-14053.
<https://doi.org/10.1073/pnas.94.25.14048>
- Quirk, G. J., Reppas, C., & LeDoux, J. E. (1995). Fear conditioning enhances short-latency auditory responses of lateral amygdala neurons: parallel recordings in the freely

- behaving rat. *Neuron*, 15(5), 1029-1039. [https://doi.org/10.1016/0896-6273\(95\)90092-6](https://doi.org/10.1016/0896-6273(95)90092-6)
- Reich, C. G., Karson, M. A., Karnup, S. V., Jones, L. M., & Alger, B. E. (2005). Regulation of IPSP Theta Rhythm by Muscarinic Receptors and Endocannabinoids in Hippocampus. *Journal of Neurophysiology*, 94(6), 4290-4299. <https://doi.org/10.1152/jn.00480.2005>
- Rodrigues, S. M., LeDoux, J. E., & Sapolsky, R. M. (2009). The Influence of Stress Hormones on Fear Circuitry. *Annual Review of Neuroscience*, 32(1), 289-313. <https://doi.org/10.1146/annurev.neuro.051508.135620>
- Rogan, M. T., Stäubli, U. V., & LeDoux, J. E. (1997). Fear conditioning induces associative long-term potentiation in the amygdala. *Nature*, 390(6660), 604-607. <https://doi.org/10.1038/37601>
- Rokosh, D. G., & Simpson, P. C. (2002). Knockout of the α 1A/C-adrenergic receptor subtype: The α 1A/C is expressed in resistance arteries and is required to maintain arterial blood pressure. *Proceedings of the National Academy of Sciences*, 99(14), 9474-9479. <https://doi.org/10.1073/pnas.132552699>
- Roozendaal, B., McEwen, B. S., & Chattarji, S. (2009). Stress, memory and the amygdala. *Nature Reviews Neuroscience*, 10(6), 423-433. <https://doi.org/10.1038/nrn2651>
- Roozendaal, B., Portillo-Marquez, G., & McGaugh, J. L. (1996). Basolateral amygdala lesions block glucocorticoid-induced modulation of memory for spatial learning. *Behavioral Neuroscience*, 110(5), 1074-1083. <https://doi.org/10.1037/0735-7044.110.5.1074>

- Rovira-Esteban, L., Gunduz-Cinar, O., Bukalo, O., Limoges, A., Brockway, E., Müller, K., Fenno, L., Kim, Y. S., Ramakrishnan, C., Andrási, T., Deisseroth, K., Holmes, A., & Hájos, N. (2019). Excitation of Diverse Classes of Cholecystokinin Interneurons in the Basal Amygdala Facilitates Fear Extinction. *eneuro*, 6(6), ENEURO.0220-0219.2019. <https://doi.org/10.1523/eneuro.0220-19.2019>
- Rovira-Esteban, L., Péterfi, Z., Vikór, A., Máté, Z., Szabó, G., & Hájos, N. (2017). Morphological and physiological properties of CCK/CB1R-expressing interneurons in the basal amygdala. *Brain Structure and Function*, 222(8), 3543-3565. <https://doi.org/10.1007/s00429-017-1417-z>
- Rumpel, S., LeDoux, J., Zador, A., & Malinow, R. (2005). Postsynaptic receptor trafficking underlying a form of associative learning. *Science*, 308(5718), 83-88. <https://doi.org/10.1126/science.1103944>
- Ryan, S. J., Ehrlich, D. E., Jasnow, A. M., Daftary, S., Madsen, T. E., & Rainnie, D. G. (2012). Spike-timing precision and neuronal synchrony are enhanced by an interaction between synaptic inhibition and membrane oscillations in the amygdala. *PLoS One*, 7(4), e35320. <https://doi.org/10.1371/journal.pone.0035320>
- Schafe, G. E., Doyère, V., & LeDoux, J. E. (2005). Tracking the Fear Engram: The Lateral Amygdala Is an Essential Locus of Fear Memory Storage. *The Journal of Neuroscience*, 25(43), 10010. <https://doi.org/10.1523/JNEUROSCI.3307-05.2005>
- Schottenbauer, M. A., Glass, C. R., Arnkoff, D. B., Tendick, V., & Gray, S. H. (2008). Nonresponse and Dropout Rates in Outcome Studies on PTSD: Review and Methodological Considerations. *Psychiatry*, 71(2), 134-168. <https://doi.org/10.1521/psyc.2008.71.2.134>

- Schrage, R., Schmitz, A.-L., Gaffal, E., Annala, S., Kehraus, S., Wenzel, D., Büllsbach, K. M., Bald, T., Inoue, A., Shinjo, Y., Galandrin, S., Shridhar, N., Hesse, M., Grundmann, M., Merten, N., Charpentier, T. H., Martz, M., Butcher, A. J., Slodczyk, T., Armando, S., Effern, M., Namkung, Y., Jenkins, L., Horn, V., Stöbel, A., Dargatz, H., Tietze, D., Imhof, D., Galés, C., Drewke, C., Müller, C. E., Hölzel, M., Milligan, G., Tobin, A. B., Gomeza, J., Dohlman, H. G., Sondek, J., Harden, T. K., Bouvier, M., Laporte, S. A., Aoki, J., Fleischmann, B. K., Mohr, K., König, G. M., Tüting, T., & Kostenis, E. (2015). The experimental power of FR900359 to study Gq-regulated biological processes. *Nature Communications*, 6(1), 10156. <https://doi.org/10.1038/ncomms10156>
- Senn, V., Wolff, Steffen B. E., Herry, C., Grenier, F., Ehrlich, I., Gründemann, J., Fadok, Jonathan P., Müller, C., Letzkus, Johannes J., & Lüthi, A. (2014). Long-Range Connectivity Defines Behavioral Specificity of Amygdala Neurons. *Neuron*, 81(2), 428-437. <https://doi.org/https://doi.org/10.1016/j.neuron.2013.11.006>
- Siderovski, D. P., & Willard, F. S. (2005). The GAPs, GEFs, and GDIs of heterotrimeric G-protein alpha subunits [Review]. *International Journal of Biological Sciences*, 1, 51-66. <https://doi.org/10.7150/ijbs.1.51>
- Sierra-Mercado, D., Padilla-Coreano, N., & Quirk, G. J. (2011). Dissociable Roles of Prelimbic and Infralimbic Cortices, Ventral Hippocampus, and Basolateral Amygdala in the Expression and Extinction of Conditioned Fear. *Neuropsychopharmacology*, 36(2), 529-538. <https://doi.org/10.1038/npp.2010.184>
- Singewald, N., Salchner, P., & Sharp, T. (2003). Induction of c-Fos expression in specific areas of the fear circuitry in rat forebrain by anxiogenic drugs. *Biological*

Psychiatry, 53(4), 275-283. [https://doi.org/https://doi.org/10.1016/S0006-3223\(02\)01574-3](https://doi.org/https://doi.org/10.1016/S0006-3223(02)01574-3)

Singh, B., Hughes, A. J., Mehta, G., Erwin, P. J., & Parsaik, A. K. (2016). Efficacy of Prazosin in Posttraumatic Stress Disorder: A Systematic Review and Meta-Analysis. *The primary care companion for CNS disorders*, 18(4). Retrieved 2016/07//, from <http://europepmc.org/abstract/MED/27828694>

<https://doi.org/10.4088/PCC.16r01943>

Smith, Y., Paré, J.-F., & Paré, D. (2000). Differential innervation of parvalbumin-immunoreactive interneurons of the basolateral amygdaloid complex by cortical and intrinsic inputs. *Journal of Comparative Neurology*, 416(4), 496-508. [https://doi.org/https://doi.org/10.1002/\(SICI\)1096-9861\(20000124\)416:4<496::AID-CNE6>3.0.CO;2-N](https://doi.org/https://doi.org/10.1002/(SICI)1096-9861(20000124)416:4<496::AID-CNE6>3.0.CO;2-N)

Sohal, V. S., Zhang, F., Yizhar, O., & Deisseroth, K. (2009). Parvalbumin neurons and gamma rhythms enhance cortical circuit performance. *Nature*, 459(7247), 698-702. <https://doi.org/10.1038/nature07991>

Sotres-Bayon, F., Sierra-Mercado, D., Pardilla-Delgado, E., & Quirk, Gregory J. (2012). Gating of Fear in Prelimbic Cortex by Hippocampal and Amygdala Inputs. *Neuron*, 76(4), 804-812. <https://doi.org/https://doi.org/10.1016/j.neuron.2012.09.028>

Spampanato, J., Polepalli, J., & Sah, P. (2011). Interneurons in the basolateral amygdala. *Neuropharmacology*, 60(5), 765-773. <https://doi.org/10.1016/j.neuropharm.2010.11.006>

- Stringfield, S. J., Higginbotham, J. A., & Fuchs, R. A. (2016). Requisite Role of Basolateral Amygdala Glucocorticoid Receptor Stimulation in Drug Context-Induced Cocaine-Seeking Behavior. *International Journal of Neuropsychopharmacology*, *19*(12). <https://doi.org/10.1093/ijnp/pyw073>
- Stujenske, Joseph M., Likhtik, E., Topiwala, Mihir A., & Gordon, Joshua A. (2014). Fear and Safety Engage Competing Patterns of Theta-Gamma Coupling in the Basolateral Amygdala. *Neuron*, *83*(4), 919-933. <https://doi.org/https://doi.org/10.1016/j.neuron.2014.07.026>
- Takasaki, J., Saito, T., Taniguchi, M., Kawasaki, T., Moritani, Y., Hayashi, K., & Kobori, M. (2004). A Novel Gαq/11-selective Inhibitor*. *Journal of Biological Chemistry*, *279*(46), 47438-47445. <https://doi.org/https://doi.org/10.1074/jbc.M408846200>
- Tamamaki, N., Yanagawa, Y., Tomioka, R., Miyazaki, J.-I., Obata, K., & Kaneko, T. (2003). Green fluorescent protein expression and colocalization with calretinin, parvalbumin, and somatostatin in the GAD67-GFP knock-in mouse. *Journal of Comparative Neurology*, *467*(1), 60-79. <https://doi.org/https://doi.org/10.1002/cne.10905>
- Taniguchi, H., He, M., Wu, P., Kim, S., Paik, R., Sugino, K., Kvitsani, D., Fu, Y., Lu, J., Lin, Y., Miyoshi, G., Shima, Y., Fishell, G., Nelson, Sacha B., & Huang, Z. J. (2011). A Resource of Cre Driver Lines for Genetic Targeting of GABAergic Neurons in Cerebral Cortex. *Neuron*, *71*(6), 995-1013. <https://doi.org/https://doi.org/10.1016/j.neuron.2011.07.026>

- Trouche, S., Sasaki, Jennifer M., Tu, T., & Reijmers, Leon G. (2013). Fear Extinction Causes Target-Specific Remodeling of Perisomatic Inhibitory Synapses. *Neuron*, 80(4), 1054-1065. <https://doi.org/10.1016/j.neuron.2013.07.047>
- Varga, C., Lee, S. Y., & Soltesz, I. (2010). Target-selective GABAergic control of entorhinal cortex output. *Nature Neuroscience*, 13(7), 822-824. <https://doi.org/10.1038/nn.2570>
- Vereczki, V. K., Veres, J. M., Müller, K., Nagy, G. A., Rácz, B., Barsy, B., & Hájos, N. (2016). Synaptic Organization of Perisomatic GABAergic Inputs onto the Principal Cells of the Mouse Basolateral Amygdala [Original Research]. *Frontiers in Neuroanatomy*, 10(20). <https://doi.org/10.3389/fnana.2016.00020>
- Veres, J. M., Nagy, G. A., & Hájos, N. (2017). Perisomatic GABAergic synapses of basket cells effectively control principal neuron activity in amygdala networks. *eLife*, 6, e20721. <https://doi.org/10.7554/eLife.20721>
- Vogel, E., Krabbe, S., Gründemann, J., Wamsteeker Cusulin, J. I., & Lüthi, A. (2016). Projection-Specific Dynamic Regulation of Inhibition in Amygdala Micro-Circuits. *Neuron*, 91(3), 644-651. <https://doi.org/10.1016/j.neuron.2016.06.036>
- Weiskrantz, L. (1956). Behavioral changes associated with ablation of the amygdaloid complex in monkeys. *Journal of Comparative and Physiological Psychology*, 49(4), 381-391. <https://doi.org/10.1037/h0088009>
- Wester, J. C., & McBain, C. J. (2014). Behavioral state-dependent modulation of distinct interneuron subtypes and consequences for circuit function. *Current Opinion in*

<https://doi.org/https://doi.org/10.1016/j.conb.2014.07.007>

- Whissell, P. D., Bang, J. Y., Khan, I., Xie, Y.-F., Parfitt, G. M., Grenon, M., Plummer, N. W., Jensen, P., Bonin, R. P., & Kim, J. C. (2019). Selective Activation of Cholecystinin-Expressing GABA (CCK-GABA) Neurons Enhances Memory and Cognition. *eneuro*, 6(1), ENEURO.0360-0318.2019. <https://doi.org/10.1523/eneuro.0360-18.2019>
- Wilensky, A. E., Schafe, G. E., & LeDoux, J. E. (1999). Functional inactivation of the amygdala before but not after auditory fear conditioning prevents memory formation. *J Neurosci*, 19(24), Rc48. <https://doi.org/10.1523/JNEUROSCI.19-24-j0006.1999>
- Wilson, R. I., Kunos, G., & Nicoll, R. A. (2001). Presynaptic Specificity of Endocannabinoid Signaling in the Hippocampus. *Neuron*, 31(3), 453-462. [https://doi.org/https://doi.org/10.1016/S0896-6273\(01\)00372-5](https://doi.org/https://doi.org/10.1016/S0896-6273(01)00372-5)
- Wilson, R. I., & Nicoll, R. A. (2001). Endogenous cannabinoids mediate retrograde signalling at hippocampal synapses. *Nature*, 410(6828), 588-592. <https://doi.org/10.1038/35069076>
- Wolff, S. B. E., Gründemann, J., Tovote, P., Krabbe, S., Jacobson, G. A., Müller, C., Herry, C., Ehrlich, I., Friedrich, R. W., Letzkus, J. J., & Lüthi, A. (2014). Amygdala interneuron subtypes control fear learning through disinhibition. *Nature*, 509(7501), 453-458. <https://doi.org/10.1038/nature13258>

- Woodruff, A. R., & Sah, P. (2007a). Inhibition and Synchronization of Basal Amygdala Principal Neuron Spiking by Parvalbumin-Positive Interneurons. *Journal of Neurophysiology*, 98(5), 2956-2961. <https://doi.org/10.1152/jn.00739.2007>
- Woodruff, A. R., & Sah, P. (2007b). Networks of Parvalbumin-Positive Interneurons in the Basolateral Amygdala. *The Journal of Neuroscience*, 27(3), 553-563. <https://doi.org/10.1523/jneurosci.3686-06.2007>
- Yoshida, T., Uchigashima, M., Yamasaki, M., Katona, I., Yamazaki, M., Sakimura, K., Kano, M., Yoshioka, M., & Watanabe, M. (2011). Unique inhibitory synapse with particularly rich endocannabinoid signaling machinery on pyramidal neurons in basal amygdaloid nucleus. *Proceedings of the National Academy of Sciences*, 108(7), 3059-3064. <https://doi.org/10.1073/pnas.1012875108>
- Zagha, E., & McCormick, D. A. (2014). Neural control of brain state. *Current Opinion in Neurobiology*, 29, 178-186. <https://doi.org/https://doi.org/10.1016/j.conb.2014.09.010>
- Zhang, J., Muller, J. F., & McDonald, A. J. (2013). Noradrenergic innervation of pyramidal cells in the rat basolateral amygdala. *Neuroscience*, 228, 395-408. <https://doi.org/https://doi.org/10.1016/j.neuroscience.2012.10.035>
- Zoellner, L. A., Ojalehto, H. J., Rosencrans, P., Walker, R. W., Garcia, N. M., Sheikh, I. S., & Bedard-Gilligan, M. A. (2020). Chapter 2 - Anxiety and fear in PTSD☆. In M. T. Tull & N. A. Kimbrel (Eds.), *Emotion in Posttraumatic Stress Disorder* (pp. 43-63). Academic Press. <https://doi.org/https://doi.org/10.1016/B978-0-12-816022-0.00002-8>

Zorawski, M., & Killcross, S. (2002). Posttraining Glucocorticoid Receptor Agonist Enhances Memory in Appetitive and Aversive Pavlovian Discrete-Cue Conditioning Paradigms. *Neurobiology of Learning and Memory*, 78(2), 458-464.
<https://doi.org/https://doi.org/10.1006/nlme.2002.4075>

7. Biography

Xin Fu attended Beijing Normal University in Beijing, China where he received his Bachelor degree of Science in Biotechnology and graduated in May 2012. He then worked as a research technician in Yingyu Sun's lab at Beijing Normal University to study the neural mechanism of vocalization in songbirds. In August 2013, he entered the master program in Neuroscience at Tulane University and received his Master degree in Neuroscience in May 2014. In August 2014, he entered the Ph.D. program in Neuroscience at Tulane University under the mentorship of Dr. Jeffrey G. Tasker to investigate the neurophysiology of stress in the basolateral amygdala.